

THE UNIVERSITY OF MICHIGAN, Ann Arbor, Mich.
EFFECT OF CREEP-EXPOSURE ON MECHANICAL PROPERTIES OF RENE' 41: Part II, Structural Studies, Surface Effects, and Re-Heat Treatment, by Jeremy V. Gluck and James W. Freeman, November 1961. 103p. incl. figs. tables and refs. (Project 7381; Task 73810) (ASD TR 61-73, Pt. II) (Contract AF 33(616)-6462)

Unclassified report
The effect of creep-exposure on room temperature mechanical properties of Rene' 41 was studied for temperatures of 1200-1800°F and times up to 200 hours. Unstressed exposures were for as long as 2012 hours at 1700°F. Thermally-induced structural changes reduced strength and ductility after exposures at 1400-1800°F. Reduced yield

(over)

UNCLASSIFIED

UNCLASSIFIED

UNCLASSIFIED

UNCLASSIFIED

UNCLASSIFIED

THE UNIVERSITY OF MICHIGAN, Ann Arbor, Mich.
EFFECT OF CREEP-EXPOSURE ON MECHANICAL PROPERTIES OF RENE' 41: Part II, Structural Studies, Surface Effects, and Re-Heat Treatment, by Jeremy V. Gluck and James W. Freeman, November 1961. 103p. incl. figs. tables and refs. (Project 7381; Task 73810) (ASD TR 61-73, Pt. II) (Contract AF 33(616)-6462)

Unclassified report
The effect of creep-exposure on room temperature mechanical properties of Rene' 41 was studied for temperatures of 1200-1800°F and times up to 200 hours. Unstressed exposures were for as long as 2012 hours at 1700°F. Thermally-induced structural changes reduced strength and ductility after exposures at 1400-1800°F. Reduced yield

UNCLASSIFIED

(over)

UNCLASSIFIED

strength was due to decreased volume fraction of gamma prime and secondarily to an increase in the particle size. Ductility was reduced by formation of massive grain boundary carbides. Up to 1500°F, creep caused strain hardening and Bauschinger effects. Except for surface effects, damage was restorable by re-heat treatment. Yield strength was restored by re-solution and re-aging to produce fine gamma prime. Complete re-solution of carbides was required to restore ultimate strength and ductility. Microcracking was not observed. Creep induced intergranular surface cracking at 1200-1300°F which reduced ductility. Surface effects for exposures above 1400°F were thermally induced. General principles were formulated for damage to properties of nickel-base alloys.

UNCLASSIFIED

UNCLASSIFIED

THE UNIVERSITY OF MICHIGAN, Ann Arbor, Mich. EFFECT OF CREEP-EXPOSURE ON MECHANICAL PROPERTIES OF RENE' 41: Part II, Structural Studies, Surface Effects, and Re-Heat Treatment, by Jeremy V. Gluck and James W. Freeman, November 1961. 103p. incl. figs. tables and refs. (Project 7381; Task 73810) (ASD TR 61-73, Pt. II) (Contract AF 33(616)-6462)

Unclassified report
The effect of creep-exposure on room temperature mechanical properties of Rene' 41 was studied for temperatures of 1200-1800°F and times up to 200 hours. Unstressed exposures were for as long as 2012 hours at 1700°F. Thermally-induced structural changes reduced strength and ductility after exposures at 1400-1800°F. Reduced yield

UNCLASSIFIED

(over)

UNCLASSIFIED

strength was due to decreased volume fraction of gamma prime and secondarily to an increase in the particle size. Ductility was reduced by formation of massive grain boundary carbides. Up to 1500°F, creep caused strain hardening and Bauschinger effects. Except for surface effects, damage was restorable by re-heat treatment. Yield strength was restored by re-solution and re-aging to produce fine gamma prime. Complete re-solution of carbides was required to restore ultimate strength and ductility. Microcracking was not observed. Creep induced intergranular surface cracking at 1200-1300°F which reduced ductility. Surface effects for exposures above 1400°F were thermally induced. General principles were formulated for damage to properties of nickel-base alloys.

UNCLASSIFIED

UNCLASSIFIED

THE UNIVERSITY OF MICHIGAN, Ann Arbor, Mich. EFFECT OF CREEP-EXPOSURE ON MECHANICAL PROPERTIES OF RENE' 41: Part II, Structural Studies, Surface Effects, and Re-Heat Treatment, by Jeremy V. Gluck and James W. Freeman, November 1961. 103p. incl. figs. tables and refs. (Project 7381; Task 73810) (ASD TR 61-73, Pt. II) (Contract AF 33(616)-6462)

Unclassified report
The effect of creep-exposure on room temperature mechanical properties of Rene' 41 was studied for temperatures of 1200-1800°F and times up to 200 hours. Unstressed exposures were for as long as 2012 hours at 1700°F. Thermally-induced structural changes reduced strength and ductility after exposures at 1400-1800°F. Reduced yield

UNCLASSIFIED

(over)

UNCLASSIFIED

strength was due to decreased volume fraction of gamma prime and secondarily to an increase in the particle size. Ductility was reduced by formation of massive grain boundary carbides. Up to 1500°F, creep caused strain hardening and Bauschinger effects. Except for surface effects, damage was restorable by re-heat treatment. Yield strength was restored by re-solution and re-aging to produce fine gamma prime. Complete re-solution of carbides was required to restore ultimate strength and ductility. Microcracking was not observed. Creep induced intergranular surface cracking at 1200-1300°F which reduced ductility. Surface effects for exposures above 1400°F were thermally induced. General principles were formulated for damage to properties of nickel-base alloys.

UNCLASSIFIED

ASD TECHNICAL REPORT 61-73
PART II

**EFFECT OF CREEP-EXPOSURE ON MECHANICAL PROPERTIES
OF RENE' 41**

**PART II: STRUCTURAL STUDIES, SURFACE EFFECTS,
AND RE-HEAT TREATMENT**

*JEREMY V. GLUCK
JAMES W. FREEMAN*

THE UNIVERSITY OF MICHIGAN

NOVEMBER 1961

DIRECTORATE OF MATERIALS AND PROCESSES
CONTRACT No. AF 33(616)-6462
PROJECT No. 7381

AERONAUTICAL SYSTEMS DIVISION
AIR FORCE SYSTEMS COMMAND
UNITED STATES AIR FORCE
WRIGHT-PATTERSON AIR FORCE BASE, OHIO

FOREWORD

This report was prepared by The University of Michigan, Department of Chemical and Metallurgical Engineering under USAF Contract No. AF 33(616)-6462. This contract was conducted under Project No. 7381, "Materials Application", Task No. 73810, "Exploratory Design and Prototype Development". The work was administered under the direction of the Directorate of Materials and Processes, Deputy for Technology, Aeronautical Systems Division, with Messrs. W. H. Hill and D. M. Forney, Jr. acting as project engineers.

This report covers work conducted between April 1, 1960 and May 31, 1961.

The research is identified in the records of the University of Michigan as Project No. 02902. The invaluable assistance of Mr. P. D. Goodell in the structural studies is gratefully acknowledged.

ABSTRACT

This report presents the results of a continued investigation of the influence of creep-exposure on the mechanical properties of Rene' 41 at room temperature beyond the results reported in ASD TR 61-73. The results show that thermally-induced structural changes reduced the strength and ductility for exposures at temperatures from 1400° to 1800°F. Reduced yield strength was due mainly to a decrease in the measured volume fraction of gamma prime precipitate and secondarily to an increase in the gamma prime particle size. Exposures beyond 100-200 hours did not further reduce the yield strength due to the attainment of a near minimum volume fraction of gamma prime. For the conditions studied, gamma prime was sufficiently stable up to 1400°F so that yield strength was not affected. Ductility was reduced by thermally-induced carbide precipitation in the grain boundaries in the temperature range from 1400° to 1800°F. Ductility reached a minimum after about 100 hours at 1700° to 1800°F and was not apparently further decreased by creep. Creep also had little effect on the gamma prime reactions. Creep did introduce strain hardening which increased ultimate strength and decreased ductility and Bauschinger effects which raised the tensile yield strength for creep-exposures up to 1500°F. Creep also induced surface cracking which reduced ductility after exposure at 1200° and 1300°F. Contact with alumel apparently accelerated the surface cracking. Where ductility was sufficiently reduced, the ultimate strength was also reduced. Thermally-induced surface reactions occurred for exposures above 1400°F. The maximum extent of such reduced ductility was attained rapidly and was independent of the exposure temperature. The removal of odd-size atom alloying elements from solution as a result of precipitation reactions was apparently responsible for a volume decrease during unstressed exposures above 1400°F.

The damage effects, except for surface reactions, were not permanent. Strength could be restored by re-dissolving and re-precipitating gamma prime. Re-solution of carbides, particularly M_6C by heating to 2150°F, was necessary to completely restore ultimate strength and ductility. Creep strength could also be restored. The absence of creep damage may have been due to the complete absence of microcracking during creep. The results are believed typical for nickel-base Ti-Al alloys except for the absence of the microcracking commonly occurring in many alloys of this type. A series of general principles was formulated for damage to mechanical properties of such alloys.

The controlling influence of the volume fraction of gamma prime on the yield strength appears to be in agreement with theories of dispersion strengthening. Better verification of this than was possible during this investigation

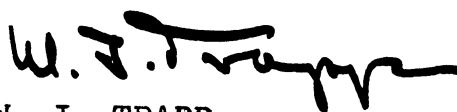
ABSTRACT (continued)

would be desirable. This is also true for the role of the types of carbides and the mechanisms of surface damage.

PUBLICATION REVIEW

This report has been reviewed and is approved.

FOR THE COMMANDER:

A handwritten signature in black ink, appearing to read 'W. J. Trapp', with a stylized, cursive flourish at the end.

W. J. TRAPP
Chief, Strength and Dynamics Branch
Metals and Ceramics Laboratory
Directorate of Materials and Processes

TABLE OF CONTENTS

	PAGE
INTRODUCTION	1
EXPERIMENTAL MATERIAL	2
TEST SPECIMENS	4
EQUIPMENT AND PROCEDURES	4
CREEP-EXPOSURE TESTS	4
TENSILE TESTS	5
IMPACT TESTS	6
DIMENSIONAL CHANGES	6
STRUCTURAL EXAMINATION	7
Specimen Preparation	7
Etchant	7
Optical Microscopy	7
Electron Microscopy	8
X-ray Diffraction	8
Lattice Parameter Determination	8
Minor Phase Identification	8
Electron Diffraction	9
RESULTS AND DISCUSSION	
EFFECT OF CREEP-EXPOSURE ON MECHANICAL PROPERTIES -- THERMALLY-INDUCED STRUCTURAL CHANGES	11
Tensile Properties after Prolonged Exposure at 1600°, 1700°, and 1800°F	11
Volume Shrinkage During Exposure at 1600°, 1700°, and 1800°F	12
Impact Tests as a Measure of Creep Damage	13
EFFECT OF RE-HEAT TREATMENT ON TENSILE PROPERTIES	14
Re-Heat Treatment after Thermally-Induced Structural Changes	15
Re-Solution of Gamma Prime and $M_{23}C_6$ Carbides Only	15
Complete Re-Solution and Re-Heat Treatment	15
Complete Re-Solution with Omission of 1950° and 1975°F Treatments	16

TABLE OF CONTENTS (continued)

	PAGE
Complete Re-Solution Without Exposure . . .	16
Re-Heat Treatment of Material Originally Heat Treated at 2050° and 1650°F	16
Complete Re-Solution after Exposure to Creep at 1800°F	17
Influence of Temperature and Time of Creep Exposure on Response to Heat Treatment	17
Summary of Tensile Property Studies	18
RE-HEAT TREATMENT AND CREEP-RUPTURE PROPERTIES	19
Re-Heat Treatment by Re-Solution of Gamma Prime and $M_{23}C_6$ Carbides Only	20
Complete Re-Solution and Re-Heat Treatment . . .	22
Influence of Surface Damage on Response to Re- Heat Treatment	22
General Principles from Study of Re-Heat Treatment on Creep-Rupture Properties	23
MICROSTRUCTURAL ASPECTS OF CREEP DAMAGE . .	25
Influence of Exposure and Re-Heat Treatment on Microstructure	26
Relation of the State of Gamma Prime after Exposure to Yield Strength	27
Effect of Exposure on Matrix Lattice Parameter .	31
Relationship of Carbides to Properties	32
Additional Observations from Structural Studies . .	33
EFFECT ON TENSILE PROPERTIES OF SURFACE REACTIONS DURING EXPOSURE	34
Exposure Without Creep	34
Exposure With Creep	35
General Effects from As-Exposed Surfaces	35
Deep Cracking During Creep at 1200° and 1300°F .	36
Examination of As-Exposed Surfaces	37
Cracking Characteristics	37
General Surface Alteration	38
Structural Characteristics of General Surface Alteration	39
GENERAL PRINCIPLES FOR CREEP-DAMAGE OF GAMMA PRIME-STRENGTHENED ALLOYS	40

TABLE OF CONTENTS (continued)

	PAGE
CONCLUSIONS	43
REFERENCES	45

LIST OF TABLES

TABLE		PAGE
1	Effect of Long-Time Aging on Tensile Properties of Rene' 41	47
2	Impact Test Data for Rene' 41 Tested at Room Temperature	48
3	Establishment of Re-Heat Treatments for Restoration of Room Temperature Tensile Properties of Rene' 41 .	49
4	Effect of Re-Heat Treatment on Tensile Properties of Rene' 41 After Initial Creep-Exposure	50
5	Effect of Re-Heat Treatment on Creep-Rupture Properties of Rene' 41 After Initial Creep Exposure .	51
6	Structural Parameters and Yield Strengths of Rene' 41 After Unstressed Exposure	52
7	Comparison Matrix Lattice Parameters and Dilatometer Shrinkage for Rene' 41 Aged Without Stress .	53
8	X-Ray Diffraction Data from Extraction Residues of Rene' 41 Specimens Used for Development of Re-Heat Treatments	54
9	Effect of Re-Machining on Response of Room Temperature Tensile Properties of Rene' 41 to Creep-Exposure	55
10	Creep Exposure Test Data for Rene' 41	56
11	Cracking Depth Data for Creep-Exposure of Rene' 41 at 1200° and 1300°F	57
12	General Surface Attack Data for Exposed Specimens of Rene' 41	58
13	X-Ray Diffraction Data from Extraction Residues of Dilatometer Aging Specimens	59

LIST OF ILLUSTRATIONS

FIGURE		PAGE
1	Details of Test Specimens	60
2	Method of Attaching Thermocouple for Long-Time Dilatometric Aging Studies	61
3	Effect of Exposure Time in Unstressed Exposures on Room Temperature Tensile Properties of Rene' 41 Alloy. ("R" Condition)	62
4	Shrinkage versus Aging Time for Dilatometer Exposures of Rene' 41	63
5	Comparison of Shrinkage Observed in Dilatometer Aging With Data Taken in Creep Units	64
6	Negative Creep Observed in Rene' 41 at 1200°F During Initial Survey Tests (Ref. 1)	65
7	Effect of 10 Hours Unstressed Exposure on Smooth Bar Charpy Impact Strength of Rene' 41	66
8	Relative Efficiencies of Tensile and Smooth Bar Impact Strengths in Showing Damage to Rene' 41	66
9	Effect of Re-Heat Treatment on Tensile Properties of Rene' 41 After Creep-Exposure at 1400°F	67
10	Effect of Re-Heat Treatment on Tensile Properties of Rene' 41 After Creep-Exposure at 1600° or 1700°F	68
11	Effect of Re-Heat Treatment on Tensile Properties of Rene' 41 After Creep-Exposure at 1800°F	69
12	Effect of Creep-Exposure on Room Temperature Tensile Properties of Rene' 41 and Subsequent Ability to Recover Original Properties by Re-Heat Treating and Re-machining	70

LIST OF ILLUSTRATIONS (continued)

FIGURE		PAGE
13	Effect of Re-Heat Treatment "R" on Rupture Life After Initial Creep-Exposure	71
14	Effect of Re-Heat Treatment to the "R" Condition and Re-machining Ratios of Actual Behavior to Theoretical Behavior of Rene' 41 After a First Creep-Exposure of 10 or 100 Hours at 1400°, 1600°, or 1800°F	72
15	Effect of Re-Heat Treatment and Re-machining on Creep of Rene' 41 After Initial Creep-Exposure for 6.9-10 Hours	73
16	Effect of Re-Heat Treatment and Re-machining on Creep of Rene' 41 After Initial Creep-Exposure for 100 Hours	74
17	Effect of Various Re-Heat Treatments on Rupture Life of Rene' 41 at 1800°F	75
18	Effect of Type of Re-Heat Treatment (Followed By Re-machining) on Creep of Rene' 41 After Initial Creep-Exposure at 1800°F for 6.8-33 Hours	76
19	Effect of Type of Re-Heat Treatment (Followed By Re-machining) on Creep of Rene' 41 After Initial Creep-Exposure at 1800°F for 100 Hours	77
20	Effect of Re-Heat Treatment and Re-machining on Creep of Rene' 41 After Initial Creep-Exposure at 1600°F	78
21	As-Heat Treated "R" Condition	79
22	Specimen R-104 Exposed Without Stress 100 Hours at 1800°F	79
23	Specimen R-105 Re-Heat Treated After 100 Hours at 1800°F (Includes One Hour Re-Solution at 2150°F)	79

LIST OF ILLUSTRATIONS (continued)

FIGURE		PAGE
24	Specimen R-111 Re-Heat Treated After 100 Hours at 1800°F (Includes Two Hour Re-Solution at 2150°F)	79
25	Optical Micrograph of Spec. R-150 Creep-Exposure 10 Hours at 1400°F to 3.52 Percent Deformation, Then Re-Heat Treated to Condition "R"	80
26	Electron Micrograph of Spec. R-150	80
27	Electron Micrograph of Spec. R-172 Creep-Exposure 100 Hours at 1400°F to 19.0 Percent Deformation, Then Re-Heat Treated to Condition "R"	80
28	Electron Micrograph of Spec. R-148 Creep-Exposure 10 Hours at 1600°F to 6.20 Percent Deformation, Then Re-Heat Treated to Condition "R"	80
29	Electron Micrograph of Spec. R-185 Creep-Exposure 100 Hours at 1600°F to 7.38 Percent Deformation, Then Re-Heat Treated to Condition "R"	81
30	Electron Micrograph of Spec. R-151 Creep-Exposure 10 Hours at 1700°F to 3.57 Percent Deformation, Then Re-Heat Treated to Condition "R"	81
31	Electron Micrograph of Spec. R-155 Creep-Exposure 10 Hours at 1800°F to 5.34 Percent Deformation, Then Re-Heat Treated to Condition "R"	81
32	Optical Micrograph of Spec. R-197 Creep-Exposure 100 Hours at 1800°F to 8.06 Percent Deformation, Then Re-Heat Treated to Condition "R"	82
33	Electron Micrograph of Spec. R-197	82
34	Optical Micrograph of Spec. R-124 Creep-Exposure 100 Hours at 1800°F to 3.46 Percent Deformation, Then Re-Heat Treated to Condition "A"	82

LIST OF ILLUSTRATIONS (continued)

FIGURE		PAGE
35	Electron Micrograph of Spec. R-124	82
36	Effect of Aging Time and Temperature on Average Gamma Prime Particle Size in Rene' 41	83
37	Effect of Exposure Time on Volume Fraction of Gamma Prime in Matrix of Rene' 41	84
38	Effect of Gamma Prime Particle Size on Yield Strength of Rene' 41	85
39	Correlation of Meiklejohn-Skoda Volume Fraction Parameter With Room Temperature Yield Strength of Rene' 41 After Unstressed Exposure	86
40	Collodion Replica of Spec. R-32	87
41	Carbon Extraction Replica of Spec. R-32	87
42	Carbon Extraction Replica of Spec. R-32	87
43	Collodion Replica of Spec. R-104. Spec. R-32 and Spec. R-104 Exposed Without Stress 100 Hours at 1800°F	87
44	Collodion Replica of Spec. R-104	88
45	Carbon Extraction Replica of Spec. R-104	88
46	Carbon Extraction Replica of Spec. R-104	88
47	Carbon Extraction Replica of Spec. R-104 (Diffraction obtained from outlined area) Spec. R-104 Exposed Without Stress 100 Hours at 1800°F	88
48	Carbon Extraction Replica of Spec. R-104 (Diffraction obtained from outlined area)	89
49	Electron Diffraction Photo of Selected Area of Figure 47	89

LIST OF ILLUSTRATIONS (continued)

FIGURE		PAGE
50	Electron Micrograph of As-Treated Condition "R" (1950°F Solution)	89
51	Electron Micrograph of Spec. R-124 Re-Heat Treated to Condition "A" (2150°F Solution) After 100 Hours Creep-Exposure at 1800°F	89
52	Effect of Re-machining on Curves of Room Temperature Tensile Properties Versus Exposure Temperature of Rene' 41 Exposed Without Stress for 10 or 100 Hours	90
53a	Effect of Exposure Temperature and Time on Difference in Room Temperature Tensile Properties Between As-Exposed and Re-machined Specimens of Rene' 41 After Unstressed Exposure	91
53b	Effect of Exposure Temperature and Amount of Prior Creep on Difference in Room Temperature Tensile Properties Between As-Exposed and Re-machined Specimens of Rene' 41 After 10 Hours Exposure	91
54	Effect of Prior Creep, Re-machining, and Thermocouple Practice on Room Temperature Tensile Properties and Cracking Tendencies of Rene' 41 Exposed at 1200° and 1300°F	92
55	Effect of Prior Creep and Re-machining on Room Temperature Tensile Properties of Rene' 41 Exposed at 1400°, 1600°, and 1800°F	93
56	Examples of Deep Cracks in Rene' 41 Exposed to Creep at 1200° or 1300°F (Low Ductility and Oxidation on Fracture Surface for Subsequent Tensile Test at Room Temperature)	94
57	Examples of Creep Curves of Rene' 41 Specimens Exhibiting Deep Cracking After 10 Hours Creep-Exposure at 1200° or 1300°F	95

LIST OF ILLUSTRATIONS (continued)

FIGURE		PAGE
58	Spec. No. R-90 (Section Showing Surface) Exposed Without Stress 100 Hours at 1000°F	96
59	Spec. No. R-99 (Section Showing Surface Attack) Creep-Exposure at 1300°F for 100 Hours to 0.63 Percent Deformation	96
60	Spec. No. R-95 (Section Showing Surface Attack and Isolated Crack) Creep-Exposure at 1300°F for 10 Hours to 2.71 Percent Deformation	96
61	Spec. No. R-93 (Section Showing Surface Attack) Exposed Without Stress 100 Hours at 1400°F	97
62	Spec. No. R-92 (Section Showing Surface Attack) Exposed Without Stress 100 Hours at 1600°F	97
63	Spec. No. R-91 (Section Showing Surface Attack) Exposed Without Stress 100 Hours at 1800°F	97
64	Longitudinal Section of Spec. D-2 Exposed Without Stress 474 Hours at 1700°F	98
65	Electron Micrograph of Spec. D-2	98
66	Longitudinal Section of Spec. D-5 Exposed Without Stress 2012 Hours at 1700°F	98
67	Electron Micrograph of Spec. D-5	98
68	Effect of Exposure Temperature and Time on Depth of Visible Surface Attack in Rene' 41	99
69	Effect of Visible Surface Attack on Room Temperature Tensile Ductility of Rene' 41 Exposed Without Stress at 1300° - 1800°F	100
70	Section of Spec. D-2 Showing Attacked Surface Layers (Arrow shows solution of grain boundary phase in advance of general attack)	101

LIST OF ILLUSTRATIONS (continued)

FIGURE		PAGE
71	Electron Micrograph of "Depleted" Layer of Spec. D-2 Exposed 474 Hours at 1700°F in Dilatometer Furnace	101
72	Section of Spec. D-5 Showing Attacked Surface Layer (Exposed 1150 Hours at 1800°F in Dilatometer)	102
73	Effect of Surface Attack on Matrix Lattice Parameter of Spec. D-2	103
74	Lattice Parameter Data for Specimen D-2 Compared to Data of Beattie and VerSnyder for Effect of Molybdenum Content on Lattice Parameter of Nickel-Base Alloys	103

INTRODUCTION

An investigation has been conducted at the University of Michigan under the sponsorship of the Materials Central, ASD, United States Air Force, under Contract AF 33(616)-6462 to obtain information and develop general principles for the influence of creep-exposure on the normal temperature mechanical properties of alloys. Changes in mechanical properties are termed "creep damage" and may be defined as any degradation in properties following exposure to stress and/or temperature under which creep can occur.

This report presents data on this subject for Rene' 41, a nickel-base Al+Ti-hardened superalloy. The results of research covering the effects of 10 to 200 hours creep-exposure over the temperature range from 1200° to 1800°F were presented previously (Ref. 1) for conditions where surface damage effects were excluded, as far as possible, from the experimental variables.

The initial results indicated that both thermally-induced structural changes and creep-strain caused alterations of room temperature mechanical properties. In addition, there was an indication that surface effects could occur that were almost as large as the thermally-induced changes, and furthermore, probably operated at lower temperatures. The major thermally-induced structural change identified was the agglomeration of dispersed gamma prime particles in the matrix. The metal carbides M_6C and $M_{23}C_6$ increased during creep-exposure and there were indications that the carbides were an important factor controlling ductility. Strain hardening and the Bauschinger effect contributed to increased strength and decreased ductility.

The research described in this report was designed to obtain additional mechanical property and microstructural information to supplement the results of Reference 1 and to extend the investigation by studying the influence of surface reactions during exposure and the feasibility of restoring properties by re-heat treatment.

Earlier research (Refs. 2-5) was confined to studies of the effects of specific exposure conditions on a number of established alloys used in sheet form in aircraft structures. The present investigation deviated from this practice by deliberately seeking damage from exposure conditions without restriction to engineering limits commonly used to avoid damage. In order

to induce changes in Rene' 41, extremes of both stress and temperature were utilized to outline exposure principles causing damage. The material was particularly outstanding in its lack of susceptibility to internal micro-cracking after substantial amounts of creep at high temperatures.

The studies of the influence of creep-exposure on room temperature properties were based mainly on tensile testing. Some compression testing and impact testing was also conducted. Surface effects were eliminated in the initial studies by re-machining the specimens following creep-exposure. Following mechanical property determinations, extensive microstructural studies were conducted in order to define the mechanisms producing the damage. Use was made of optical and electron microscopy and x-ray and electron diffraction.

The selection of Rene' 41 as an experimental material was made to provide specific data for the alloy and to develop general principles for the numerous nickel-base alloys of the same metallurgical type that might be used in aircraft structures.

EXPERIMENTAL MATERIAL

The primary requirement for the experimental material was that it be a complex high-strength heat resistant alloy with considerable future applicability by the Air Force. Preliminary experiments, discussed in detail in Reference 1, led to the selection of the nickel-base alloy Rene' 41 as a promising representative of this class of material.

Approximately 107 pounds of Rene' 41 alloy were procured from the Metallurgical Products Department, General Electric Company, in the form of 0.516-0.520-inch diameter centerless ground bar stock from vacuum induction-melted Heat R-134. The material was reported to have the following chemical composition:

<u>Element</u>	<u>Weight Percent</u>
Nickel	55.32 (by difference)
Chromium	19.27
Cobalt	11.06
Molybdenum	9.06
Titanium	3.28
Aluminum	1.44
Carbon	0.12

Chemical Composition for Rene' 41 (Continued)

<u>Element</u>	<u>Weight Percent</u>
Boron	0.0040
Iron	<0.30
Sulfur	0.006
Manganese	0.07
Silicon	0.07

The producer reported the grain size to be ASTM 3-6 and the Brinell Hardness to be 241-269. The material was shipped in the mill annealed condition (1975°F solution treatment plus water quench).

Most of the material was tested in the heat treatment condition recommended by General Electric for applications limited in service by tensile properties (Ref. 6). This treatment, coded "R" for the purposes of the investigation, consisted of the following:

- 1) Solution treatment: 1950°F - 1/2 hour plus air cool
- 2) Aging treatment: 1400°F - 16 hours plus air cool

The Vickers Hardness after treatment was 367 (equivalent to a Brinell Hardness of 347).

A minor amount of experimental work was performed on specimens heat treated according to a specification by General Electric for rupture-limited applications (Ref. 6). This treatment was coded "R2" and consisted of the following:

- 1) Solution treatment: 2050°F - 1/2 hour plus air cool
- 2) Aging treatment: 1650°F - 4 hours plus air cool

This treatment produced a Vickers Hardness of 348 and was shown in Reference 1 to produce substantially the same short-time creep-rupture properties as the "R" treatment and a similar response to creep-exposure.

For the original heat treatments, batches of 24 specimen blanks, 4 inches long by 0.516-inch diameter, were heat treated in 4 bundles of 6 blanks each. Re-heat treatments were generally conducted as convenient -- in some cases, groups of up to 6 specimens were treated at one time. The details of the re-heat treatments will be discussed more fully in the section on Results.

TEST SPECIMENS

Details of the test specimens employed in this investigation are shown in Figure 1. The original creep-exposures were generally conducted on specimens having a 0.350-inch diameter gage section with a reduced section approximately 2 inches long. For high stress tests, gage section diameters of 0.300-inches were occasionally used in order to reduce the absolute load on the creep testing machine. The specimens for subsequent mechanical property tests were designed to be machined from the gage sections of the creep-exposure specimens.

Where surface damage was to be eliminated as a variable, approximately 0.025-inches were machined from the gage section diameter. Following rough turning on a lathe, all gage sections were draw-filed and then hand polished with crocus cloth. The impact specimen employed for smooth bar tests was the ASTM Type-W sub-sized bar. The dimensions, 0.197-inches square by 2.16 inches long, were such that it could be conveniently milled from the reduced section of a creep specimen.

Exposure tests without stress were also conducted on cylindrical specimens 4.0-inches long by 0.4-inches in diameter in a dilatometer so that volume changes could be measured. Care was taken that the specimen ends were flat and parallel.

EQUIPMENT AND PROCEDURES

CREEP-EXPOSURE TESTS

The creep-exposure tests were conducted in individual University of Michigan creep-testing machines. In these units, the stress is applied through a third class lever system having a lever-arm ratio of about 10 to 1. The specimens were gripped by threaded holders fitting into a universal joint system that insured uniaxial loading. Heating was accomplished by a wire-wound resistance furnace fitting over the entire specimen holder assembly. Strain measurements were made with the modified Martens extensometer system, an optical lever-arm system which permits the detection of specimen elongations of approximately 10 millionths of an inch. Because this system required the attachment of extensometer bars to collars threaded to the specimen shoulders, it was necessary to correct the observed deformations for the diminished contribution of the fillets and shoulders. A detailed description of the extensometer system and the method of making

"effective gage length" calculations was given previously (Refs. 1 and 3) and will not be repeated here.

Temperature measurements were generally made from three Type-K thermocouples, one at the center of the reduced section and at either end. All thermocouples were shielded from direct furnace radiation. Prior to starting a test, the furnace was heated to within 50°F of the desired temperature. The specimen was then placed in the hot furnace and brought up to the test temperature and distribution in a standard period of four hours. ASTM Recommended Practices were followed in controlling the test temperature and distribution. For several tests where exposure was desired without thermocouple contact on the gage section, temperature measurement was made from couples wired to the specimen shoulders. The validity of this procedure was checked on a specimen with five couples attached -- the three on the gage section and one at either shoulder. The shoulder-to-shoulder temperature deviation was less than 5°F

Strain measurements were made as each weight was applied during loading and then periodically throughout the tests. At the end of the exposure period, a final reading was made and the power to the furnace turned off. The specimen then cooled under load in order to minimize the effects of creep recovery. In the tests exposed without stress, the same procedure was followed in order to make the total time at temperature equivalent to the case of a stressed exposure. The Martens extensometers were also used in the unstressed exposures as an expedient to obtain information on dimensional changes due to structural reactions. For the 0.350-inch diameter specimens, the weight of the necessary holder and extensometer system produced a specimen stress of 54.5 pounds per square inch. The data obtained with this system were later checked by conventional dilatometer tests.

Where the creep tests were allowed to run until failure, an automatic timer, accurate to one-tenth of an hour, was actuated by the fall of the specimen holder to measure the rupture time.

TENSILE TESTS

Short-time tensile tests were conducted at room temperature in a hydraulic testing machine. Elongation was measured with a microformer strain gage and recorded automatically in the form of a load versus strain curve. A strain pacer was used to insure a strain rate of 0.005 inches per inch per minute.

The data determined in the tensile tests were the ultimate tensile

strength, the 0.2-percent offset yield strength, the elongation, reduction of area, and the modulus.

IMPACT TESTS

Both Izod and Charpy smooth bar impact tests were utilized in this investigation. In the Izod test, the specimen is supported vertically at one end as a cantilever, while in the Charpy test the specimen is supported horizontally at both ends as a simple beam. A special holding fixture was used to accommodate the sub-sized specimen. In all tests, the impact machine pendulum was set to produce a striking energy of 120 foot-pounds. Prior to conducting a test, the scale of the machine was zeroed by allowing the pendulum to swing through its cycle with no specimen in place.

DIMENSIONAL CHANGES

The dimensional change data obtained using the optical extensometer system during the unstressed exposures were checked by using more conventional dilatometric techniques. A quartz tube dilatometer assembly conforming to ASTM Recommended Practices was available for these determinations. A wire-wound resistance furnace was used to heat the assembly. The test specimen employed was a cylinder 4.0-inches long by 0.4-inches in diameter. Care was taken that the ends of the specimen were flat, parallel, and perpendicular to the specimen axis. Dimensional changes were measured with a mechanical dial gage graduated in 10,000ths of an inch. Since the aim of these tests was to obtain information on dimensional changes with time at temperature and not the thermal coefficient of expansion, minor modifications of conventional procedure were employed. To reduce the effects of heating time, the tests were hot started, that is, the specimens were placed in the hot unit which had been previously brought to about 10°F below the desired aging temperature. The specimen was then "nursed" to the proper temperature as quickly as possible, generally 40 minutes or less, and the dial gage readings were started. From two to four readings per day were then made throughout the exposure period.

Temperature measurement was made from a thermocouple attached to the center of the specimen. It was not possible to spot weld a thermocouple to the specimen because the 28-gage wire necessary for a couple that could be spot welded would not stand up during the long aging times contemplated. The standard dilatometer rod was modified to permit the use of 18-gage thermocouples as shown in Figure 2. This was accomplished by using a hollow quartz tube for the push rod. The heavy gage thermocouple wires were covered with ceramic insulators and fed through the push rod. At the bottom end, the bare wires were brought out around the specimen,

fusion welded to form a bead, and then fastened to the specimen with asbestos cord. The top of the thermocouple was brought out around a special cap.

A thermocouple that had been attached in this manner to a specimen during aging for 2012 hours at 1700°F was subsequently checked against a virgin couple at 1700°F and found to read only 5°F hot.

STRUCTURAL EXAMINATION

The techniques used in this investigation for structural examination included optical microscopy, electron microscopy, x-ray diffraction of powder samples and extracted residues, and electron diffraction of extraction replicas.

Specimen Preparation

Specimens for microscopic examination were sectioned longitudinally along the center line with a water-cooled cut-off wheel and then mounted in Bakelite. The mounted specimens were wet ground on a rotating lap through a series of silicon carbide papers finishing at 600-mesh grit. Final polishing was accomplished on a cloth-covered rotating lap using fine diamond compound and then on a vibratory polisher in an aqueous media of Linde "B" polishing compound. The samples were cleaned in an ultrasonic cleaner with a detergent solution.

Etchant

The specimens for optical and electron microscopy were etched electrolytically in "G" etch, an etchant developed by Bigelow, Amy, and Brockway (Ref. 7). Etching was conducted at 6 volts and a current density of approximately 0.8 amperes per square inch for a period of 5-7 seconds. The composition of the etchant follows:

"G" Etch

H₃PO₄ (85%) 12 parts
H₂SO₄ (96%) 47 parts
HNO₃ (70%) 41 parts

Optical Microscopy

Conventional methods were employed for general optical examination. Crack depths and oxide penetrations were determined with a 10x filar micrometer eyepiece at a system magnification of 600x.

Electron Microscopy

Electron microscopy was carried out in an RCA EML Electron Microscope. For examination in the microscope, collodion replicas mounted on nickel grids were prepared from the surface of the etched specimens. The replicas were shadowed with palladium to increase the contrast and reveal surface contours. Polystyrene latex spheres of either 2580 or 3400 Å diameter were placed on the replicas prior to shadowing to indicate the angle and direction of shadowing and to provide an internal standard for the measurement of magnification. The micrographs reproduced in this report are direct prints from the original negatives; consequently, the polystyrene spheres appear black and the shadows appear white. Since the spheres are raised from the surface of the replica, a particle casting a shadow opposite to that of the latex spheres is in relief on the metal specimen; conversely, areas casting shadows in the same direction as those cast by the latex spheres are depressions in the surface of the metal specimen and correspond to material that was attacked or eaten out by the etchant.

X-ray Diffraction

X-ray diffraction analysis was used both for the identification of minor phases and the determination of matrix lattice parameters.

Lattice Parameter Determination. Determinations of the matrix lattice parameters were made from Debye-Scherrer diffraction photographs of filings. The filings were made with a very fine file, sifted with a magnet to remove any extraneous iron particles that might have come from the file, and then sifted through a 200-mesh screen. The resultant fine powder was rolled into a thin wire using a binder of Duco cement. Exposure was made to nickel-filtered copper radiation for 4 hours in a 114.6 mm diameter Debye camera. An optical comparator was used to determine diffraction line positions. Lattice parameters were determined by the extrapolation method of Nelson and Riley (Ref. 8).

Minor Phase Identification. The identification of minor phases was made from x-ray diffraction analysis of residues extracted either from solid samples or from filings by immersion in a bromine-alcohol solution. Filings were made for the identification of the constituents in various surface layers of an aged dilatometer sample. Layers approximately one-thousandth of an inch thick were removed from the sample with a fine file as it was rotated in a lathe.

After initial preparation, the samples for extraction were soaked in pure bromine liquid, cleaned with distilled water, and completely dried.

Each specimen was then placed in an individual centrifuge tube. Approximately 25 ml. of a 10:1 mixture of anhydrous methyl alcohol and bromine was added. Boiling took place in about 10 minutes, after which the tube was cooled under tap water. The reaction was allowed to continue until a sufficient quantity of extract had been obtained, after which the specimen was removed and rinsed with methyl alcohol. The tube was centrifuged and the extract washed repeatedly with alcohol until the supernatant liquid was clear. The extract was scraped onto a filter paper, dried, and formed into a thin wire using a Duco cement binder. X-ray exposures were conducted either in a 57.3 or a 144.6 mm diameter Debye camera using nickel-filtered copper radiation for periods of four hours. The line positions were determined on an optical comparator and "d" values were calculated. The patterns were then analyzed by comparison with standard patterns available from the literature and, in particular, the ASTM Powder Data File.

Electron Diffraction

Electron diffraction studies were carried out in a 50 kilo-volt RCA EML Electron Microscope on extraction replicas mounted on nickel grids. Although this process has the advantage of allowing study of phases in situ, it is a time-consuming, rather delicate operation, particularly sensitive to preparation techniques. Results once obtained, must be analyzed carefully. Considerable experimentation was required before usable replicas could be prepared, with best results finally being obtained from bromine-extracted carbon replicas. Replicating media discarded due to inability to find a satisfactory extracting agent that would not also destroy the replica included collodion and Fax-film. A vinyl chloride polymer appeared to have promise in standing up to a number of extracting reagents, however, the polymerization often continued to the point of cracking.

The metallographic specimens selected for extraction replication were repolished and etched with "G" etch in order to bring the minor phases well into relief. On some samples, the etching conditions were varied to also etch out the gamma prime phase. A carbon film was then vapor-deposited on the surface. This acted not only as a replica of the surface but was also the medium for holding the extracted particles in place. A 3/16-inch grid was then scribed in the carbon film with a razor blade to permit the penetration of the extracting agent to the specimen surface and to facilitate handling of the individual replicas. The mounted specimen was then immersed in a 10:1 bromine-absolute methyl alcohol solution for 4-6 hours. Following extraction, individual grid squares were floated off the surface by immersing the specimen in distilled water. The squares were washed and lifted out of the solution on nickel grids.

Each grid was dried and a thin film of aluminum was vapor-deposited on the replica to act as an internal standard for diffraction analysis.

The completed grids were handled in the microscope in the same manner as conventional collodion replicas. An electron micrograph was taken to identify each area from which diffraction was obtained. The relatively low accelerating potential of the microscope made it difficult to obtain a diffraction pattern from anything other than thin films or particles.

The completed patterns were analyzed by indexing the diffraction spots by a trial and error procedure analogous to the study of a front-reflection Laue x-ray pattern. The lattice constant of the diffracting phase was determined by the relationship of its pattern to the known pattern produced by the aluminum standard.

RESULTS AND DISCUSSION

The previous report (Ref. 1) demonstrated that creep damage to mechanical properties at room temperature occurred in Rene' 41 by:

- (1) Residual mechanical effects from creep which caused Bauschinger effects and strain hardening
- (2) Thermally-induced structural changes
- (3) Surface reactions in air.

This report extends the data for the second and third effects and presents results of investigations of the causes for the observed changes in properties as a basis for developing general principles for creep damage in gamma prime-strengthened alloys.

EFFECT OF CREEP-EXPOSURE ON MECHANICAL PROPERTIES -- THERMALLY-INDUCED STRUCTURAL CHANGES

A study was carried out of the effect of prolonging exposure time on tensile properties. A short study of the changes in impact properties for unnotched specimens was conducted. Volume shrinkage during exposure was studied. The effects studied were confined to thermally-induced structural changes by remachining specimen surfaces after exposure.

Tensile Properties after Prolonged Exposure at 1600°, 1700°, and 1800°F

Prolonging exposures at 1700° and 1800°F without stress did not appreciably reduce tensile properties at room temperature (Table 1 and Fig. 3) from those resulting from the 100-200 hour exposures reported in Reference 1. The data covered exposures as long as 2012 hours at 1700°F and 1700 hours at 1800°F. Short-time exposures at 1600°F did not reduce properties as much as they did at 1700° and 1800°F. An exposure of 401 hours at 1600°F reduced the properties to those after exposure for 100 to 200 hours at 1700° and 1800°F. Longer exposures at 1600°F were not available to establish whether or not the properties would also level off at the same value as for exposure at 1700° and 1800°F.

The approximate levels of tensile properties at room temperature for exposures longer than 100 to 200 hours at 1700° and 1800°F and for 400 hours at 1600°F in comparison to original material were as follows:

<u>Property</u>	<u>Exposed Material</u>	<u>Original Material</u>
Ultimate strength (psi)	140,000	190,000
0.2% offset yield strength (psi)	95,000	130,000
Elongation (%)	5	20
Reduction of area (%)	6	28

Values somewhat above and below these approximate levels after exposures were obtained in the actual tests.

All exposures longer than 200 hours were carried out in a dilatometer so that volume changes could be measured. Those up to 200 hours were carried out in creep units under a dead load of 54.5 psi.

Volume Shrinkage During Exposure at 1600°, 1700°, and 1800°F

The prolonged exposures without stress were carried out in a thermal expansion unit to measure volume changes accompanying structural changes. The data obtained (Fig. 4) indicated continued shrinkage at least up to 1150 hours at 1800°F and up to 2012 hours at 1700°F. Exposure for 401 hours at 1600°F also resulted in shrinkage. The amount of shrinkage was larger for a given time of exposure the higher the exposure temperature. The rate of shrinkage decreased with time but continued for the full period of exposure. Exposure for 1000 hours at 1800°F resulted in a shrinkage of 0.004 inch and 0.0028 inch at 1700°F. A similar value for 1600°F was not established but would apparently have been less than at 1700°F.

These data indicate that there was a real and substantial shrinkage during exposure at 1600° to 1800°F. Due to the stresses which can be induced by shrinkage, the characteristics of the shrinkage are in themselves important. It will be noted, however, that shrinkage continued after there was little further change in tensile properties at room temperature with continued exposure (Fig. 3). It is, therefore, uncertain as to what degree the structural changes causing shrinkage were responsible for the changes in mechanical properties.

The shrinkage offsets and reduces the amount of creep measured during stressed exposure. Figure 5 compares creep curves with the shrinkage during unstressed exposure for the first 100 to 200 hours of exposure. This comparison indicates the amount the measured creep was reduced by the shrinkage. It does not, however, show whether or not stress accelerated shrinkage.

The data of Figure 5 indicated that the unstressed tests reported in Reference 1 resulted in less shrinkage that was measured by the dilatometer. The testing procedure used for the previous tests was then

checked. These exposures were carried out in creep units with all adapters in place so that the extensometer system would operate. The stress imposed by the adapter system was 54.5 psi. This was not sufficient stress to account for the difference from the amounts measured in the dilatometer. It is known that the extensometer method of measurement is subject to errors under loads too low to eliminate the misalignment associated with joints. It is, therefore, considered that the initial data correctly indicated shrinkage but that due to the conditions of measurement, the absolute amount was slightly low. In fact, one of the reasons for using the dilatometer was the question regarding the prior method of measuring the shrinkage. This allowed verification of the shrinkage by another method.

The unstressed exposures at 1200° and 1400°F in the creep units indicated little change in length in 100 to 200 hours. However, creep curves for stressed exposure at 75,000 psi at 1200°F did show a small amount of shrinkage, exhibited as "negative creep" (Fig. 6). The phenomenon of "negative creep" has also been reported in the literature for a number of other alloy systems (Refs. 9, 10). Presumably, the shrinkage offsets some of the normal creep at higher stresses so that the amount of creep measured, such as for the curve at 114,000 psi in Figure 6, was less than actually occurred. It is assumed that the normal creep at 75,000 psi was extremely small and the indicated shrinkage was about the total amount which occurred. The indicated shrinkage probably represents the extensometer functioning correctly under load, whereas it did not in the unstressed exposures. It is possible, however, that the stress did accelerate shrinkage.

Impact Tests as a Measure of Creep Damage

Impact tests are frequently a most sensitive method of determining that properties are being changed as a result of exposure to creep. This method was abandoned in the initial studies (Ref. 1) when it was discovered that the subsize notched specimens had only about 3 foot-pounds of energy absorption in the as-treated condition. Subsequent discussion of this test with a representative of the Materials Central suggested that impact tests on unnotched specimens might provide useful results.

The usefulness of this test was studied with the data obtained being given in Table 2 along with the original data for notched specimens from Reference 1. The unnotched specimens bent in the Izod tests at 30 foot-pounds and fractured at about 29 foot-pounds in Charpy tests. These values were sufficiently large so that reductions in properties due to exposure to creep might be useful for measuring damage.

Charpy tests on smooth specimens after unstressed exposure (Table 2 and Fig. 7) gave the following results:

- (1) Exposure for 10 hours at 1600°F did not significantly change impact strength. When the time was increased to 401 hours, there was a significant decrease.
- (2) Exposure for 10 hours at 1700° or 1800°F did reduce impact strength significantly.
- (3) The scatter between individual tests could be quite large. For this reason, replicate testing would be necessary.

Comparison of the information obtained from tensile and impact tests (Fig. 8) using average percentages of as-treated strength indicated a more pronounced decrease for impact properties. The impact strength of the smooth specimens was approaching low values so rapidly that with slightly more exposure all values would be very low and not show any change. As previously shown (Fig. 3), tensile properties continued to decrease with longer exposure. It was concluded that the impact tests were not showing changes where tensile tests did not show any change. The replicate exposures necessary were also undesirable. For these reasons, it was decided to discontinue impact tests.

EFFECT OF RE-HEAT TREATMENT ON TENSILE PROPERTIES

The study of the effects of re-heat treatments after creep-exposure was undertaken for the information it would provide regarding the factors causing creep damage to tensile properties at room temperature. The experiments had the following objectives:

(1) To determine if the damage was permanent or if the properties could be restored by re-heat treatment. If any part of the damage were permanent, it would indicate that damage by internal cracking could have been a factor in addition to microstructural effects. If properties could be restored, it would indicate that microstructural changes alone were responsible.

(2) To obtain information on the damage mechanism by varying the conditions of re-heat treatment. Beattie (Ref. 11) had determined for Rene' 41 that gamma prime dissolves between 1900° to 1950°F, $M_{23}C_6$ carbides dissolve between 1700° and 1800°F, and 2150°F is required to dissolve M_6C carbides. For the present studies, the assumption was made that re-resolution plus re-aging would result in nearly the same structure as the original material.

In all experiments, the specimens were re-machined after heat treatment. Surface effects from the prior creep-exposure as well as those from the re-heat treatment were thus eliminated. The tensile properties were calculated on the basis of the specimen dimensions after re-machining. The results will show that re-heat treatment was very effective in restoring properties at room temperature. It must be clearly recognized, however, that restoration would not be nearly as effective if the damaged surface is not removed.

Re-Heat Treatment after Thermally-Induced Structural Changes

The first step in the studies of re-heat treating was to evaluate the permanency of thermally-induced structural changes. The data are summarized in Table 3. Severe reduction in room temperature properties was induced by unstressed exposures at 100 hours at 1800°F (Table 3, Spec. R-32 and Spec. R-104 indicate the effect of this exposure). In all the re-heat treatments studied, complete re-solution of the gamma prime was then induced. By varying the temperature of re-solution, the effect of leaving the M_6C undissolved or dissolved was studied.

Re-Solution of Gamma Prime and $M_{23}C_6$ Carbides Only:

Re-heat treatment by reproducing the original treatment of one-half hour at 1950°F, air cooling and aging at 1400°F for 16 hours (coded "R" in this investigation) would be expected to re-dissolve and re-precipitate gamma prime as a fine dispersion. Heating at 1950°F would also be expected to dissolve at least part of any $M_{23}C_6$ carbides present. The treatment brought the yield strength up to nearly the original level (Table 3, Spec. R-136). However, the ultimate strength was only partially restored and the ductility was not restored at all. This suggests that the solution of gamma prime was effective in restoring yield strength, but incomplete solution of carbides, particularly M_6C , restricted ductility and thereby ultimate strength.

Complete Re-Solution and Re-Heat Treatment:

After 100 hours exposure at 1800°F, Specimens R-105 and R-110 were heated to 2150°F and air cooled after 1 hour in one case and 2 hours in another. They were then re-heated at 1975°F for 1 hour and water quenched to simulate the original mill anneal. The original "R" heat treatment was then duplicated by heating to 1950°F for one-half hour, air cooling and aging at 1400°F for 16 hours. Both treatments nearly restored the original properties with the two-hour treatment at 2150°F (Spec. R-110) possibly slightly more effective. Taking into

account the probable differences in structure between the original and re-heat treatments, it can be concluded that the effects of the thermally-induced structural changes were eliminated and the original properties completely restored.

Complete Re-Solution with Omission of 1950° and 1975°F Treatments:

After 100 hours exposure at 1800°F, re-treatment at 2150°F for 2 hours, plus simulation of the mill anneal at 1975°F and aging at 1400°F for 16 hours resulted in essentially the same properties (Table 3, Spec. R-111 and Spec. R-201) as the complete treatment. Ductility may have been sufficiently high to represent a significant increase. This treatment was coded "A". Omission of both the 1950° and 1975°F treatments resulted in essentially the same properties (Spec. R-135). Evidently, the intermediate treatments at 1975° and 1950°F had very little effect on tensile properties at room temperature. If these treatments did cause some re-precipitation of M_6C while at 1975° and 1950°F, it did not have much effect.

Complete Re-Solution Without Exposure:

Because the treatment at 2150°F was so effective after the 100-hour exposure at 1800°F, it seemed desirable to determine what the effect of this treatment would be if no exposure was involved. Accordingly, Specimen R-141 in the as-treated "R" condition was re-heated for 2 hours at 2150°F, air cooled, re-heated to 1975°F, water quenched and aged at 1400°F for 16 hours. Ultimate and yield strengths were lower than for the original material or the exposed specimens given the same re-treatment, while ductility was higher. While only one test was involved, it seems evident that the prior exposure at 1800°F for 100 hours resulted in some effect that slightly raised tensile strength and slightly reduced ductility in relation to unexposed material with the same treatment.

Re-Heat Treatment of Material Originally Heat Treated at 2050° and 1650°F:

The heat treatment of one-half hour at 2050°F, air cool plus aging for 4 hours at 1650°F (code "R2") which had been recommended for rupture-limited applications (Ref. 6) was applied to several specimens. These were then exposed at 1800°F for 100 hours to induce marked reduction of tensile properties at room temperature (Table 3, Spec. R2-8).

Re-heat treatment with the original conditions of heat treatment restored yield strength but not ultimate strength and ductility (Table 3, Spec. R2-13). Evidently, treatment at 2050°F was not sufficiently high to dissolve enough carbides to restore properties.

Re-heat treatment at 2150°F with or without the treatment at 2050°F restored both ultimate and yield strengths (Table 3, Spec. R2-14 and Spec. R2-15). Ductilities, however, may not have been completely restored. Because no creep was involved, any inability to completely restore ductility must have resulted from some difference in structure before and after re-heat treatment and not to a permanent damage arising from creep.

Complete Re-Solution after Exposure to Creep at 1800°F

The ability of the "A" treatment to restore thermally-induced changes after 100 hours unstressed exposure at 1800°F was demonstrated on specimens R-111 and R-201. Creep-exposure for the same time period also had a severe effect on the tensile properties (Table 3, Spec. R-26 and Spec. R-45).

An indication of the effect of the "A" treatment in restoring properties after creep-exposure was obtained by exposing specimens to 3.46 and 28.4 percent of creep in 100 hours at 1800°F prior to re-heat treatment. These specimens were then heated at 2150°F for 2 hours, air cooled, re-heated to 1975°F for 1 hour, water quenched, and aged at 1400°F for 16 hours. Both specimens had about the same ultimate and yield strengths as the specimen (R-141) simply re-heat treated. The ductility of Specimen R-124 with 3.46-percent creep may have been slightly reduced and was definitely reduced for Specimen R-116 with 28.4-percent creep. The restoration of properties after 28.4-percent creep was, however, remarkably effective and indicated that if there was permanent damage from creep at 1800°F it was very small.

Influence of Temperature and Time of Creep Exposure on Response to Heat Treatment

The experiments involving material exposed at 1800°F for 100 hours demonstrated that a complete re-solution essentially restored tensile properties at room temperature when the exposure conditions were the most severe used in this investigation. Presumably, any less drastic exposures would also respond to a similar heat treatment. The data did suggest, however, that information could be obtained on the structural changes reducing properties from less drastic exposure if the re-heat treatment was limited to gamma prime and $M_{23}C_6$ re-solution by using the original "R" heat treatment of 1950°F solution and 1400°F aging.

A group of specimens were exposed for 10 hours at 1400°, 1600°, 1700°, and 1800°F under stresses producing from 3 to 6 percent of creep (Table 4). This exposure generally was about 70 to 80 percent of the

estimated rupture life. The specimens were then re-heated to 1950°F for one-half hour, air cooled, aged at 1400°F for 16 hours, and finally re-machined. The creep curves for each exposure are plotted in Figures 9-11 together with bar graphs indicating the level of room temperature tensile properties at each stage of the exposure and re-heat treatment cycle. Summary plots to illustrate the effects of exposure temperature and time are included in Figure 12.

Properties were essentially unchanged from the original condition (Table 4) for specimens exposed at 1400° and 1600°F (Figs. 9, 10, and 12). The increase in yield strength from the Bauschinger effect was removed by re-heat treatment. The loss in ductility at 1600°F was restored. The ultimate and yield strength reductions from exposure to 1700° and 1800°F were restored, but the accompanying losses in ductility were not (Figs. 10, 11, and 12).

When the exposure time was increased to 100 hours, the re-heat treatment only returned both strength and ductility to near original values for exposure at 1400°F (Figs. 9 and 12). Strengths were restored after exposure at 1600°F but not ductility (Figs. 10, 12). Yield strength was restored after exposure at 1800°F but not ultimate strength or ductility (Figs. 11, 12). As previously discussed, the re-heat treatment apparently had to be 2150°F to include re-resolution of M_6C carbides for exposure for 100 hours at 1800°F (Fig. 12). Presumably, this temperature would also be required to restore ductility after 100 hours exposure at 1600°F.

The results for either time of exposure (Fig. 12) showed no appreciable influence of creep on the ability for property restoration by re-heat treatment.

Summary of Tensile Property Studies

The results indicate that deterioration of tensile properties during prior creep exposure involves the following processes:

(a) Any changes in yield strength can be substantially restored by a treatment at 1950°F. When exposures are at a sufficiently low temperature to introduce Bauschinger effects or strain hardening, the re-heat treatment provides stress relief. When the temperature and time of exposure are high enough to cause reductions in yield strength due to loss of the original fine dispersion by agglomeration of gamma prime, re-resolution of the gamma prime at 1950°F and re-aging restores yield strength.

(b) The initial losses in ductility for short time or low temperature of exposure apparently can be restored by a treatment at 1950°F. Either these are due to removal of $M_{23}C_6$ carbides which are redissolved at 1950°F; the treatment at 1950°F changes carbide distribution so that it does not effect ductility; or strain hardening is relieved.

(c) When the exposure temperature is increased above 1600°F and time of exposure is increased beyond 10 hours, ductility cannot be restored by re-heat treatment at 1950°F (Fig. 12). Because treatment at 2050°F was not effective in one case while 2150°F was effective in all cases (Table 4), it appears that the re-resolution treatment must be high enough to dissolve M_6C carbides when they have formed or reached a given size or dispersion.

(d) Ultimate strength will not be restored by gamma prime re-resolution when this treatment does not restore the more severe cases of reduced ductility.

(e) Creep in itself did not appreciably change the response to re-heat treatment. The only effect it might have would be to accelerate the structural changes previously discussed. (This is based on specimens with 3 to 6 percent of creep in 10 and 100 hours at 1400° to 1800°F. One case of 28-percent creep at 1800°F also responded.) The indications are that internal cracking was not occurring during creep; or, if it did occur, it was not sufficient to noticeably effect properties.

In considering this general summary, it is important to again recognize that surface damage from prior exposure and during re-heat treatment was eliminated by re-machining the specimen surfaces. If this had not been done, the degree to which ultimate strength and ductility were restored would have been considerably less.

RE-HEAT TREATMENT AND CREEP-RUPTURE PROPERTIES

Differences in the plastic flow mechanism between room temperature and the creep-exposure temperatures could be responsible for the ability to restore the room temperature tensile properties by re-heat treatment after creep. That is, permanent damage from prior creep might have little effect on tensile properties due to differences in the mechanism of plastic flow. Accordingly, it appeared that a study of the effect of re-heat treatment on creep-rupture properties after creep-exposure for part of the rupture life would provide information further delineating the principles governing creep damage. This procedure also would extend the measure of creep damage by assessing it in terms of

properties quite different than the mechanical properties at room temperature. The information could have considerable practical utility in those cases where such re-heat treatments would be feasible and surface damage effects could be controlled.

It is generally considered that creep-rupture life which has been used up cannot be restored by re-heat treatment. When such treatments are successful in prolonging creep-rupture life, structural deterioration reducing creep-rupture life presumably has been restored. The reason for the permanency of creep-damage to subsequent creep-rupture life has never been fully explained. The explanation based on microcracking has appeared to be deficient.

For interrupted creep-rupture tests, the rupture time after re-heat treatment should be no longer than the difference between the expected uninterrupted (i. e., "normal") rupture life and the time at which the test was interrupted. (This is an expression of the so-called "life fraction rule".) Interrupting and re-starting a test on a re-heat treated and re-machined specimen involves an adjustment of stress which might increase the rupture time slightly. Also, the re-machining could increase life if surface attack was an important factor controlling rupture. However, any marked increase in rupture life would presumably be due to the restoration of a structural change which was markedly reducing creep resistance with time of testing.

Re-Heat Treatment by Re-Solution of Gamma Prime and $M_{23}C_6$ Carbides Only

A group of specimens were exposed to creep at 1400°, 1600°, 1700°, and 1800°F generally for 10 or 100 hours. The stresses were such that the time periods represented 60 to 90 percent of the expected rupture life (Table 5). The initial "R" heat treatment of one-half hour at 1950°F, air cool, plus aging at 1400°F for 16 hours was then reapplied. After re-machining to eliminate surface damage and confine the results to creep damage to the internal structure, the specimens were returned to creep-rupture testing under the original conditions. Because the loads were changed to give the same stress as the initial stress, any stress intensification from reduction of area during the initial exposure was eliminated.

In every case (Table 5 and Fig. 13), the rupture life after re-heat treatment was considerably longer than the additional time expected for rupture to occur in uninterrupted testing. It ranged from 1.82 to 4.60 times as long as expected on the basis of no restoration of creep life ("life fraction" rule) (Fig. 14a). This measure is, perhaps, not as im-

portant as the fraction of expended life recovered by the heat treatment. The percentage recovered tended to decrease with increasing test temperature and time (Fig. 14b). The specimen exposed for 10 hours at 1600°F apparently completely recovered its creep-rupture life during the re-heat treatment. The specimen exposed for 10 hours at 1400°F, while it recovered a substantial amount of life, did not reach 100 percent. It did, however, rupture with low ductility (Fig. 14d) and it is suspected, for this reason, that something may have been wrong with the test. (This specimen also represented the maximum expenditure of life during the first exposure of any of the specimens studied.) The general trend in Figure 14b for decreasing recovery with increasing temperature would be in agreement with the general trend of the data for the effects on properties at room temperature (Fig. 12). On the other hand, if the high recovery tests are due to erratic test behavior, then all the specimens were damaged to the extent that only about 50 percent of the original life was restored by the re-heat treatment (Fig. 14b and 14c).

The elongation during the first creep exposure plus that during the second generally totalled more than for uninterrupted testing. They were as high during the second exposure as for uninterrupted testing, except for prior creep at 1400°F (Fig. 14d).

The re-heat treatment initially returned the creep resistance very nearly to that of the material at the start of the first exposure. Examination of the creep curves (Figs. 15 and 16), however, indicates that the creep rates increased with time during the second exposure faster than during the first. This tendency was more apparent the higher the temperature of the first exposure (Fig. 14e). Some factor inherited from the first creep exposure affected creep after re-heat treatment.

From these data, it appears that:

(1) Complete recovery of creep-rupture life by re-heat treatment and re-machining after exposure at 1400°F was prevented by incomplete recovery of ductility.

(2) When the exposure temperature was 1600°F, nearly 100-percent recovery was obtained because both creep-resistance and ductility were recovered.

(3) The inheritance factor preventing complete recovery of prior creep-exposure at higher temperatures appeared to be the faster rate of increase of creep with testing time.

Complete Re-Solution and Re-Heat Treatment

The response to re-heat treatment at 1950°F was somewhat similar to that observed in tensile tests at room temperature. This suggested that solution was incomplete and that a full solution treatment would completely restore creep-rupture life. Accordingly, specimens exposed to creep at 1800°F were heated at 2150°F for 2 hours and air cooled. Like the specimens used for tensile tests, a treatment of 1 hour at 1975°F, water quench and age at 1400°F for 16 hours was then applied. (This sequence was designated the "A" treatment) After re-machining, the specimens were returned to rupture testing at 1800°F under the same stress as the first creep exposure.

The rupture times were longer than those expected for uninterrupted testing of the original material (Table 5 and Fig. 17). In other words, the complete solution treatment at 2150°F not only resulted in complete recovery from the prior creep but also added more rupture life.

In view of this result, the influence of the treatment on specimens which had not been exposed to creep was determined. The rupture times were the same as those for the specimens which had been exposed to creep (Fig. 17). From the viewpoint of rupture life, there was no residual effect from creep after complete re-solution.

The ductility during the second creep-exposure was about the same as for specimens heat treated at 2150°F without prior creep (Table 5). The creep curves were virtual reproductions of those for similarly heat-treated specimens which had not been exposed to creep (Figs. 18 and 19).

Apparently, the inclusion of a complete re-solution at 2150°F in the re-heat treatment resulted in complete recovery from prior creep. The inheritance factor after re-heat treatment at 1950°F of a more rapid increase in creep with time of testing was eliminated. Because the testing was limited to prior creep at 1800°F, it is not known if the reduced ductility found after creep at 1400°F and re-heat treatment at 1950°F would also have been eliminated.

Influence of Surface Damage on Response to Re-Heat Treatment

Part of the prolongation of rupture life from re-heat treatment could be due to the removal of surface damage by re-machining. In order to obtain some information on this point, two tests were carried out. Limitation of time and funds prevented a more thorough study.

Specimen R-183 with the original heat treatment at 1950°F was exposed to creep at 1600°F for 10 hours to 2.5-percent creep strain. After re-heat treatment at 1950°F and aging at 1400°F, it was returned to creep-rupture testing without re-machining. The rupture time was nearly the same as for the specimen which was both re-heat treated and re-machined (Table 5). Ductility was lower and was probably responsible for a slightly shorter rupture life. Creep resistance appeared to be similar to that during first exposure (Fig. 20).

Specimen R-187 was similarly exposed to creep, re-machined but not re-heat treated. The rupture time during the second exposure was 60 percent of that for the specimen both re-heat treated and re-machined. This did, however, represent a considerable prolongation of life beyond that of an uninterrupted test. The prolongation of life was apparently due to the increased elongation after re-machining. Creep resistance was somewhat reduced (Fig. 20).

These very limited data suggest that re-heat treatment restores creep resistance while re-machining is required to restore ductility. The indication is based on only two tests limited to prior creep at 1600°F. It was previously shown that re-machining presumably did not restore ductility when the exposure temperature was 1400°F and the re-heat treatment was limited to 1950°F.

If these results are indicative of the magnitude of the two effects, re-heat treatment is considerably more effective in prolonging rupture life than re-machining. This is possibly related to the shape of the creep curves. The restoration of ductility by only re-machining operated when the creep resistance had already deteriorated to a considerable extent. The rapid creep used up the ductility in less time.

General Principles from Study of Re-Heat Treatment on Creep-Rupture Properties

In general, re-heat treatment and re-machining had the same effects on future creep-rupture properties as it did on tensile properties at room temperature. A re-solution treatment at 1950°F followed by aging at 1400°F to restore the gamma prime dispersion, did not completely restore properties. Complete re-solution by including a re-heat treatment at 2150°F did completely restore properties. In fact, this treatment actually increased the creep-rupture life beyond that expected for the original material heat treated at 1950°F.

The inheritance factors when the re-heat treatment was limited to 1950°F were apparently somewhat different than for tensile properties.

When the first creep-exposure was at a relatively low temperature (1400°F), ductility during the re-exposure to creep was reduced. After higher temperatures of exposure to creep, ductility was restored but the creep rates increased with time faster than during the original exposure. The tensile properties at room temperature could be restored after creep exposure at the lower temperatures but not after the higher temperatures. The latter was due to non-recovery of ductility. Possibly, the same structural feature, incomplete solution of M_6C carbides, was responsible for both effects. The cause for the inability to recover creep-rupture ductility after creep exposure at the lower temperatures is not clear. Possibly, the M_6C formed affects creep-rupture ductility but not tensile at room temperature. The data suggest that restoration of gamma prime by re-heat treatment restores both yield strength at room temperature and creep-resistance.

The removal of surface damage by re-machining restores ductility in creep-rupture tests. Due to concurrent increases in creep resistance from re-heat treatment, this was less effective in prolonging creep-rupture life than it was in restoring properties at room temperatures. In other words, the restoration of creep-resistance apparently was the predominant factor.

The absence of permanent loss of creep-rupture life by prior creep indicates that the principal damage factors during prior creep were structural changes. The potential creep resistance of the material is such that considerable creep extension introduces little damage if the structure is restored. Certainly, there was no result suggesting that internal cracking was involved. The difference in plastic flow between room temperature tensile tests and creep-rupture conditions only reflected itself in the differing ways the structures control the two properties when the re-solution during re-heat treatment was incomplete.

Table 5 includes tabulations to show the degree by which re-heat treatment prolonged rupture life and changed total ductility. These values were obtained by summing the respective values for the exposure to creep before and after re-heat treatment. It should be recognized that these values cannot be considered for practical applications without consideration of the effects of surface damage and the possibility of re-machining. The latter is frequently impossible. Surface damage can have serious deleterious effects on other properties than those considered. In addition, such factors as warpage during re-heat treatment could be serious. The investigation also did not consider possible deleterious effects of a 2150°F treatment on other properties, particularly at temperatures below 1800°F.

MICROSTRUCTURAL ASPECTS OF CREEP DAMAGE

As has previously been indicated, the experimental program was based, in many ways, on the expected effects of creep-exposure on the microstructure of Rene' 41 alloy. In particular, the following features were used:

1) The main strengthening feature of the microstructure was the precipitation of $\text{Ni}_3(\text{Al, Ti})$, commonly referred to as gamma prime. Alloys containing gamma prime are known to undergo losses in strength as it agglomerates during exposure at elevated temperatures. The previous report (Ref. 1) showed electron micrographs which indicated qualitatively that yield strength decreased as the size of the gamma prime particles increased with exposure temperature and time. This feature of damage from exposure has now been examined in more detail by making quantitative measurements of the gamma prime as a function of exposure conditions.

2) The role of gamma prime was studied further by determining the influence of re-heat treatment to dissolve agglomerated gamma prime and reprecipitate it in the original dispersion. This was done for both mechanical properties at room temperature and subsequent creep-rupture properties. Studies of the influence of re-heat treatment on microstructure were then carried out.

3) One of the objectives of the re-heat treatment program was to determine if there was permanent damage from creep which could not be restored by heat treatment. In particular, the possibility of micro-cracking as a source of permanent damage was examined microscopically.

4) Other research on nickel-base gamma prime-strengthened alloys had demonstrated that carbides precipitated at grain boundaries could be damaging to ductility (Refs. 11, 12). In this research, it was previously shown (Ref. 1) that reduced ductility at room temperature was associated with the growth of fairly massive carbides in the grain boundaries during exposure. X-ray diffraction analyses of extraction residues from exposed samples had shown that both M_{23}C_6 and M_6C carbides could be present in material with either high or low ductility. The choice of re-heat treatment temperatures for the present studies was based on the restoration of gamma prime by heating at 1950°F but not re-resolution of M_6C carbides. The choice of 2150°F was based on the expected re-resolution of M_6C carbides. The actual structures and types of carbides after exposure and after re-heat treatment were accordingly investigated for this report.

Influence of Exposure and Re-Heat Treatment on Microstructure

The series of photomicrographs showing the coarsening of gamma prime with increasing exposure temperature for 10 and 100 hours from Reference 1 have not been repeated for this report. The original optical microstructure (Fig. 21) shows some grain boundary precipitation and titanium carbonitrides. The fine gamma prime precipitate present is not evident optically but is shown by the electron micrograph of Figure 50. The exposures up to 1400°F did not noticeably change the microstructure. As shown in the previous report, starting at 1500°F, exposure at higher temperatures coarsened the gamma prime and increased the amount of precipitate in the grain boundaries. Figures 22, 40, 43 and 44 show the extreme changes developed by 100 hours at 1800°F. Figures 65 and 67 show the influence of prolonged exposure at 1700°F. The gamma prime particles became large enough so that they were evident in the optical microstructure. The grain boundary precipitates became continuous. As shown in Reference 1, both massive gamma prime and carbides formed in the grain boundaries.

Exposure at 1600° to 1800°F would be expected to result in solution of gamma prime as required by the phase relationships. This took place and as a result, during cooling, fine gamma prime re-precipitated in the matrix between the larger undissolved gamma prime particles as is shown by Figures 40, 43, 44, 65, and 67. In the previous report, it was shown that this fine re-precipitation did not always occur under conditions and for reasons which have not been established.

The re-heat treatments at 1950°F dissolved the gamma prime and on re-aging developed about the same gamma prime dispersion as the original material. Figures 25 through 33 show, however, that as the carbides in the grain boundaries increased with creep-exposure temperature and time, they remained in the grain boundaries in increasing amounts after re-heat treatment. Apparently, this is the reason why re-heat treatment, simply involving re-solution of gamma prime, was not always successful in restoring ductility at room temperature. (The effects on mechanical properties are shown in Figure 12.) These micrographs show that massive gamma prime was dissolved from the grain boundaries and, therefore, was not involved in the loss in ductility. (It should be noted that the electron micrographs of these figures do not show gamma prime reprecipitated. This was due to the low magnification necessary to properly show the carbides.)

Re-heat treatments involving complete re-solution at 2150°F were, however, effective in reducing the grain boundary carbides (Figs. 23, 24, 34, 35).

Relation of the State of Gamma Prime after Exposure to Yield Strength

The qualitative observations between gamma prime particle size and yield strength after exposure (Ref. 1) suggested the possibility that quantitative measures of gamma prime would provide a useful means of defining the general principles governing creep damage. Accordingly, measurements were made to define the volume fraction of gamma prime, its particle size, and spacing as a function of exposure conditions with the results given in Table 6. The method used was to carry out lineal analyses on electron micrographs, using the adaptation developed by Rowe (Ref. 13) to correct for the particle size being smaller than the etching depth. These structural parameters were then correlated with the yield strength.

In making these measurements, only samples exposed without stress were used to avoid the complication due to residual stresses influencing yield strength. The samples given prolonged exposure in the dilatometer were added to the study. In attempting to measure specimens exposed up to and including 1400°F, it was found that the change in gamma prime for the exposure conditions considered was so slight that the time-consuming measurements would not show a significant change. This is quite certainly the reason that there was no change in yield strength after these exposures.

The measurements of structures exposed at 1600°, 1700°, and 1800°F gave the following results:

1) The average particle size increased with both temperature and time of exposure (Fig. 36).

2) The volume fraction of gamma prime decreased with exposure time with a strong tendency towards a constant minimum value (Fig. 37).

The objective of these measurements was to relate the state of the gamma prime to the yield strength at room temperature after exposure. Both the increase in size of gamma prime particles and the decrease in volume would commonly be expected to reduce yield strength. The scatter in data and lack of time to conduct check and additional tests where desirable made it necessary to analyze the results in terms of general trends. Within this limitation, it appears from the data that:

1) The yield strengths at room temperature (Fig. 3) tend to approach a common level with exposure time. The common level is attained in shorter times with increasing temperature of exposure.

2) The particle size of gamma prime increases with both exposure temperature and time.

3) The volume fraction of gamma prime tends to approach a common level with exposure time. This is attained in somewhat less time with increasing exposure temperature.

In other words, the yield strengths tend to level out along with the volume fraction of gamma prime while the particle size continued to grow with exposure time. The time required for this condition decreased slightly with increasing exposure temperature. Particle size, however, continued to increase with both exposure temperature and time.

An extensive study of the explanations for strengthening from dispersed phases was carried out with the aid of the literature survey of Bunshah and Goetzel (Ref. 14). The treatment developed by Meiklejohn and Skoda (Ref. 15) from studies of iron particles dispersed in solid mercury seemed to best explain the results. Moreover, their treatment seems best substantiated from a theoretical viewpoint (Ref. 16). The experiments of Meiklejohn and Skoda showed that strengthening from a dispersed phase -- if the phase is truly a dispersion -- depends on the ratio of h/λ , where h is the particle diameter and λ is the interparticle spacing. In turn, from geometric considerations, it can be shown that h/λ is a function of the volume fraction of the dispersed phase; namely, h/λ is proportional to $f^{1/3}$. Thus, the yield strength is a function of the volume fraction of the precipitate, i. e., $\sigma_y - \sigma_0 = \frac{a f^{1/3}}{0.82 - f^{1/3}}$, where σ_y is the strength with the dispersion, σ_0 is the strength of the matrix, and "a" is a constant.

However, if the yield strength, at a constant volume fraction, f , does vary with the particle size, h , then the foregoing conditions are not being met. Meiklejohn and Skoda explain this on the basis of coherency effects, and show that in the case of coherency, an effective volume fraction, f' , must be used; defined as the stressed region through which dislocations will not pass. Thus, the operative effect is the blocking of dislocations by the actual or effective dispersion.

In applying these considerations to the present data, a plot of σ_y versus h (Fig. 38) showed some dependence of yield strength on particle size -- although the data did not permit comparison to be made at constant volume fraction. Thus, the conditions for a "true" dispersion were not entirely met.

With this in mind, the yield strength data were all tested with the Meiklejohn-Skoda volume fraction parameter, $\frac{f^{1/3}}{0.82 - f^{1/3}}$, with the results being plotted in Figure 39. Allowing for experimental scatter, the correlation appears to be good, and in particular, shows excellent agreement with one facet of the Meiklejohn-Skoda equation in that the intercept,

σ_0 , at zero volume fraction, is the experimentally determined yield strength of the matrix (mill annealed) material prior to aging. The correlation of Figure 39 thus suggests that the volume fraction, f , was the strong variable governing yield strength, with the particle size effect suggested by Figure 38 of secondary importance.

The break in the curve, or limiting yield strength, indicated in Figure 39 for large volume fractions was also reported by Meiklejohn and Skoda for their iron-mercury dispersions. Their explanation for the effect was that at the maximum stress either cross-slip occurred with dislocation loops climbing over the particles or that dislocations passed through the particles.

For precipitation hardening alloys, Meiklejohn and Skoda suggested that after attainment of maximum strength, as the particles continue to grow, a decrease in yield strength is expected until the particles attained a certain size. At this point, the strength would be expected to level out with increasing particle size and become only a function of volume fraction. The general trends of the data of Figure 38 show a rather remarkable similarity to this prediction and suggest that:

- 1) The yield strengths initially decreased when the particles of gamma prime were small due both to the increase in particle size and to the decrease in volume fraction.

- 2) The yield strengths levelled out and became virtually independent of exposure time and temperature because the particles of gamma prime attained a size where volume fraction was the controlling feature and the volume fraction attained nearly a constant value independent of the exposure temperature.

- 3) Yield strengths did not continue to decrease with exposure time (Fig. 3) because the gamma prime particles attained a size beyond which size changes had no further effect.

- 4) The variations in yield strength with exposure temperature and time for exposures of 10 to 100 hours reflect the combined effects of rate of increase in size of gamma prime particles and the rate of decrease in volume fraction as they were influenced by exposure conditions before the limiting conditions were attained.

Extensive attempts were made to utilize the data to correlate the properties in other terms of the fundamental characteristics of the particle size and interparticle spacing. The literature is not clear on the proper way to do this and attempts to correlate the data in this manner

led to a number of fair correlations and others which did not correlate. It is believed, however, that more time to obtain more data in the proper ranges of properties and particle size together with proper recognition of the limiting size effect would have resulted in considerable progress in further clarifying the factors controlling yield strength of gamma prime-strengthened alloys.

The as-treated yield strength of material aged at 1400°F ("R" condition) was higher than that for material aged at 1650°F ("R2" condition). The data of Figures 38 and 39 indicate that this was due to both the larger volume fraction and smaller particle size of the gamma prime. Both heat treatment conditions rapidly attained the same yield strength as a result of exposure because both of the structural parameters rapidly attained the same value.

There are a number of features of the data which limit the generality and reliability of the explanation proposed:

1) The decrease in measured volume fraction of gamma prime with exposure is not understood. Rowe (Ref. 13) encountered the same effect in M252 and Inconel 700 alloys. Bigelow (Ref. 17) had also reported this phenomena. Bigelow proposed that it was due to the entrapment of matrix atoms in the gamma prime which during exposure had an opportunity to diffuse out of the gamma prime. Rowe was unable to completely explain his results on this basis and suggested the possibility that coherency effects where particles were small may have somehow resulted in the measured volume fraction being increased beyond the true volume fraction. In all cases, the initial measured volumes were larger than would be predicted from known phase relations.

2) The measurements of gamma prime were confined to the particles freely dispersed in the matrix. The massive gamma prime accumulated in the grain boundaries was not counted. As Rowe (Ref. 13) observed, the gamma prime in the grain boundaries was, however, nowhere near sufficient to account for the decrease in measured volume.

3) In this investigation, the exposure conditions and phase relationships required solution of gamma prime from that present after aging in accordance with the increasing solubility with temperature. In some cases, this resulted in reprecipitation on slow cooling in the form of fine particles in the matrix between the larger particles of undissolved gamma prime. In the measurements, the unsatisfactory procedure of merely averaging the particle size was used. In other samples, the fine precipitate was absent. Time did not permit clarification of these two effects. It must be recognized, however, that part of the measured

volume decrease could be due to re-resolution of gamma prime. The attainment of a volume fraction nearly independent of exposure temperature suggests that this was not much of a factor.

4) Meiklejohn and Skoda (Ref. 15) treated the case where the dispersed phase was hard in a soft matrix and was chemically and structurally widely different from the matrix (i. e., little opportunity for coherency). It must be recognized that in alloys such as Rene' 41 gamma prime is very similar to the matrix (gamma phase) in both crystal structure and hardness. Thus, the present conditions are widely different than were postulated by Meiklejohn and Skoda.

5) The particle size at which the strengthening from the dispersed phase became a function only of volume fraction in Meiklejohn and Skoda's work (Ref. 15) was smaller than the point of apparent levelling-off in this investigation (Fig. 38). The latter data are not, however, too definite due to the difficulty of accounting for the volume fraction and particle size varying simultaneously. In addition, data scatter could have played a part. There seemed to be a tendency for higher strength for smaller particle size in the range where volume fraction was decreasing. It is possible that this apparent discrepancy was due to the similarity of gamma prime and gamma and to the retention of coherency to larger particle size for gamma prime.

Effect of Exposure on Matrix Lattice Parameter

Measurements of the lattice parameter of the matrix showed a decrease (Table 7) with increasing temperature and time of exposure. Calculations of shrinkage based on these measurements agreed with those measured in the dilatometer. Table 7 also includes measurements made by Beattie (Ref. 11) which show good agreement between the two sets of measurements when allowance is made for the lower solution temperature and aging at 1400°F for the present investigation.

These data suggest that the volume shrinkage was due to precipitation removing odd-sized atoms from solution. In this case, this would presumably mainly be carbon and molybdenum. There are, however, uncertainties involving the role of the apparent volume fraction change of gamma prime. If the apparent volume change of gamma prime was due to some preferential segregation of other atoms not involving size differences, there could have been a shift in matrix lattice parameter and volume. It should be noted, however, that shrinkage continued after the volume fraction of gamma prime apparently became nearly constant. The indications are, therefore, that precipitation of odd-sized atoms as carbides was the major reason, even though the amount of shrinkage seems large for this to be the sole cause.

Relationship of Carbides to Properties

The microstructural studies of carbides were qualitative in nature. Attempts were made to make this more definite. As was shown in Reference 1, x-ray diffraction analysis of extraction residues after exposure showed both $M_{23}C_6$ and M_6C carbides present when ductility was high as well as when it was low. Additional diffraction data for the dilatometer specimens given prolonged exposure at 1600° to 1800°F are included in Table 13.

The main correlation of properties with carbides seemed to be the deterioration in ductility as the total amount of carbide increased. Other investigations (Refs. 11, 18) had shown that $M_{23}C_6$ tends to break down to M_6C as the exposure temperature and time are increased. Moreover, it had been found that $M_{23}C_6$ redissolved between 1700° and 1800°F. Because $M_{23}C_6$ had been found in samples exposed as high as 1900°F for 10 hours, this was difficult to understand.

Further information on this point was obtained by carrying out x-ray diffraction analysis of extracted carbides after re-heat treatment (Table 8). After exposure for 100 hours at 1800°F, both $M_{23}C_6$ and M_6C were present in Specimen R-104 (see also Fig. 22). (The TiC was originally present and remained constant with re-heat treatment and apparently was inactive.) After re-heat treatment at 2150°F for 1 and 2 hours (Figs. 23 and 24), the patterns for $M_{23}C_6$ and M_6C became weaker. The two-hour treatment reduced the $M_{23}C_6$ and M_6C to quite small amounts with possibly more $M_{23}C_6$. These results again confirmed that treatment at 2150°F was effective in dissolving carbides (compare Figs. 33 and 35). In this case, the carbides found could have formed during aging at 1400°F. This also suggests that they may have been present in exposed samples as a result of opportunity to form during cooling.

Considerable effort was expended to produce extraction replicas to isolate the carbides in place in the microstructure and then use electron diffraction for identification purposes. The specimens used had been exposed at 1800°F for 100 hours (Fig. 40). When the technique of leaving the gamma prime in the structure before extraction of the carbides was used, the replicas illustrated by Figures 41 and 42 were obtained. The dark areas are the extracted carbides. The very light areas adjacent to the carbide in Figure 41 were due to a tear in the replica, a major difficulty with the technique. In Figure 42, the massive gamma prime adjacent to the carbide can still be seen. When the gamma prime was etched out prior to applying the extraction replication procedure, the replicas shown by Figures 45 through 48 were obtained. These included areas of what appeared to be thin films of carbide. Normal electron micro-

graphs of collodion replicas of this sample are shown in Figures 43 and 44. Satisfactory electron diffraction patterns of these, characteristic of thin films (Fig. 49), were obtained. The patterns indexed as $M_{23}C_6$. Useful patterns could not be obtained from the more massive carbide particles which were extracted since they were not suitable for electron diffraction purposes. It should be recognized that the thin films of $M_{23}C_6$ could have formed during cooling after exposure and may not be entirely characteristic of prolonged exposures.

To summarize the carbide studies, the decrease in $M_{23}C_6$ and M_6C carbides during re-solution treatment at 2150°F was substantiated. Extraction replicas further identified carbides in exposed samples. The association of reduced ductility with massive carbides was, therefore, given further substantiation. The simultaneous presence of $M_{23}C_6$ after exposure and after heat treatment was proven by additional data. The occurrence of $M_{23}C_6$ as thin films was shown. The reason why $M_{23}C_6$ was found after exposure or heat treatment above the reported solution temperature of 1700° to 1800°F was not determined, although it probably was formed during cooling after exposure or during aging after re-heat treatment. The presence of $M_{23}C_6$ as thin films would be consistent with its formation under those conditions.

Increasing the re-heat treatment temperature to 2150°F did result in extensive carbide re-solution (Figs 23, 24, 34, and 38). The carbides after 2 hours at 2150°F were even less than in the original condition of heat treatment (Figs 50 and 51). The re-solution of carbides, therefore, did coincide with the restoration of ductility. The reprecipitated gamma prime particles (Fig. 51) were finer than when the material was heat treated at 1950°F (Fig. 50). This coincided with the increase in creep-rupture strength when the re-heat treatment temperature was raised to 2150°F from 1950°F.

Additional Observations from Structural Studies

A relationship between structure and the inheritance factor of more rapid increase in creep rate with time after re-heat treatment at 1950°F than in the first exposure was not identified. As discussed previously (page 27), there were volume differences in measured gamma prime as well as changes in particle size during aging and exposure. It might be that if such measurements had been made, it would be found that the volume of gamma prime was less whenever carbides were not redissolved and that re-solution of carbides increased the volume percentage of gamma prime. Presumably, the re-solution of carbides at 2150°F was responsible for the reduced size of the gamma prime particles after aging, although

other factors associated with nucleation and growth could have been involved.

One of the most important results of the microstructural examinations was the absence of microcracking after creep in any of the samples examined. The authors have found that microcracking is a prominent feature of creep in all other nickel-base gamma prime-strengthened alloys with which they have had experience. At present, this absence of microcracking appears to be unique to Rene' 41 and may be the reason why creep damage was negligible.

EFFECT ON TENSILE PROPERTIES OF SURFACE REACTIONS DURING EXPOSURE

Although the previous portion of this investigation (Ref. 1) was concentrated on re-machined specimens, a few tensile tests were conducted on specimens which were not machined to remove surface damage after exposure. The results suggested that the reduction in ultimate strength and ductility at room temperature from surface damage was similar in magnitude to that due to structural changes. Additional data have now been obtained for exposure without and with creep.

Exposure Without Creep

The exposure conditions were 10 hours at 1200° to 1800°F and 100 hours at 1000° to 1800°F without stress. The tensile properties (Table 9) and the graphical comparisons (Figs. 52 and 53a) to specimens with re-machined surfaces indicate the following:

- 1) Yield strengths (Figs. 52 and 53a) were the same for both re-machined and as-exposed surfaces.
- 2) After exposure for 10 or 100 hours, the as-exposed surfaces resulted in lower ultimate tensile strength and ductility (Figs. 52 and 53a) than for the re-machined specimens for exposure at 1400°F and higher temperatures. The degree of reduction increased somewhat with exposure temperature. An exception was exposure for 100 hours at 1800°F where the limited data indicate little difference between as-exposed and re-machined specimens. Exposure at 1200° and 1300°F did not result in reduced properties from surface effects.
- 3) The amount the as-exposed surfaces reduced properties below those of the machined specimens (Figs. 52 and 53a) was essentially the same for either 10 or 100 hours of exposure at a given temperature,

except for 1800°F.

4) Specimens with as-exposed surfaces exhibited reduced ductility after exposure for 10 hours above 1300°F, while the re-machined specimens exhibited no change (Figs. 52 and 53a). The tensile strength was also reduced below that due to structural changes. When exposed for 100 hours, the surface and structural change effects were approximately equal. The exception was 1800°F when the structural changes appeared to be responsible for nearly all the reduction.

Exposure With Creep

Specimens were exposed to creep for 10 hours from 1200° to 1800°F and for 100 hours at 1200° and 1300°F and then tensile tested at room temperature with as-exposed surfaces. The data obtained (Table 9) indicate:

1) The introduction of creep caused the as-exposed surfaces to reduce ductility for exposure at 1200° and 1300°F (Fig. 54). This did not occur for specimens exposed without creep (Fig. 52). Specimens re-machined after creep exposure also showed no loss in ductility, except when deep cracking occurred. As will be shown in the next section, this was due to an extraneous effect.

2) The surfaces as exposed to creep at 1200° and 1300°F had no effect on yield or ultimate tensile strengths (Fig. 54). The reduced ductility did not affect ultimate strength since the residual effects of creep which manifested themselves as the Bauschinger effect and strain-hardening caused a change in the shape of the stress-strain curve such that the yield strength and ultimate strength were almost equal.

3) The ductility after exposure above 1300°F for 10 hours was essentially constant at each temperature for specimens with as-exposed surfaces (Figs. 55 and 53b) with increasing amounts of creep. The damage from exposure without creep was the same as when creep occurred. Ultimate tensile strengths were also reduced by as-exposed surfaces. Creep had little effect except possibly to increase damage at 1800°F. At 1400° and 1600°F, it may have reduced the surface damage.

General Effects from As-Exposed Surfaces

Surface alterations which can include such things as surface cracking, oxidation, decarburization, and de-molybdenumization reduced ultimate tensile strength and ductility at room temperature after exposure.

Surprisingly, the only significant effect from creep was reduced ductility for the 1200° and 1300°F creep-exposures. The damage was not significantly increased by increasing exposure times from 10 to 100 hours. There was some increase from increasing temperature of exposure. The mechanism of damage, therefore, appears to be fairly complicated because surface reactions certainly increase both with time and temperature of exposure, and creep would be expected to intensify cracking.

Deep Cracking During Creep at 1200° and 1300°F

Exposure to creep at 1200° and 1300°F resulted in progressive reduction in ductility with increasing creep up to about 4-percent strain (Fig. 54). For larger amounts of creep, there was a marked increase in the loss in ductility along with a tendency for reduced ultimate strength where the ductility was particularly limited. These specimens exhibited oxidized fracture surfaces (Fig. 56) extending in from the surface to varying degrees, indicating that cracks had penetrated during exposure deeper than the 0.025-inch machined off before testing. This phenomena has been designated "deep cracking". Measurements of the depth of deep cracking are summarized in Table 11 and plotted as a function of prior strain in Figure 54.

Re-examination of these specimens disclosed that the deep cracks were associated with points of thermocouple attachment. When this was noted, three specimens were exposed at 1300°F with the thermocouples attached only to shoulders. Even when the creep strain was 5.4-percent there was no evidence of deep cracking (Table 11 and Fig. 54). The ductility values were in accordance with a prolongation of the curves for smaller creep strains where there had been no deep cracking.

Further examination showed that the cracks generally originated at a point about one-third around the circumference from the point where the thermocouple beads were in contact with the specimen. This is the point at which the wire fastening the thermocouple to the specimen first comes in contact with the specimen. The cracks as revealed by dye-penetrant testing are shown by Figure 56.

Further testing (Tables 9, 11 and Fig. 54) showed that the condition developed most extensively when alumel wire was used to attach the thermocouple. When chromel was used, the penetration was reduced. Specimen R-152 was exposed to 5.6-percent creep at 1300°F with a loop of alumel wire wrapped around one end. When tested at room temperature, deep cracking which had occurred where the alumel loop was attached, had reduced ductility (Fig. 54). One-half of the gage length of Specimen

R-156 was wrapped with alumel and the other half with chromel before exposure to 5.9-percent creep in 10 hours at 1300°F. Dye-penetrant examination showed numerous cracks on the end wrapped with alumel, with practically none on the chromel half. When 0.046-inches was machined off the surface and the specimen then subjected to tensile testing, the properties (Fig. 54) were in agreement with those to be expected for samples not subject to deep cracking. Most of the deep cracks previously formed were 0.045-inch or less (Table 11). The removal of 0.046-inch apparently removed all cracks.

Since a thermocouple is a joint between chromel and alumel, even when only chromel wire was used to attach the thermocouples there was a good chance of some contact with alumel from the thermocouple itself. This was manifested in a reduced tendency for deep cracking (Spec. R-196 and Spec. R-189 -- compared with Spec. R-193). However, alumel wire fastening or thermocouple contact itself did not completely explain the cracking. Specimens which had exhibited deep cracking in tensile tests were cooled to -320°F and broken at other locations by striking. In no case were other deep, oxidized cracks found than the one in the tensile test fracture. This suggests that the cracking started at one point and proceeded rapidly before it had a chance to occur at other points.

Apparently deep cracking did not occur until creep strain exceeded 4 percent at 1200° and 1300°F. It did not occur at higher temperatures. The presence of only one crack together with no apparent effect on creep curves up to 4-percent strain (Fig. 57) indicates that alumel catalyzed the cracking at one particular location and the crack grew quite rapidly. Otherwise, there should have been noticeable acceleration of creep and cracks present at the location of the other thermocouples. The absence at higher temperatures seems to be evidence that the reaction with alumel was not specific to the development of cracks at these temperatures.

Examination of As-Exposed Surfaces

Microstructural examination of as-exposed surfaces was carried out. The results showed that depending on the exposure temperature there was normally a relatively shallow zone of intergranular cracks and an area of oxidation together with probable removal of alloying elements by diffusion to the surface. In addition, the deep cracks previously discussed as arising from contact with alumel wire were observed in specimens exposed to more than 4-percent creep at 1200° and 1300°F.

Cracking Characteristics

No cracking or other attack was noticeable (Fig. 58) in the specimens exposed for 100 hours at 1000°F without stress. Exposure at 1200° and

1300°F under stress resulted in intergranular cracks (Figs. 59 and 60), usually one to a few grains deep. The depth of these surface cracks was less than 0.001 to 0.005-inch for specimens exposed to 2 to 4 percent creep (Table 11). The crack depth increased with the amount of prior strain (Fig. 54). The 0.0125-inch of metal removed during re-machining removed these cracks, accounting for the absence of any effect on properties. When tensile tested with as-exposed surfaces, these cracks apparently were responsible for the reduced ductility. No cracks and no reduction in properties resulted from exposure without stress at 1200° and 1300°F.

When deep cracking occurred for creep strain of more than 4 percent due to contact with alumel, crack depths (Table 11) as deep as 0.081-inch were observed. Measurements of the indicated depth of cracking by oxide coloration on specimens crept to rupture in 5.1 to 9.2 hours at 1300°F showed cracking depths ranging from 0.07- to 0.11-inch at the time of rupture. The deep cracks were intergranular.

The reason why deep cracking occurred for more than 4-percent creep at 1200° and 1300°F when in contact with alumel wire is not clear. These temperatures are those for minimum ductility and maximum notch sensitivity for the alloy. However, the cracks did not grow deeply in the absence of alumel. The brittleness at 1200° and 1300°F alone could not be responsible. Some reaction with alumel causing a stress corrosion-type of effect at the grain boundaries was necessary. The notch sensitivity at these temperatures may have made the material more sensitive to attack by alumel and could thus explain its lack of effect at higher temperatures.

General Surface Alteration

When exposure temperatures were increased above 1300°F, general surface alteration occurred (Figs. 61, 62, and 63). There was penetration into grains and not just at grain boundaries. In addition, there was a layer of alloy depletion. This was probably due to decarburization and demolybdenumization as well as depletion of Al and Ti to cause the disappearance of gamma prime. Some internal oxidation and nitrogenation may have also occurred as is more evident in specimens exposed for prolonged times (Figs. 64 and 66).

Measurements of the depth of visible general surface attack were made (Table 12) and plotted as a function of exposure time in Figure 68. The curves agree in general with a parabolic rate law similar to scaling (Ref. 19). The depth of detectable attack corresponded with the amount of attack first reducing properties.

The visible depth of penetration was correlated with ductility measurements (Fig. 69). This figure shows, as a function of depth of penetration, the ratio of ductility for specimens in the as-exposed condition to ductility with the surface attack machined off. The maximum effect was obtained with relatively little penetration. There was little difference between 10 and 100 hours of exposure. Evidently, only about 0.0002-inch of penetration was required to give a maximum effect. Beyond this amount, there was no further deterioration. This was the cause for the absence of any change from 10 to 100 hours exposure. This also shows why there was relatively little additional effect from exposure above 1400° to 1600°F

Figure 69 indicated that Specimen R-188 (Table 9) should have had a visible attack depth of 0.0003-inch after 10 hours exposure at 1600°F to 2.81-percent creep. The surface was remachined to remove 0.001-inch and then the specimen tensile tested. The results (Fig. 55), however, showed that the properties were still the same as for specimens with as-exposed surfaces. Examination showed that all of the surface attack had not been removed. Evidently creep did accelerate attack but it was not evident in the tensile properties due to the saturation at about 0.0002-inch penetration.

Structural Characteristics of General Surface Alteration

The details of the microstructure of the altered surfaces are shown by Figures 70 and 72 for samples exposed 474 and 2012 hours at 1700°F without stress. The overaged gamma prime of the matrix is bounded by an area free from gamma prime. Figure 70 shows by the arrow that there was little, if any, preferential penetration along grain boundaries. The carbides and massive gamma prime are, however, removed from the grain boundaries in the layer next to unaltered matrix. The electron micrograph of Figure 71 shows in greater detail that no gamma prime was present.

The next layers contained gamma prime-free matrix and a new phase in the form of needles. There was a layer next to this with some oxidation fissures as well as needles. The outside layer was free from needles but contained numerous fissures. Electron micrographs of the unattacked interiors of these specimens are shown in Figures 65 and 67.

Four layers were machined from the surface of Specimen D-2 which had been exposed for 472 hours at 1700°F without stress. These layers were subjected to x-ray diffraction analysis. There was a linear decrease in the matrix lattice parameter (Fig. 73) from the base material out through the altered layers. Comparative parameter data (Fig. 74) from the work of Beattie and Ver Snyder (Ref. 20) on the effect of molybdenum on lattice parameters of a somewhat similar alloy make a good case for

the change in parameter being due to de-molybdenumization. There was good agreement with the present material for the lattice parameter at the Mo content of Rene' 41 and also at the parameter of 3.564 Å for the Mo-free material and the surface of the present material.

It does not seem possible that the lack of Mo would prevent gamma prime from forming. It seems quite likely, however, that Al and/or Ti were preferentially removed from solution in the alloy to account for the absence of gamma prime. Extraction residues from the layers machined from Sample D-2 showed considerable amounts of TiN (Table 13) in the altered surface. This points to the needle-like structure at least being TiN. This, in itself, could account for the absence of gamma prime. The data also suggest that Al₂O₃ was concentrated in the scale (Ref. 21). The presence of TiN plus Al₂O₃ probably account for the removal of Ti plus Al from solution. Both were, therefore, removed from gamma prime (i. e. , Ni₃(Al, Ti)) to form more stable compounds. Even a partial removal of Ti plus Al could result in gamma prime depletion by lowering its solution temperature.

The outside scale was mainly Cr₂O₃ as would be expected. It was also present in the sub-scale layer as the microstructure indicated. There was also some possibility of NiCr₂O₄ (Ref. 22). The layer next to the matrix showed M₆C and M₂₃C₆, although these could have come from inadvertently including some of the unaltered matrix in the layer. The absence of carbides in the outer layers would be expected from the exposure conditions being favorable for decarburization.

GENERAL PRINCIPLES FOR CREEP-DAMAGE OF GAMMA PRIME-STRENGTHENED ALLOYS

The results of this investigation permit definition of several general principles regarding damage from elevated temperature creep-exposure to mechanical properties of nickel-base Ti+Al alloys strengthened by precipitation of gamma prime phase. These can be grouped into two broad categories.

The first group includes principles for effects which can be considered reversible, that is, recoverable by heat treatment:

1. The measured volume fraction of gamma prime in the matrix decreases with exposure temperature and time. Yield and tensile strengths will decrease mainly as a result of the decrease in volume fraction of gamma

prime and only secondarily as a function of the accompanying increase in particle size. When the measured volume fraction reaches a constant value, the yield strength remains constant even though the particle size continues to increase.

For Rene' 41, the measured volume fraction of gamma prime decreased during exposure above 1400°F. It tended to reach constant values in 100 to 300 hours at 1600° to 1800°F.

2. The thermally-induced formation of massive carbides at the grain boundaries reduces ductility. These apparently can be both $M_{23}C_6$ and M_6C with the total amount being the controlling factor.

For Rene' 41, ductility began to be reduced after creep-exposure for 10 hours at 1600°F and continued to decrease with higher exposure temperature and longer times.

3. Creep, in itself, had very little effect on mechanical properties at room temperature in comparison to the thermally-induced effects. Its main effect was for exposures below 1600°F and was to increase tensile yield strength and decrease compressive yield strength through residual stresses of the Bauschinger-type and to increase ultimate strength and decrease ductility through strain hardening.
4. The changes in mechanical properties from thermally-induced structural changes could be restored by heat treatment. Restoring the gamma prime dispersion by re-heat treatment restored yield strength but not ductility. Restoration of ductility requires the re-resolution of carbides as well.

The restoration of gamma prime dispersion nearly restores creep-rupture strength. Re-resolution of carbides as well as gamma prime is required for complete restoration. Recovery effects during re-heat treatment remove the Bauschinger effect and relieve strain hardening.

The second group includes principles for those effects which cannot be recovered by heat treatment and are in this sense irreversible:

5. The lack of damage from creep itself and the ability to restore properties by heat treatment after creep is

probably unique to Rene' 41 due to its freedom from microcracking. Most other alloys of the nickel-base gamma prime-strengthened type are subject to microcracking during creep and, therefore, probably creep damage as well as thermally-induced structural damage. Microcracking would be expected to reduce all subsequent properties both due to a decrease in the load-carrying area and the possible introduction of stress-concentration effects.

The deterioration of properties by thermally-induced structural changes in Rene' 41 is a major factor in the reason for lack of creep damage. Apparently, deterioration of strength is so much greater than creep itself that very few of the expected manifestations of creep damage were observed.

6. Surface damage during creep exposure also influences properties when it is not removed by re-machining. Creep caused reduction in ductility after exposures as low as at 1200°F by inducing intergranular cracking at the surface. There was evidence that contact with alumel accelerated surface cracking. At 1400°F and above, the surface was damaged by other reactions as well as cracking. However, the damage from exposure without creep was as much as when creep occurred. Moreover, it reached its maximum effect in less than 10 hours even though the visible surface damage increased markedly with exposure time. The temperature of exposure was not a major factor since there was no further effect once the minimum attack requirement was attained.

Surface damage did not influence yield strength. When the reduction in ductility was sufficient from either surface attack or structural changes, the tensile strength was reduced unless the yield strength was very high.

With the exception of the absence of microcracking and, therefore, the absence of permanent damage, it is believed that these general principles developed from studies of Rene' 41 have wide applicability to all nickel-base Ti+Al strengthened alloys. Presumably, there will be differences in the details of the effects with composition variations. The general trends, however, should otherwise be the same. It is important, however, to recognize that the structure of the alloy and the marked influence of the instability of gamma prime are rather unique to alloys of this type. Other types of alloys might be quite different in response to creep damage.

CONCLUSIONS

Mechanical properties of Rene' 41 alloy were changed by creep exposure through these main mechanisms:

1. Yield strength was reduced by a thermally-induced decrease in the measured volume fraction and, to a lesser extent, by an increase in particle size of the strengthening precipitate gamma prime in the matrix after exposure at temperatures above 1400°F.
2. Ductility was reduced progressively by a thermally-induced increase in massive carbides in the grain boundaries with increasing temperature and time of exposure at 1400°F and higher. When the carbide build up was sufficiently severe, this also reduced ultimate tensile strength but not yield strength.
3. Tensile creep mainly increased tensile yield strength and reduced compressive yield strength by a Bauschinger effect when the exposure temperature was below about 1500°F. For such creep-exposure temperatures, recovery from the responsible residual stresses was insufficient to remove the effect. Some strain hardening also occurred at these temperatures. Creep had relatively little effect on the gamma prime effects.
4. Thermally-induced surface reactions reduced ductility over and above that due to carbides for exposure temperatures above 1400°F with apparently no added effect from creep. The maximum extent of reduction in ductility was attained in a very short time and, once attained, was independent of the exposure temperature. These reactions included loss of molybdenum, oxidation, and decarburization.
5. Creep progressively reduced ductility at 1200° to 1400°F by inducing surface cracking. There was evidence that contact with alumel accelerated the surface cracking.

The thermally-induced structural changes were not permanent. After exposure, restoration of the volume fraction and particle size of gamma prime by re-solution and re-heat treatment restored yield strength. When the temperature of re-solution was high enough to dissolve M_6C carbides,

both strength and ductility could be restored. Creep-rupture life was nearly restored by re-dissolving and re-precipitating gamma prime and was completely restored by re-solution of both gamma prime and carbides. The surface damage was not restored by re-heat treatment.

No evidence of creep-induced microcracking was found in Rene' 41 alloy. Because this is not typical of many nickel-base Ti+Al hardened alloys, the lack of damage from creep itself may not be typical. The pronounced weakening from overaging of gamma prime may also have been a factor in the lack of permanent damage.

The thermally-induced structural changes were accompanied by a volume decrease. The data suggest that this was due to removal of odd-sized atoms from solid solution by precipitation reactions.

The yield strength decreased to a minimum in 100 to 200 hours at 1400° to 1800°F which apparently coincided with attainment of near minimum measured volume fraction of gamma prime in the matrix. The particle size of undissolved gamma prime continued to increase with exposure time. The volume fraction of gamma prime was the controlling factor; an observation in accordance with published theory for dispersion strengthening.

The results are believed to be reasonably typical for nickel-base Ti+Al hardened alloys, except for the absence of microcracking. A series of general principles were formulated for damage to mechanical properties of such alloys. There are, however, many points about the results, particularly the mechanisms of the effects, where additional research would be desirable for better verification.

REFERENCES

1. Gluck, J. V. and Freeman, J. W. "Effect of Creep-Exposure on Mechanical Properties of Rene' 41", ASD TR 61-73 (1961)
2. Gluck, J. V., Voorhees, H. R., and Freeman, J. W. "Effect of Prior Creep on Mechanical Properties of Aircraft Structural Metals", WADC TR 57-150, Parts I, II, III. Part I: 2024-T86 Aluminum (1957), Part II: 17-7PH (TH 1050 Condition) (1957), Part III: C110M Titanium Alloy (1958)
3. Gluck, J. V. and Freeman, J. W. "Effect of Prior Creep on Short-Time Mechanical Properties of 17-7PH Stainless Steel (RH 950 Condition Compared to TH 1050 Condition)", WADC TR 59-339 (1959)
4. Gluck, J. V. and Freeman, J. W. "Effect of Prior Creep on the Mechanical Properties of a High-Strength Heat-Treatable Titanium Alloy, Ti-16V-2.5Al", WADC TR 59-454 (1959)
5. Gluck, J. V. and Freeman, J. W. "Further Investigations of the Effect of Prior Creep on Mechanical Properties of C110M Titanium with Emphasis on the Bauschinger Effect", WADC TR 59-681 (1960)
6. Letter from W. H. Coutts, Jet Engine Dept., General Electric Co., Dated January 7, 1960
7. Bigelow, W. C., Amy, J. A., and Brockway, L. O. "Electron Microscope Identification of the Gamma Prime Phase of Nickel-Base Alloys", Proc. ASTM, v. 56, p. 945 (1956)
8. Nelson, J. B. and Riley, D. P. Proc. Phys. Soc. v. 57, p. 160 (1945)
9. Gluck, J. V. and Freeman, J. W. "A Study of Creep of Titanium and Two of its Alloys", WADC TR 54-54, p. 83 (March 1956)
10. Fountain, R. W. and Korchynsky, M. "The Phenomenon of 'Negative Creep' in Alloys", Trans. ASM, v. 51, p. 108-122 (1959)
11. Beattie, H. J. "Aging Reactions in Rene' 41", General Electric Co. Report No. DF59SL314 (May 1959)

12. Morris, R. J. "Rene' 41...New Higher Strength Nickel Base Alloy", *Metal Progress*, v. 76, No. 6, pp. 67-70 (December 1959)
13. Rowe, J. P. "Relations Between Microstructure and Creep-Rupture Properties of Nickel-Base Alloys as Revealed by Over-Temperature Exposures", University of Michigan PH. D. Thesis, 1960
14. Bunshah, R. F. and Goetzel, C. G. "A Survey of Dispersion Strengthening of Metals and Alloys", WADC TR 59-414 (March 1960)
15. Meiklejohn, W. H. and Skoda, R. E. "Dispersion Hardening", *Acta Metallurgica*, v. 8, No. 11, p. 773 (November 1960)
16. Dew-Hughes, D. "On Meiklejohn and Skoda's letter 'Dispersion Hardening' ", Letter to the Editor, *Acta Metallurgica*, v. 8, No. 11, p. 816 (November 1960)
17. Bigelow, W. C. and Amy, J. A. "Electron Metallographic Studies of Nickel-Base Heat-Resistant Alloys", WADC TR 58-406, ASTIA Document AD 155767 (August 1958)
18. Beattie, H. J. and Hagel, W. C. "Intragranular Precipitation of Intermetallic Compounds in Complex Austenitic Alloys", *Trans. Met. Soc. AIME*, v. 221, No. 1, February 1961, p. 31
19. Barrett, C. A., Evans, E. B., and Baldwin, W. M. "Thermodynamics and Kinetics of Metals and Alloys. High Temperature Scaling of Ni-Cr, Fe-Cr, Cu-Cr, and Cu-Mn Alloys", U. S. Office of Ordnance Research Tech. Report, Dec. 1955 (declassified) Summarized in *The Nickel Bulletin*, v. 32, No. 2 (February 1959), The Mond Nickel Co., London.
20. Beattie, H. J. and VerSnyder, F. L. "The Influence of Molybdenum on the Phase Relationships of a High Temperature Alloy", *Trans. ASM*, v. 49, p. 894 (1957)
21. Radavich, J. F. and Wilson, J. E. "Phase Identification in Nickel-Base Alloys", *Metal Progress*, v. 79, No. 5, p. 94 (May 1961)
22. Ignatov, D. V. and Shamgunova, R. D. "Mechanism of the Oxidation of Nickel and Chromium Alloys", NASA Technical Translation F-59, March 1961 (published in Russian, 1960)

Table 1

Effect of Long-Time Aging on Tensile Properties of Rene' 41*

Exposure Conditions		Room Temperature Tensile Properties After Exposure					
Spec. No.	Temp (°F)	Time (hr)	Ult. Tensile Str. (psi)	.2% Offset Yield Str. (psi)	Elong. (%)	Red. of Area (%)	Modulus, E x10 ⁶ psi
As Treated			189,800	129,733	20.5	27.9	30.5
R-59	1600	200	172,100	106,000	13.5	15.0	31.3
D-3	1600	401	142,400	91,500	7.6	11.0	30.0
R-76	1700	200	128,000	96,400	3.8	6.0	32.2
D-2	1700	474	137,200**	101,800	3.3	3.3	31.8
D-5	1700	2012	141,400	94,500	6.0	8.0	38.0
R-78	1800	200	155,000	109,800	6.3	8.5	32.2
D-4	1800	1150	142,000	83,000	6.0	9.7	34.5
D-6	1800	1700	149,000	--	5.2	6.7	31.1

Notes: D = dilatometer aging

R = conventional "unstressed" exposure (54.5 psi)

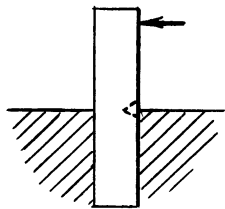
* = "R" condition: 1950°F - 1/2 hr + AC; 1400°F - 16 hr + AC

** = Broke at gage mark

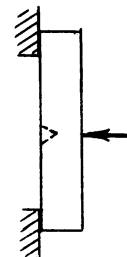
Table 2

Impact Test Data for Rene¹ 41
Tested at Room Temperature

Exposure Conditions			Impact Properties		
Temp (°F)	Time (hrs)	Stress	Type of Test *	Smooth or Notched	Impact Strength ft-lb
As Heat Treated			Izod	N	3
			Izod	N	3
					avg. 3
			Charpy	N	3.5
			Izod	S	>30 **
					>30
					avg. >30
			Charpy	S	37
					17
					34
					avg. 29
<hr/>					
1600	10	none	Charpy	S	29
			Charpy	S	27
					avg. 28
1600	401	none	Charpy	S	6
<hr/>					
1700	10	none	Charpy	S	16
			Charpy	S	27
					avg. 21.5
<hr/>					
1800	10	none	Charpy	S	18
			Charpy	S	12
					avg. 15



Izod Test - Specimen
Supported as Vertical Cantilever



Charpy Test - Specimen
Supported as Horizontal Beam

Specimen Dimensions: 2.16 x .197 x .197 inches

If Notched: 45°V notch at mid-point

0.039" deep - 0.010 root radius

** Specimen bent but did not break

Table 3

Establishment of Re-Heat Treatments for Restoration of Room Temperature Tensile Properties of Rene' 41

Spec. No.	Initial Heat Treatment	Temp* (°F)	Time (hrs)	Stress (psi)	Exposure Conditions		Creep Def. (%)	Total Def. (%)	Re-Heat Treatment	Code (if any)	Room Temperature Tensile Properties After Exposure, Re-Heat Treatment (if any), and Remachining			
					Total Load Def. (%)	Plastic Load Def. (%)					Ult. Str. (psi)	.2% Offset Yield Str. (psi)	Elongation (%)	Red. of Area (%)
--	Mill Anneal (As Received)	--	--	--	--	--	--	--	--	--	128,400	57,400	52.0	57.9
--	"R" 1950°F - 1/2 hr+AC	--	--	--	--	--	--	--	R	avg.	189,800	129,733	20.5	27.9
--	"R" 1400°F - 16 hr+AC	--	--	--	--	--	--	--	avg.	avg.	143,650	104,900	5.4	6.6
R-32	R	1800	100.0	Nil	--	--	--	None	--	--	137,500	102,600	4.2	5.9
R-104	R	1800	100.0	Nil	--	--	--	None	--	--	149,800	107,200	6.7	7.2
									avg.	avg.	143,650	104,900	5.4	6.6
Exposure Plus Re-Solution of Gamma Prime and M ₂₃ C ₆ Carbides Only:														
R-136	R	1800	100.0	Nil	--	--	--	--	1950°F - 1/2 hr+AC 1400°F - 16 hr+AC	R	160,200	121,800	6.2	6.8
Exposure Plus Complete Re-Solution and Re-Heat Treatment:														
R-105	R	1800	100.0	Nil	--	--	--	--	2150°F - 1 hr+AC 1975°F - 1 hr+WQ 1950°F - 1/2 hr+AC 1400°F - 16 hr+AC	--	179,800	121,000	17.6	18.2
R-110	R	1800	100.0	Nil	--	--	--	--	2150°F - 2 hr+AC 1975°F - 1 hr+WQ 1950°F - 1/2 hr+AC 1400°F - 16 hr+AC	--	183,000	122,000	21.1	21.4
R-111	R	1800	100.0	Nil	--	--	--	--	2150°F - 2 hr+AC 1975°F - 1 hr+WQ 1400°F - 16 hr+AC	A	179,200	119,000	23.4	25.7
R-201	R	1800	100.0	Nil	--	--	--	--	see above	A	183,200	127,200	24.0	28.2
R-135	R	1800	100.0	Nil	--	--	--	--	2150°F - 2 hr+AC 1400°F - 16 hr+AC	--	185,000	126,000	24.0	25.6
Complete Re-Solution Without Exposure:														
R-141	R	none	---	--	--	--	--	--	see above	A	174,000	111,000	30.4	36.3
Complete Re-Solution After Exposure to Creep at 1800°F:														
R-26	R	1800	100.0	7500	0.04	Nil	1.70	1.74	None	--	130,200	106,800	3.4	11.7
R-45	R	1800	100.0	7900	0.07	Nil	5.17	5.24	None	--	139,500	119,000	3.5	4.1
R-124	R	1800	100.0	7000	0.04	Nil	3.46	3.50	see above	A	173,200	115,200	22.6	31.2
R-116	R	1800	100.0	7500	0.06	Nil	28.40	28.46	see above	A	170,500	116,000	16.9	20.2
Re-Heat Treatment of Material Originally Heat Treated at 2050° and 1650°F:														
R2-8	"R2"	2050°F - 1/2 hr+AC	--	--	--	--	--	--	--	--	180,300	115,100	25.3	29.6
R2-13	R2	1650°F - 4 hr+AC	--	--	--	--	--	--	None	--	140,500	105,100	5.0	4.9
R2-14	R2	1800	100.0	Nil	--	--	--	--	2050°F - 1/2 hr+AC 1650°F - 2 hr+AC	R2	169,500	113,800	11.3	13.0
R2-15	R2	1800	100.0	Nil	--	--	--	--	2050°F - 1/2 hr+AC 1650°F - 4 hr+AC 2150°F - 2 hr+AC	--	176,200	113,400	19.9	20.8
									2150°F - 4 hr+AC	A2	177,200	115,000	19.8	21.4

* plus 4 hours pre-heat

Table 4

Effect of Re-Heat Treatment on Tensile Properties of Rene' 41 After Initial Creep-Exposure

Spec. No.	Temp (°F)	Time** (hrs)	Stress (psi)	Frac. of Rupt. Life (est.)	Exposure Conditions			Creep Def. (%)	Total Plastic Def. (%)	Total Def. (%)	Re-Heat Treatment*	Room Temperature Tensile Properties After Re-Heat Treatment and Remachining .025-inch from Dia.				
					Plastic Load Def. (%)	Plastic Load Def. (%)	Plastic Load Def. (%)					Ult. Tensile Str. (psi)	.2% Offset Yield Str. (psi)	Elongation (%)	Red. of Area (%)	Modulus, E x10 ⁶ psi
As Treated "R"	-	-	-	-	-	-	-	-	-	-	-	189,800	129,733	20.5	27.9	30.5
R-150	1400	10.0	84,700	0.91	0.38	Nil	3.14	3.52	3.52	3.52	R	182,800	116,000	23.5	31.4	30.6
R-172	1400	100.0	61,000	0.80	0.24	0.01	19.0	19.01	19.01	19.01	R	192,200	132,000	19.6	38.0	29.4
R-148	1600	10.0	39,000	0.71	0.21	0.02	6.20	6.20	6.22	6.22	R	185,500	118,800	22.4	29.6	31.8
R-185	1600	100.0	23,500	0.74	0.12	Nil	7.38	7.38	7.50	7.50	R	182,200	137,200	12.0	13.6	31.4
R-171	1600	100.0	23,500	0.74	0.10	Nil	25.50	25.50	25.60	25.60	R	183,000	132,000	10.3	12.5	30.1
R-151	1700	10.0	23,000	0.60	0.12	0.01	3.56	3.57	3.68	3.68	R	190,000	142,500	15.6	17.0	33.8
R-155	1800	9.2	12,600	0.65	0.07	Nil	5.34	5.34	5.41	5.41	R	187,000	138,800	13.5	15.2	29.1
R-197	1800	85.5	7,900	0.74	0.04	Nil	8.06	8.06	8.10	8.10	R	161,400	140,800	3.1	5.2	30.9
R-141 As Treated "R"	-	-	-	-	-	-	-	-	-	-	A	174,000	111,000	30.4	36.3	31.4
R-116	1800	100.0	7,500	0.77	0.06	Nil	28.40	28.40	28.46	28.46	A	170,500	116,000	16.9	20.2	29.8
R-124	1800	100.0	7,000	0.59	0.04	Nil	3.46	3.46	3.50	3.50	A	173,200	115,200	22.6	31.2	32.2
As Treated "R2"	-	-	-	-	-	-	-	-	-	-	--	180,300	115,100	25.3	29.6	31.2
R2-16	1800	100.0	7,500	0.77	0.03	Nil	1.54	1.54	1.57	1.57	A2	168,200	111,800	15.4	16.5	31.6

*R : 1950° - 1/2 hr + AC; 1400° - 16 hr + AC
R2: 2050° - 1/2 hr + AC; 1650° - 4 hr + AC
A : 2150° - 2 hr + AC; 1975° - 1 hr + WQ; 1400° - 16 hr + AC
A2: 2150° - 2 hr + AC; 1650° - 4 hr + AC

** Plus 4 hours pre-heat prior to load application

Table 5

Effect of Re-Heat Treatment on Creep-Rupture Properties of Rene' 41 After Initial Creep Exposure

Spec. No.	Temp (°F)	Stress (psi)	Time**		Creep Def. (%)	Red. of (Uninterrupted Est. Rupt. Area)(%)		Expected Life Remaining		Second Exposure Rupt. Time**Elong. Red. of (hrs) Area(%)		Total Life (hrs) Area(%)		Fraction Recovered of Expended Life	Total Elong.	Total Elong. Est. Rupt. Elong.	Fraction Recovered of Expended Ductility
			(hrs)	Normal Life (hrs)		(%)	(%)	(hrs)	(%)	(hrs)	(%)	(hrs)	(%)				
Original Condition: "R": Re-heat Treatment "R"																	
R-153	1400	84,700	10,0	11,5	0,91	4,29	5,7	1,5	25	6,9	3,7	7,6	17,6	0,54	8,0	0,32	-3,97
R-179	1400	61,000	100,0	125,0	0,80	14,5	16,4	25,0	25	85,9	18,3	34,3	185,9	0,61	32,8	1,31	0,54
R-149	1600	39,000	10,0	14,0	0,71	7,3	7,8	4,0	25	14,0	22,9	41,5	24,0	1,00	20,2	1,21	-1,67
R-183	1600	39,000	10,0	14,0	0,71	2,35	3,4	4,0	25	b) 11,1	13,5	22,4	21,1	0,71	15,9	0,64	-3,90
R-187	1600	39,000	10,0	14,0	0,71	2,73	3,0	4,0	25	c) 8,4	22,5	43,4	18,4	0,4	25,2	1,0	0,7
R-178	1600	23,500	100,0	135,0	0,74	10,76	11,2	35,0	26	85,7	26,4	41,5	185,7	0,51	37,1	1,43	1,04
R-154	1700	23,000	9,0	15,0	0,60	6,28	8,8	6,0	27	10,9	28,4	52,3	19,9	0,55	34,7	1,29	1,23
R-157	1800	12,600	6,8	10,4	0,65	5,34	6,2	3,6	34	8,6	33,8	51,8	15,4	0,73	39,1	1,15	0,96
R-181	1800	7,300	100,0	145,0	0,69	8,36	9,0	45,0	41	94,0	33,0	46,0	194,0	0,49	41,4	1,01	0,5
Original Condition: "R": Re-heat Treatment "A"																	
R-126	1800	12,500	10,0	12,0	0,93	7,77	8,8	2,0	34	23,4	20,0	42,0	33,4	2,14	27,8	0,82	-0,80
R-132	1800	9,500	33,0	45,0	0,73	9,10	11,0	12,0	43	93,9	18,6	46,6	126,9	2,48	27,7	0,54	-1,68
R-133	1800	7,300	100,5	145,0	0,69	6,93	7,3	45,0	43	414,5	10,6	33,1	515,0	3,70	17,5	0,41	-3,68
R-166	1800	12,500	No first	-	-	-	-	-	-	21,4	32,0	49,0	-	-	-	-	-
R-167	1800	9,500	Exposure	-	-	-	-	-	-	67,5	34,2	53,6	-	-	-	-	-
R-173	1800	9,500	Exposure	-	-	-	-	-	-	144,1	21,0	36,0	-	-	-	-	-
R-168	1800	7,300	Exposure	-	-	-	-	-	-	357,8	20,6	32,8	-	-	-	-	-
Original Condition: "R": Re-heat Treatment "R3"																	
R-170	1600	23,500	100,0	135,0	0,74	3,78	3,9	35,0	26	122,0	19,8	35,2	222,0	0,87	23,6	0,95	-0,62
Original Condition: A# Rec. (Mill Anneal) Heat Treatment "A"																	
R-174	1800	9,500	No first exposure	-	-	-	-	-	-	-	-	-	-	-	-	-	-

Heat Treatments
 "R": 1400 - 16 hr + AC
 "A": 2150 - 2 hr + AC
 "R3": 1950 - 1/2 hr + AC
 1975 - 1 hr + WC
 1400 - 16 hr + AC

a) premature failure?

b) Re-heat treated - NOT re-machined
 c) Remachined ONLY

** Plus 4 hours pre-heat prior to load application

Table 6

Structural Parameters and Yield Strengths of Rene' 41 after Unstressed Exposure

Spec. No.	Exposure Temp (°F)	Exposure Time (hrs)	Volume Fraction of γ' (f)	Average Inter-Particle		Average Particle Size, \bar{h} Å	Meiklejohn-Skoda Parameter $\frac{f\bar{h}}{0.82 - f\bar{h}}$	0.2% Offset Yield Str., psi
				Spacing, λ Å	Spacing, λ Å			
As Treated	-	-	.37	546	1000	7.03	130,000	
R-52	1600	14	.27	512	870	3.72	129,000	
R-31	1600	104	.23	835	1245	2.68	109,000	
R-59	1600	204	.22	1110	1610	2.66	106,000	
D-3	1600	401	.18	2250	2780	2.22	91,500	
R-42	1700	14	.25	1010	1600	3.31	108,200	
R-73	1700	104	.21	1945	2660	2.64	94,500	
R-76	1700	204	.18	2520	3110	2.22	96,400	
D-2	1700	474	.21	2540	3480	2.64	101,800	
D-5	1700	2012	.19	3155	3990	2.35	94,500	
R-61	1800	14	.24	1635	2520	3.12	102,500	
R-32*	1800	104	.19	1025	1300	2.35	102,600	
D-4	1800	1150	.12	5120	4650	1.52	83,000	
R-2	As HT		.26	755	1240	3.50	115,100	
R2-7	1600	104	.21	1035	1440	2.64	108,000	
R2-12	1800	14	.14	1945	1945	1.73	98,300	

* fine γ' reprecipitated on cooling

Table 7

Comparison Matrix Lattice Parameters and Dilatometer Shrinkage
for Rene' 41 Aged Without Stress

<u>Spec. No. *</u>	<u>Aging Treatment</u>	<u>Lattice Parameter</u>	<u>Calculated Shrinkage</u>	<u>Dilatometer Shrinkage</u>
As Heat Treated	-	3.6050	-	-
D-3	1600°F - 401 hr.	3.5996	0.15%	0.18%
D-2	1700°F - 474 hr.	3.5948	0.29%	0.21%
D-5	1700°F - 2012 hr.	3.5940	0.31%	0.36%
D-4	1800°F - 1150 hr.	3.5926	0.34%	0.40%

* All Specimens Originally in
Condition "R": 1950°F - 1/2 hr + AC
1400°F - 16 hr + AC

Comparative Results from Data of Beattie (Ref. 11)	2150°F - 2 hr + WQ	3.607	-	-
	above plus 1600°F - 1000 hr.	3.592	0.42%	-

Table 8

X-Ray Diffraction Data from Extraction Residues of Rene' 41 Specimens Used for Development of Re-Heat Treatments

Spec. No.	R-104		R-105		R-111		Standard Patterns for Indicated Phases		
	Exp. Temp.	1800° - 100 hr	1800° - 100 hr	1800° - 100 hr	1800° - 100 hr	1800° - 100 hr	TiC	M ₆ C	M ₂₃ C ₆
Re-Heat Treatment	None	2150° - 1 hr+AC 1975° - 1 hr+WQ 1950° - 1/2 hr+AC 1400° - 16 hr+AC	2150° - 1 hr+AC 1975° - 1 hr+WQ 1950° - 1/2 hr+AC 1400° - 16 hr+AC	2150° - 2 hr+AC 1975° - 1 hr+WQ	1800° - 2 hr+AC 1975° - 1 hr+WQ	1800° - 2 hr+AC 1975° - 1 hr+WQ	a = 4.32	a = 11.10	a = 10.71
Tensile Test Elong.	6.7	17.6	17.6	1400° - 16 hr+AC	23.4	23.4			
Red. of Area	7.2	18.2	18.2	25.7	25.7	25.7			
"d" Range	"d"	I	"d"	I	"d"	I	"d"	I	"d"
	2.89	5	2.86	20	2.88		2.77	m	2.68
	2.76	5	2.77	5	2.67		2.54	ms	w
	2.60-2.69						2.49	s	2.46
	2.50-2.59						2.48		vw
	2.39-2.49	80	2.49	100	2.49	100			
	2.40	40	2.41	5					
	2.30-2.39		2.36	5	2.38	10			
	2.20-2.29	30	2.25	10	2.25	10	2.263	s	2.399
	2.10-2.19	40	2.19	40					
		60	2.15	100	2.15	90	2.16	s	2.185
		100	2.13	10	2.13	10			
	2.00-2.09	100	2.067	10	2.06	80			
		20	2.03	5	2.00	40			
	1.89-1.99	20	1.96	5	1.96		1.959	m	1.892
	1.80-1.88	30	1.88	30			1.875	w	m
		30	1.84	5			1.850	w	
	1.69-1.79	10	1.79	10	1.82	30			1.810
		5	1.71	5			1.753	vw	1.785
		10		10	1.74	20	1.69	w	1.692
	1.60-1.68		1.66	10			1.67	w	1.632
		10							1.615
	1.50-1.59	5	1.55	5			1.552	mw	1.545
		50	1.52	80	1.52	60	1.528	m	1.500
	1.40-1.49		1.43	5			1.481		1.431
			1.40	5			1.443	mw	
	1.30-1.39		1.35	5			1.385		1.395
			1.303	70	1.30	50	1.302	mw	1.340
			1.15	40	1.27	20			w
					1.03	30			
		TiC M ₆ C M ₂₃ C ₆		TiC medium M ₆ C medium M ₂₃ C ₆		TiC slight M ₆ C slight-medium M ₂₃ C ₆			

"d" - interplanar spacing

I - relative intensity (to strongest line)

Table 11

Cracking Depth Data for Creep-Exposures of Rene' 41 at 1200° and 1300°F

Spec. No.	Temp (°F)	Exposure Conditions			Room Temp. Elongation (%)	Tensile Ductility Red. of Area (%)	Attack Depth		Deep Crack Depth (in.)	% of Fracture Surface Oxidized	Remarks -- normal thermocouple procedure except as noted -- .300-inch dia. gage section except as noted 0.250-inch dia. gage section
		Time (hrs)	Stress (psi)	Total Plastic Def. (%)			Edge Crack Depth (in.)	Edge Crack Depth (in.)			
R-101	1200	10.0	129,000	1.43	14.0	17.6	Nil	nd	-		
R-112	1200	10.0	132,000	1.79	13.1	18.6	.0005-.0017	nd	-		
R-142	1200	10.0	134,000	2.26	14.2	17.6	.0005-.0013	nd	-		
R-108	1200	10.0	130,000	3.67	11.0	13.2	.0014-.0054	nd	-		
R-128	1200	10.4	133,000	4.02	2.1	6.0	.0004-.0010	.023	-		
R-146	1200	10.0	136,000	4.70	1.3	2.0	-	.036	-		
R-66	1200	10.0	133,000	3.49	4.7	5.3	-	.022	-		
R-115	1300	10.0	108,000	.44	17.3	19.2	.0010	nd	-		
R-99	1300	10.0	106,000	.63	17.6	17.2	-	nd	-		
R-119	1300	10.0	108,000	.68	11.9	13.7	.0005	nd	-		
R-102	1300	4.5	108,000+	1.90	15.5	14.5	.0014-.0020	nd	-		
R-95	1300	10.0	108,000	2.71	10.2	12.9	.0007-.0021-(.014)	nd	-	No TC on gage section	
R-130	1300	10.0	112,500	3.74	8.0	11.3	.0005-.0038-(.035)	nd	-	3 TC, all tied on with alumel	
R-193	1300	7.7	113,000	4.04	2.0	4.1	-	.020	-	3 TC, all tied on with chromel	
R-189	1300	9.4	113,000	4.07	6.5	6.7	-	.015	-		
R-127	1300	10.0	112,000	4.30	0.9	4.1	-	.030	-		
R-63	1300	10.0	108,397	4.60	0.4	0.7	-	.081	-	.350-inch dia. gage section	
R-196	1300	8.4	113,500	4.64	6.4	6.8	-	.006	-	3 TC, all tied on with chromel	
R-140	1300	10.0	113,500	4.85	2.1	3.0	-	.045	-		
R-120	1300	100.0	86,000	5.19	1.2	2.9	.0007-.0042	.035	-	.350-inch dia. gage section	
R-147	1300	97.3	88,000	5.21	1.5	5.5	-	.026	-		
R-145	1300	10.0	114,000	5.34	5.9	8.7	.0013-.0036	nd	-	No TC on gage section	
R-152	1300	9.2	114,000	5.59	2.9	4.1	-	.021	-	No TC on gage section; alumel looped around spec. Spec. completely wrapped; half with alumel, half with chromel, but 0.0455- inches remachined before tensile test	
R-156	1300	8.7	114,000	5.88	6.2	22.6	-	nd	-		

nd = not detected
- = not measured

Table 12

General Surface Attack Data for Exposed Specimens of Rene' 41

<u>Spec. No.</u>	<u>Temp (°F)</u>	<u>Time (hrs)</u>	<u>Stress (psi)</u>	<u>Total Plastic Def. (%)</u>	<u>Attack Depth (in.)</u>
R-15	1300	36.2	100,000	2.6 (R)	.00006-.00013
R-147	1300	101.3	88,000	5.21	.000075-.00018
R-113	1400	8.0	85,500	6.47	.00006
R-109	1400	14.0	84,000	1.36	.00006
R-8	1400	14.2	80,000	~ 2.0	.00006-.00010
R-11	1400	14.0	None	Nil	.00006-.00013
R-6	1400	21.3	80,000	25.5 (R)	.00013-.00020
R-93	1400	104.0	None	Nil	.00020-.00033
R-13	1500	14.0	55,000	1.24	.00017-.00039
R-10	1600	14.0	None	Nil	.00020-.00033
R-92	1600	104.0	None	Nil	.00096-.0011
D-3	1600	401.0	None	Nil	.0017-.0019
R-57	1700	99.7	13,000	27.1 (R)	.0019-.0021
D-2	1700	474.0	None	Nil	.0034-.0040
D-5	1700	2012.0	None	Nil	.0052-.0062
R-56	1800	10.9	13,500	32.8 (R)	.0007-.0012
R-12	1800	14.0	None	Nil	.0010-.0014
R-64	1800	13.6	13,000	35.4 (R)	.0010-.0013
R-91	1800	104.0	None	Nil	.0025-.0027
D-4	1800	1150.0	None	Nil	.0072-.0078

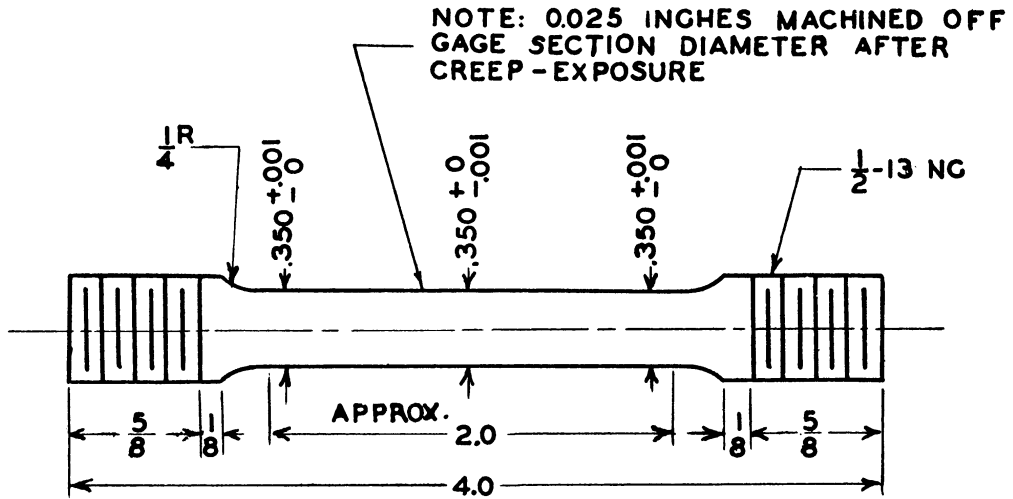
(R) Rupture ductility

Table 13

X-Ray Diffraction Data from Extraction Residues of Dilatometer Aging Specimens

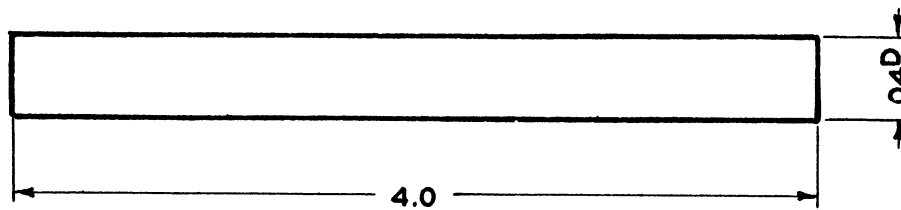
Location: Surface Depth Examined: .0012 (in.)	Surface Layers of Specimen D-2 Exposed 474 Hours at 1700°F						Interior of Dilatometer Specimens							
	Layer 1 .0010 (A) "d" I	Layer 2 .0011 (A) "d" I	Layer 3 .0014 (A) "d" I	Cr ₂ O ₃ "d" I	Y-Al ₂ O ₃ "d" I	TiN "d" I	TiC "d" I	NiCr ₂ O ₄ "d" I	M ₆ C "d" I	M ₂₃ C ₆ "d" I	Specimen No. and Exposure Condition		D-1 1800°-1150 hrs	
(A) "d" I	(A) "d" I	(A) "d" I	(A) "d" I	(A) "d" I	(A) "d" I	(A) "d" I	(A) "d" I	(A) "d" I	(A) "d" I	(A) "d" I	(B) "d" I	(B) "d" I	(B) "d" I	(B) "d" I
3,610 20	3,628 20	3,616 30	3,610 10	3,653 74	3,479 74	2,479 74	2,49 *	2,93 30	3,20	3,105	3,12 5	3,05 5	2,796 10	2,772 10
3,268 10	3,575 20	3,237 5 2,926 5	2,660 30	2,67 100	2,552 92	2,54 ms 2,48	2,45 *	2,77 m	2,68 w	2,546 10 2,49 10	2,534 10	2,535 5	2,394 15	2,252 20
2,913 10	2,666 20	2,649 40	2,486 40	2,48 96	2,379 42	2,263 *	2,16 *	2,50 100	2,185 *	2,264 40 2,235 5	2,252 20	2,196 60	2,190 20	
2,650 80	2,554 20	2,554 20	2,19 50	2,26 12	2,165 <1	2,135 vs		2,17 38	2,135 vs	2,130 40	2,126 100	2,105 5	2,105 5	
2,467 80	2,450 90 2,382 10	2,448 90	2,126 80	2,17 38	2,085 100	2,12 5		2,126 80		2,068 100	2,065 80	2,069 100	2,069 100	
2,166 20	2,173 5	2,166 10	2,064 100	2,05 9	2,085 100			2,07 35	2,062 *	1,953 10 1,892 40	1,955 30 1,894 20	1,961 20 1,901 20	1,961 20 1,841 10	
1,810 40	1,817 10	1,811 20	1,860 10 1,894 20 1,803 5	1,82 39	1,740 43				1,959 m 1,875 w 1,810 w 1,753 vw	1,892 m 1,785 mw	1,894 20 1,841 10	1,846 5 1,819 20	1,810 20 1,788 10	
1,666 100	1,738 10	1,665 70	1,685 5 1,670 30	1,67 90	1,601 81 1,546 3 1,510 7			1,70 15	1,69 w 1,67 w	1,692 vw 1,632 vw 1,615 mw	1,694 10 1,665 10 1,634 5	1,714 10 1,667 5 1,642 5	1,714 10 1,694 10 1,618 15	1,665 10 1,618 15
1,463 30	1,600 20	1,602 10	1,616 10	1,58 13	1,404 32 1,374 48			60	1,60	1,545 1,552 mw 1,500 vw	1,548 10 1,525 10	1,528 20 1,486 vw	1,528 20 1,446 10	1,496 5
1,430 40	1,497 80	1,497 60 1,478 20	1,500 20	1,46 12 1,43 40	1,374 48	1,50 M		80	1,47	1,443 1,385	1,447 10 1,374 10	1,447 10 1,344 10	1,442 10 1,352 10	1,342 5
	1,401 10 1,375 10	1,430 30	1,465 10 1,434 10	1,30 20	1,31 10			10	1,31	1,345 10	1,345 10	1,345 10	1,345 10	
Cr ₂ O ₃	Cr ₂ O ₃ TiN	Cr ₂ O ₃ ? TiN	TiC? TiN Cr ₂ O ₃ ? M ₆ C? M ₂₃ C ₆ ?			1,28 M				M ₆ C M ₂₃ C ₆ TiC		M ₆ C M ₂₃ C ₆ slight TiC	M ₆ C M ₂₃ C ₆	

"d" interplanar spacing
I - relative intensity
(A) - 57.3 mm camera
(B) - 114.6 mm camera

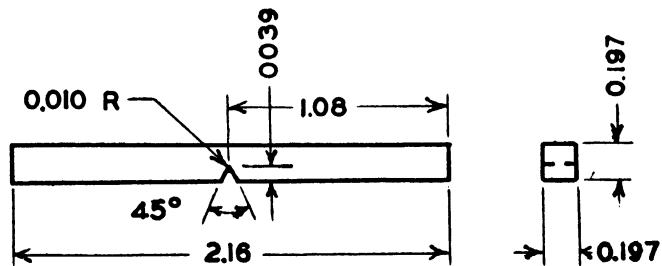


TENSILE AND CREEP SPECIMEN

GRIND BOTH ENDS
 FLAT AND PARALLEL



DILATOMETER SPECIMEN



TYPE -W IMPACT SPECIMEN

Note: Center of the Compression and Impact Specimen to Coincide with the Center of the Creep Specimen.

Figure 1 Details of Test Specimens

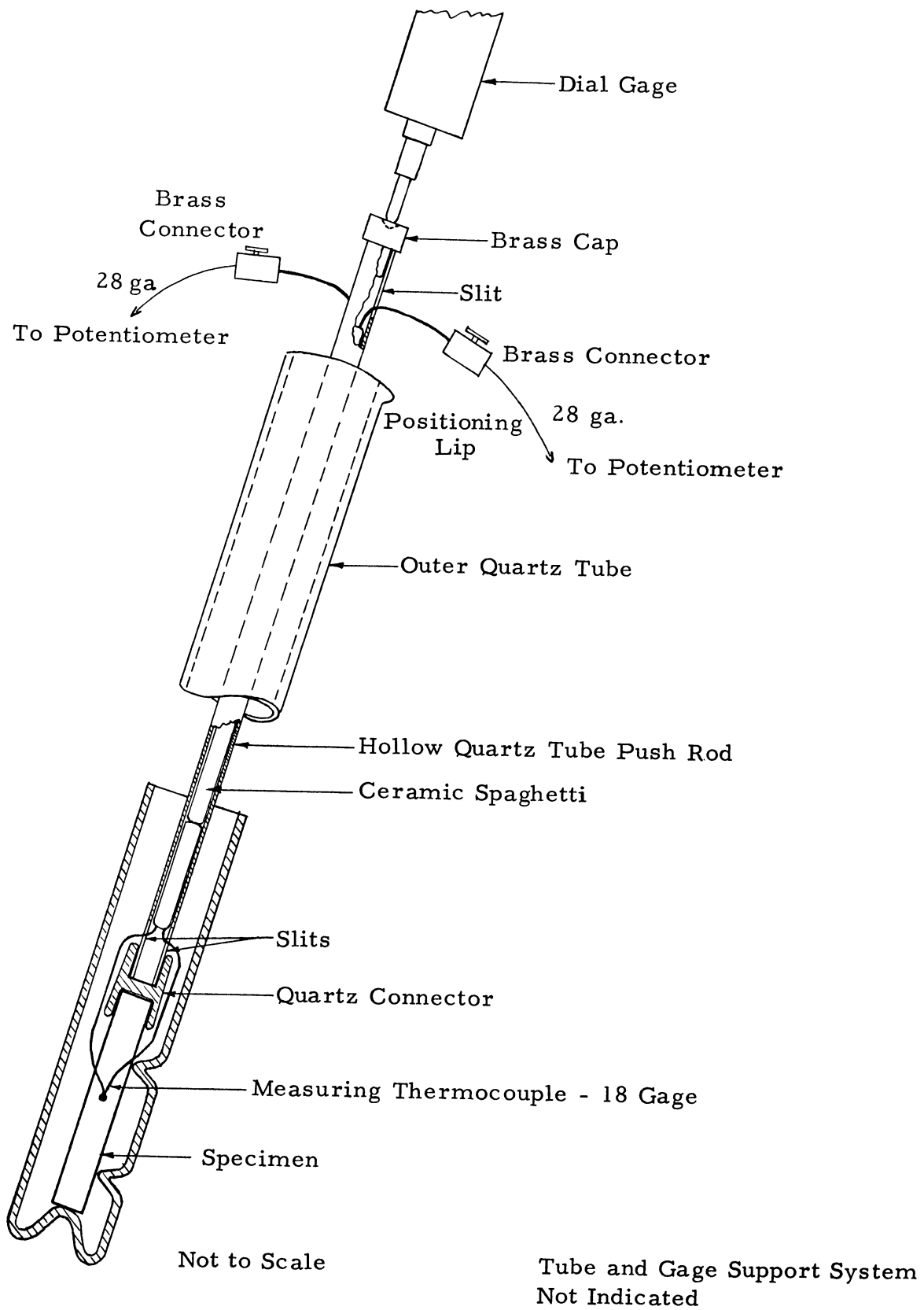


Figure 2 Method of Attaching Thermocouple For Long-Time Dilatometric Aging Studies

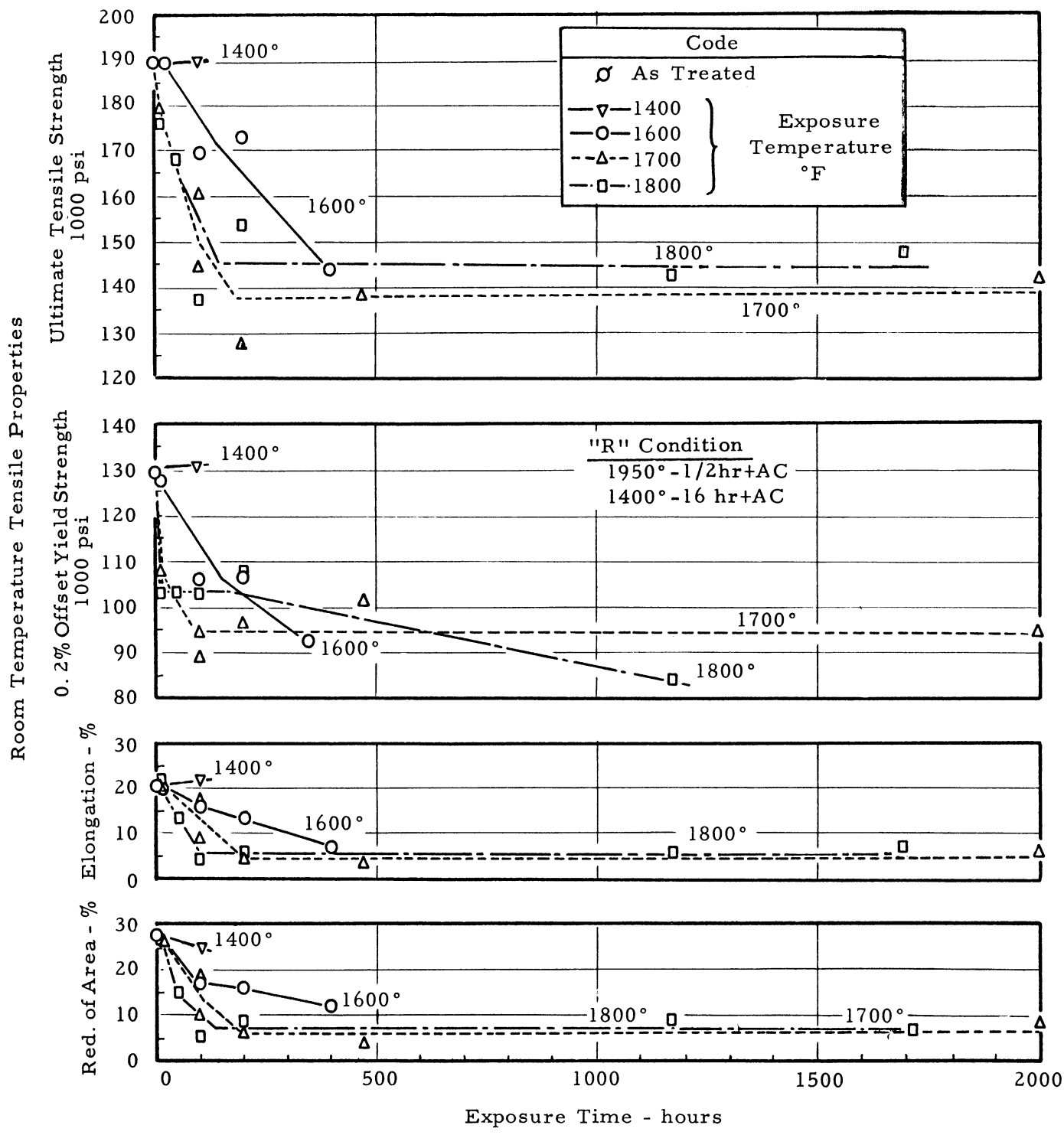


Figure 3 Effect of Exposure Time in Unstressed Exposures on Room Temperature Tensile Properties of Rene' 41 Alloy. ("R" Condition)

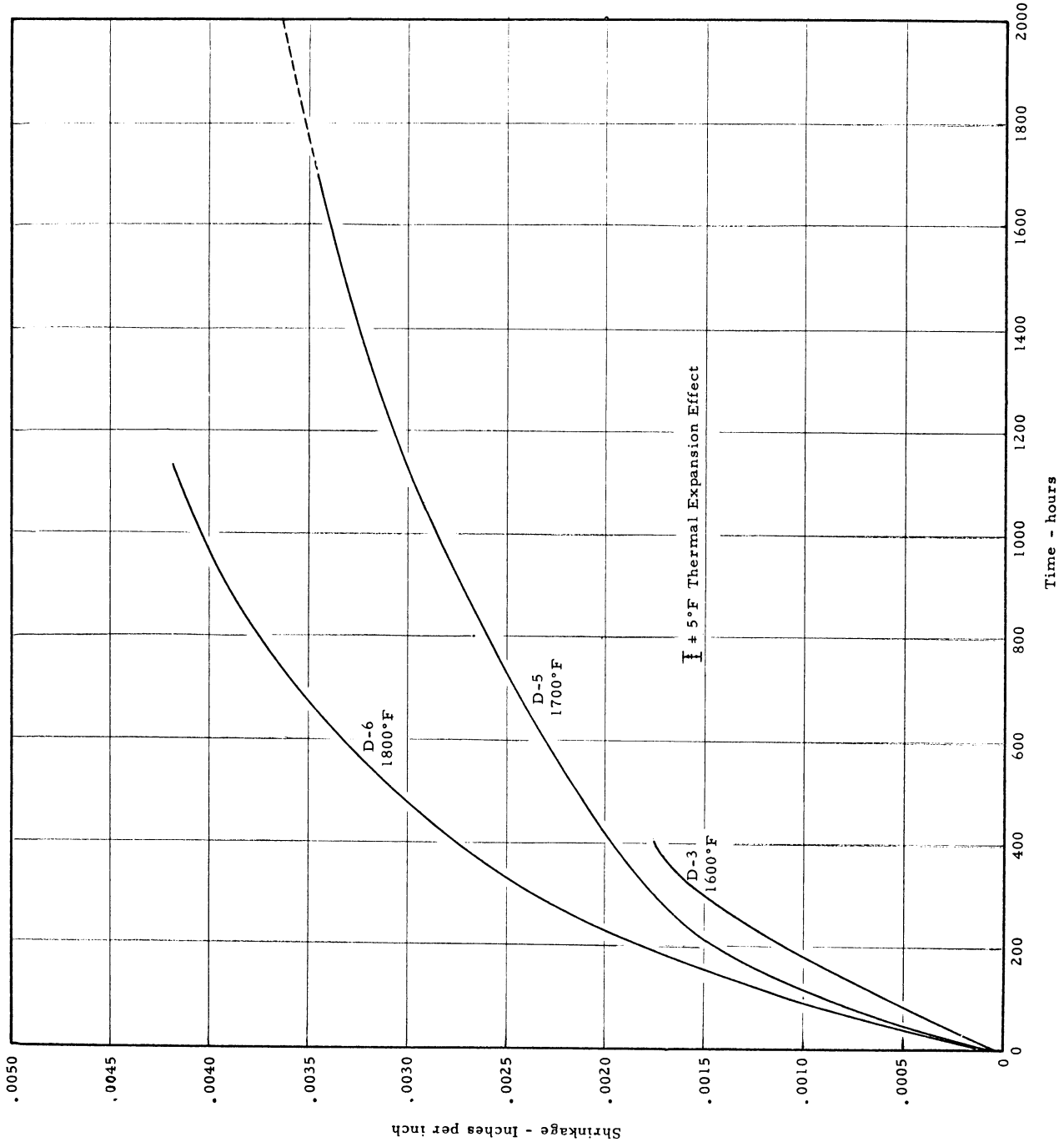


Figure 4 Shrinkage versus Aging Time for Dilatometer Exposures of Rene' 41

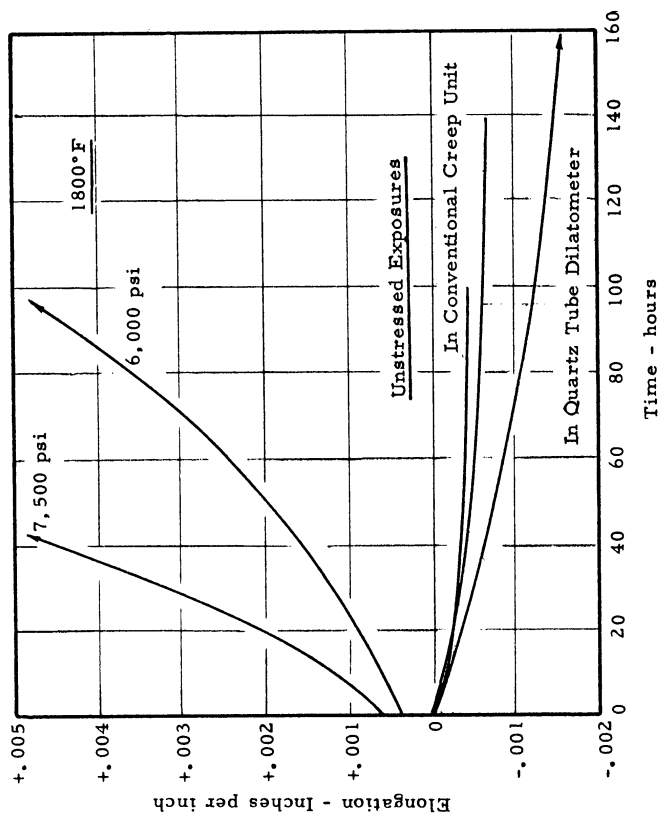
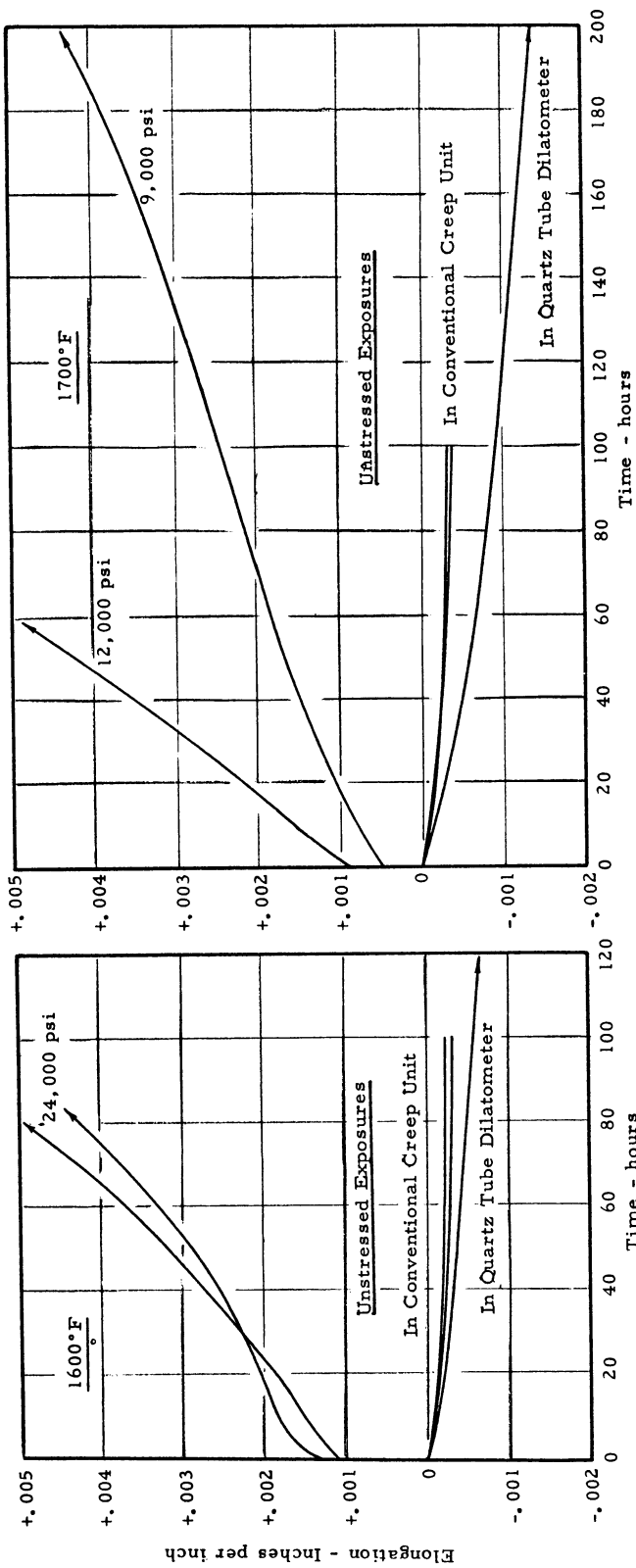


Figure 5 Comparison of Shrinkage Observed in Dilatometer Aging With Data Taken in Creep Units

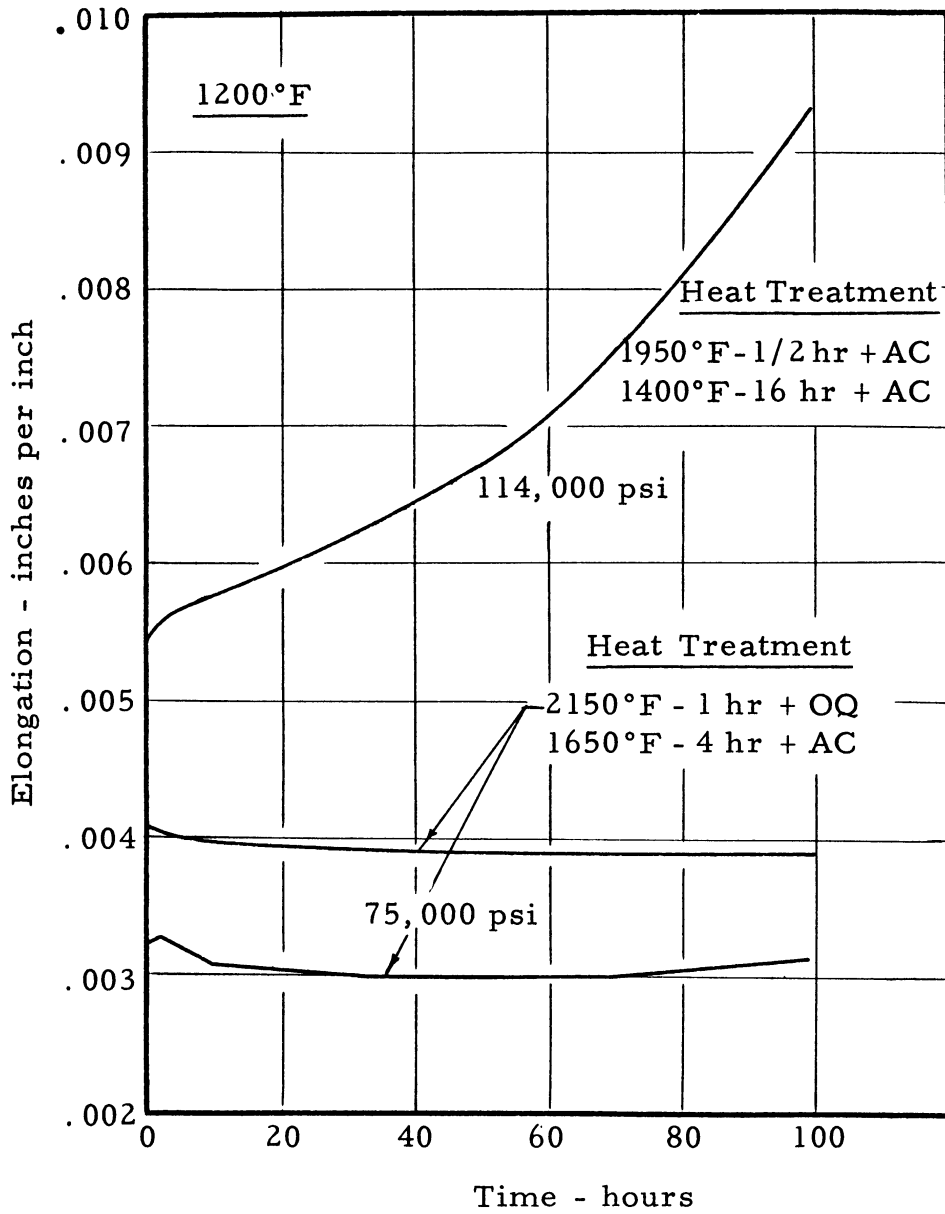


Figure 6 Negative Creep Observed in Rene' 41 at 1200°F During Initial Survey Tests (Ref. 1)

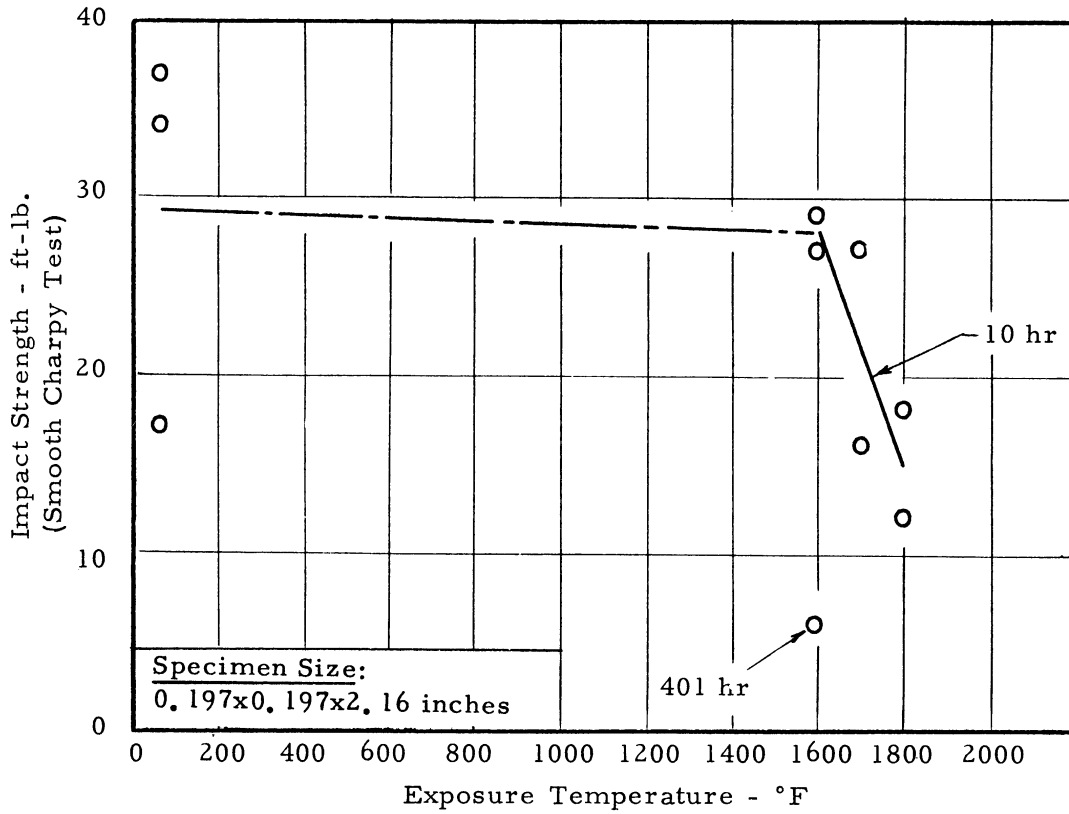


Figure 7 Effect of 10 Hours Unstressed Exposure on Smooth Bar Charpy Impact Strength of Rene' 41

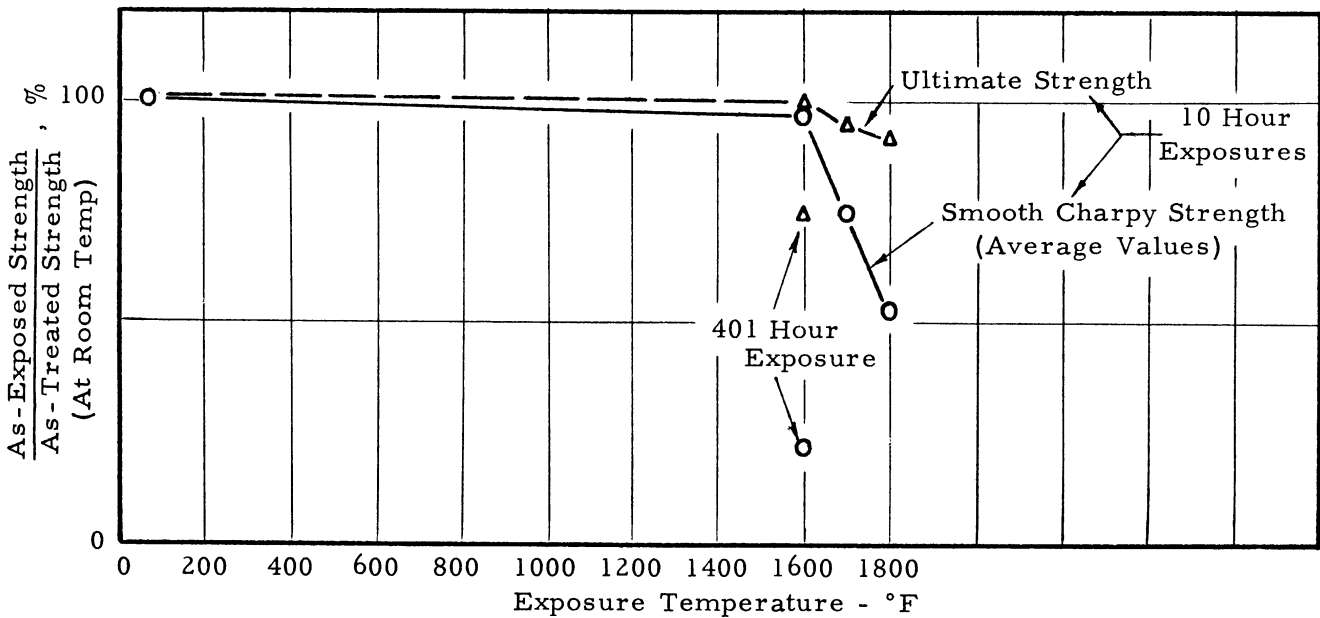


Figure 8 Relative Efficiencies of Tensile and Smooth Bar Impact Strengths in Showing Damage to Rene' 41.

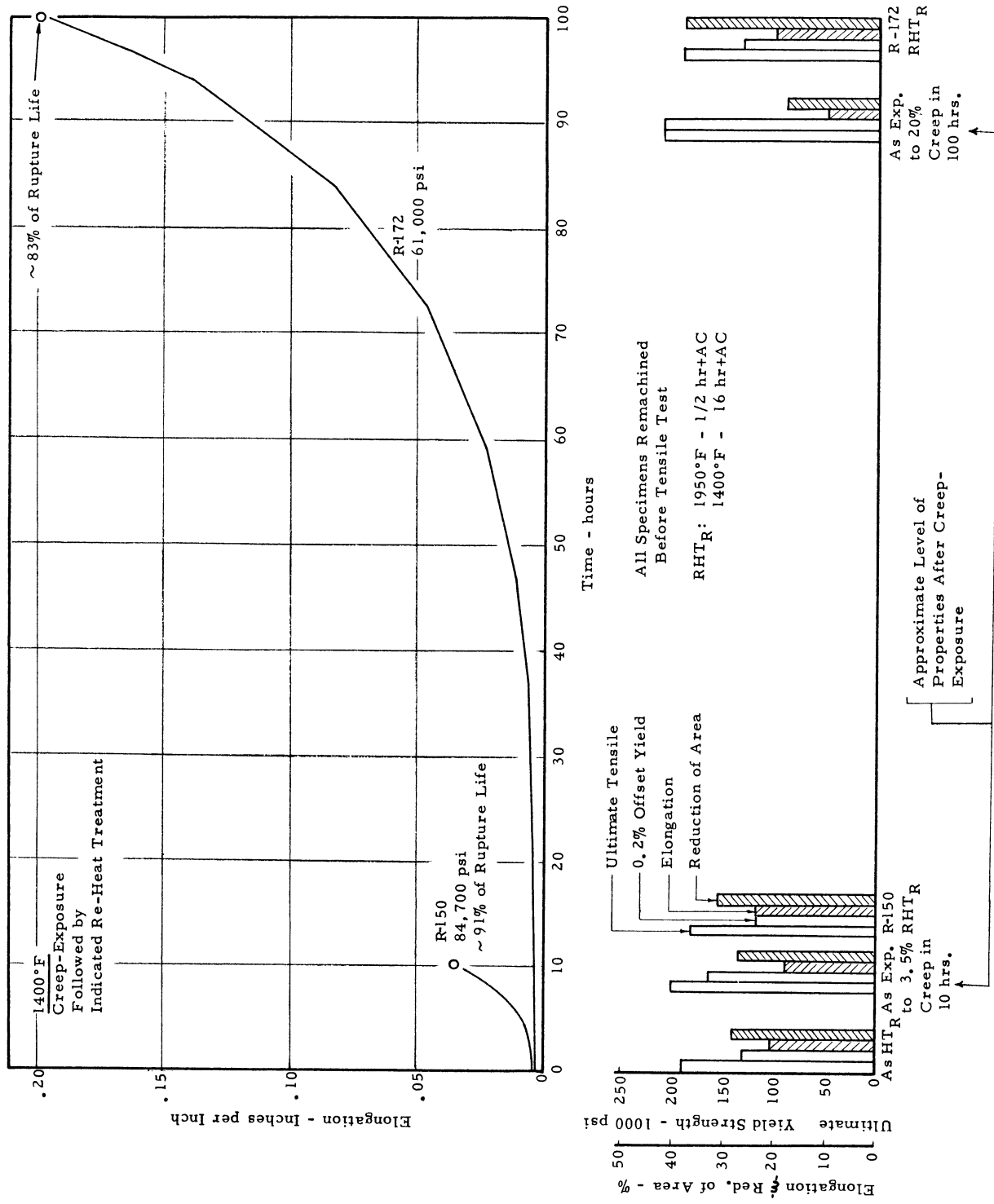


Figure 9 Effect of Re-Heat Treatment on Tensile Properties of Rene' 41 After Creep-Exposure at 1400°F

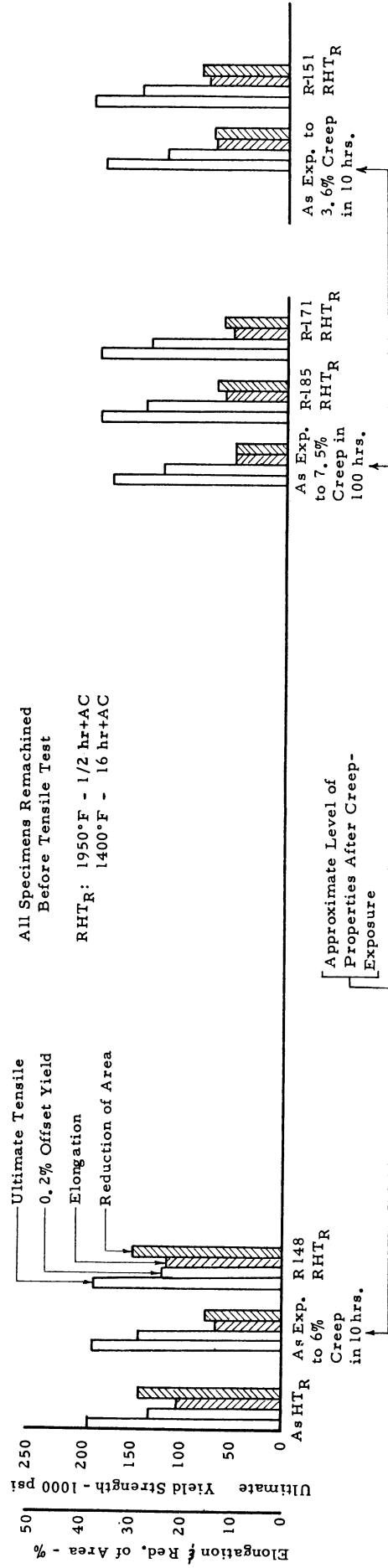
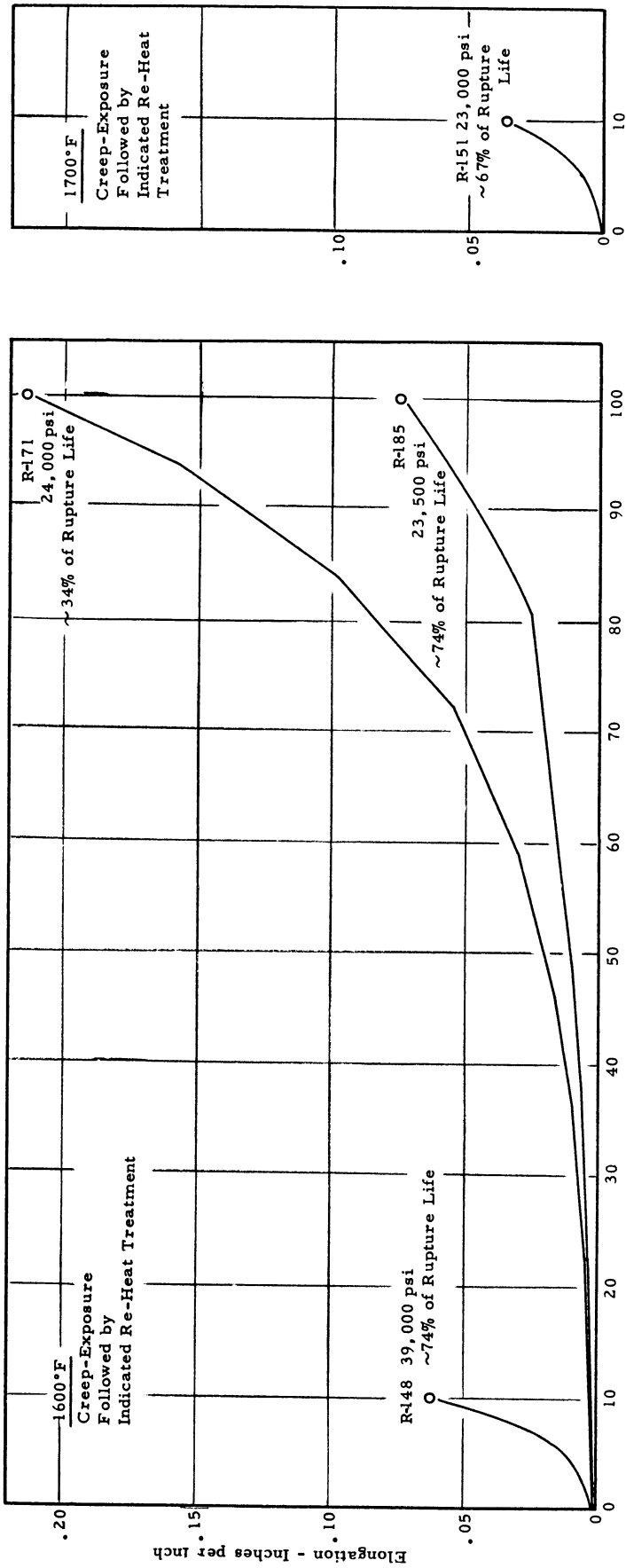


Figure 10 Effect of Re-Heat Treatment on Tensile Properties of Rene' 41 After Creep-Exposure at 1600° or 1700°F

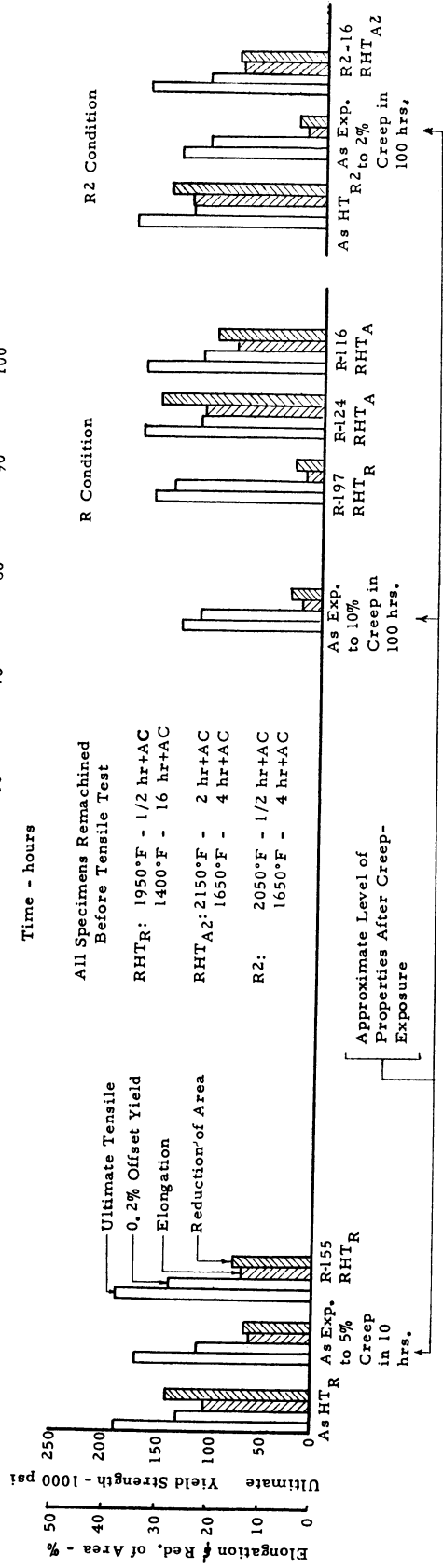
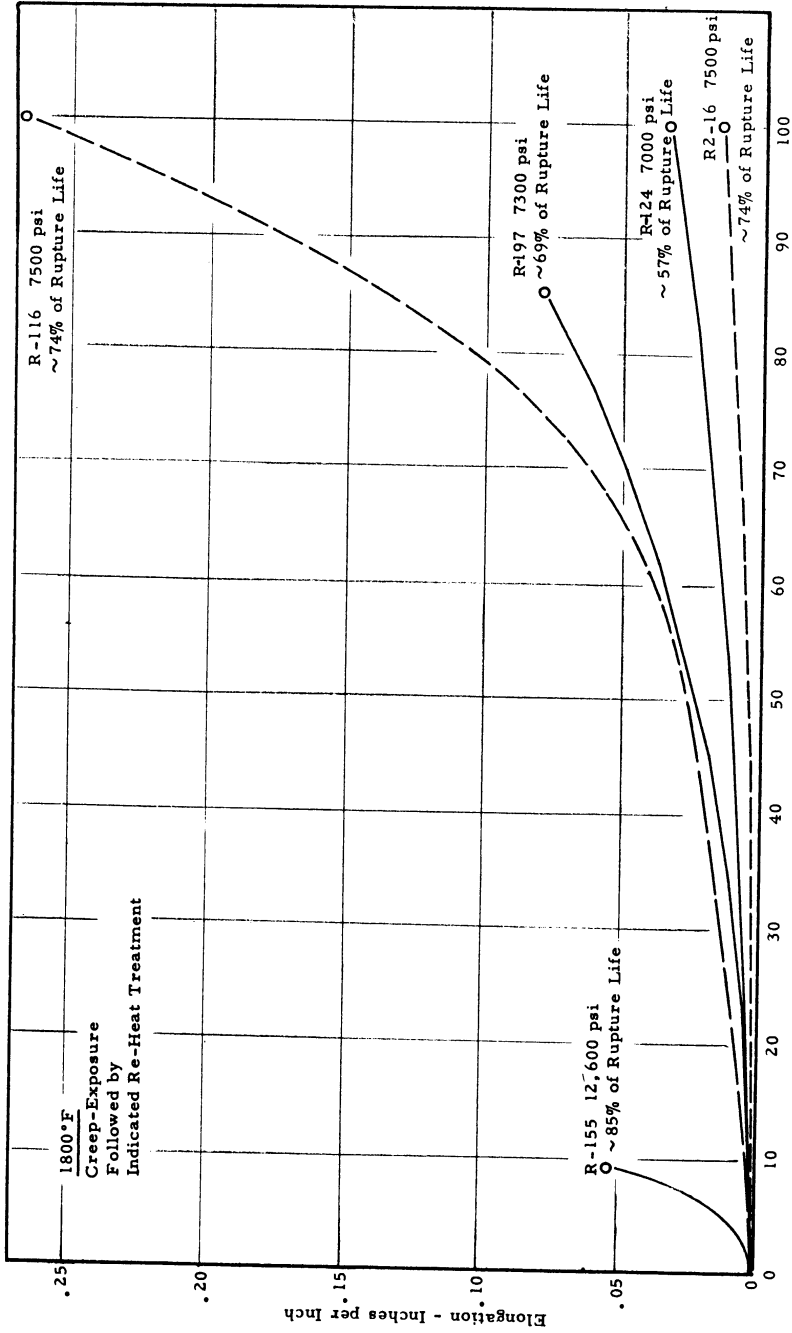


Figure 11 Effect of Re-Heat Treatment on Tensile Properties of Rene' 41 After Creep-Exposure at 1800°F

Ratio of Room Temp. Properties After Creep-Exposure or Creep-Exposure Plus Re-Heat Treatment to Original Room Temp. Properties

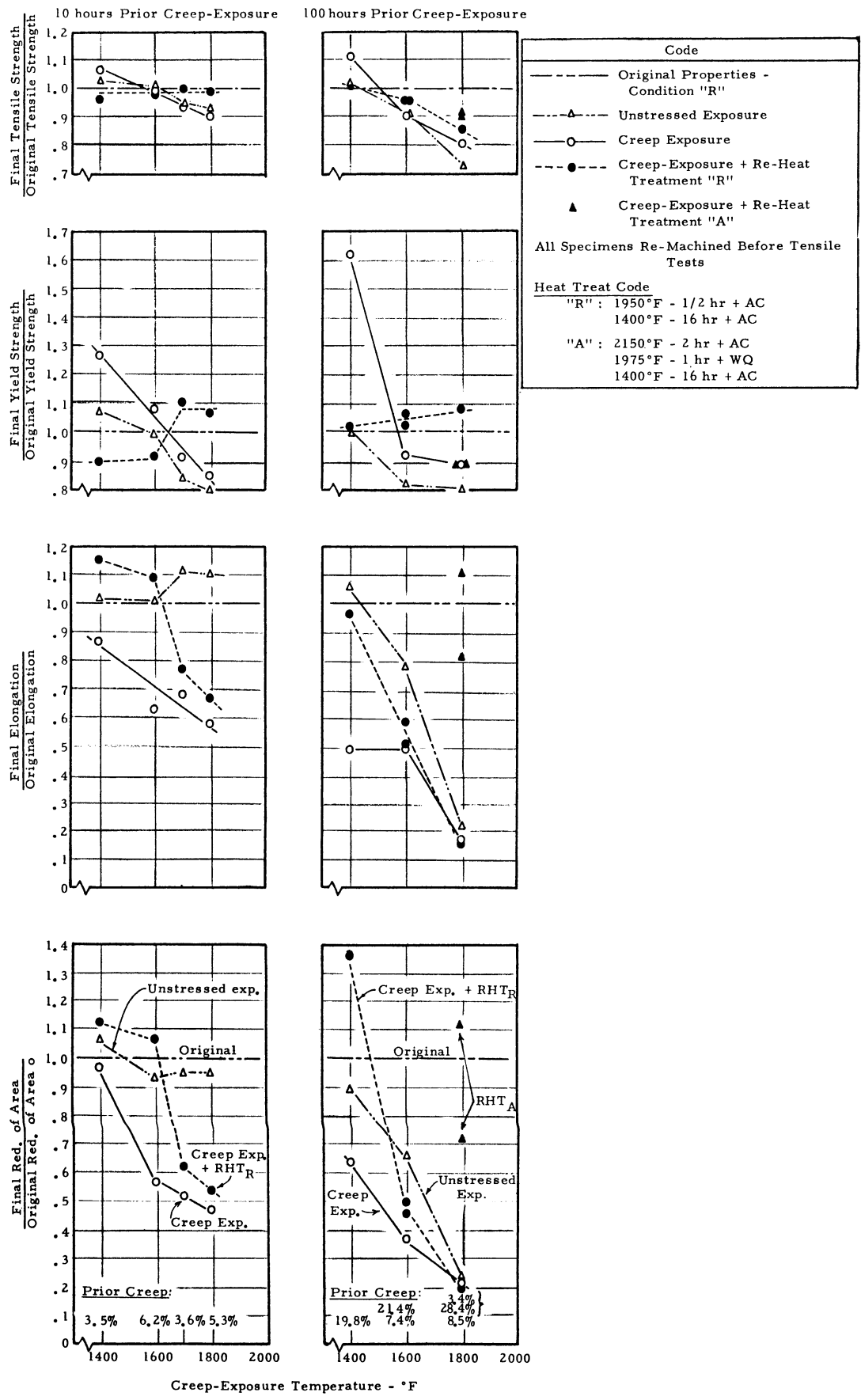


Figure 12 Effect of Creep-Exposure on Room Temperature Tensile Properties of Rene 41 And Subsequent Ability to Recover Original Properties by Re-Heat Treating and Remachining

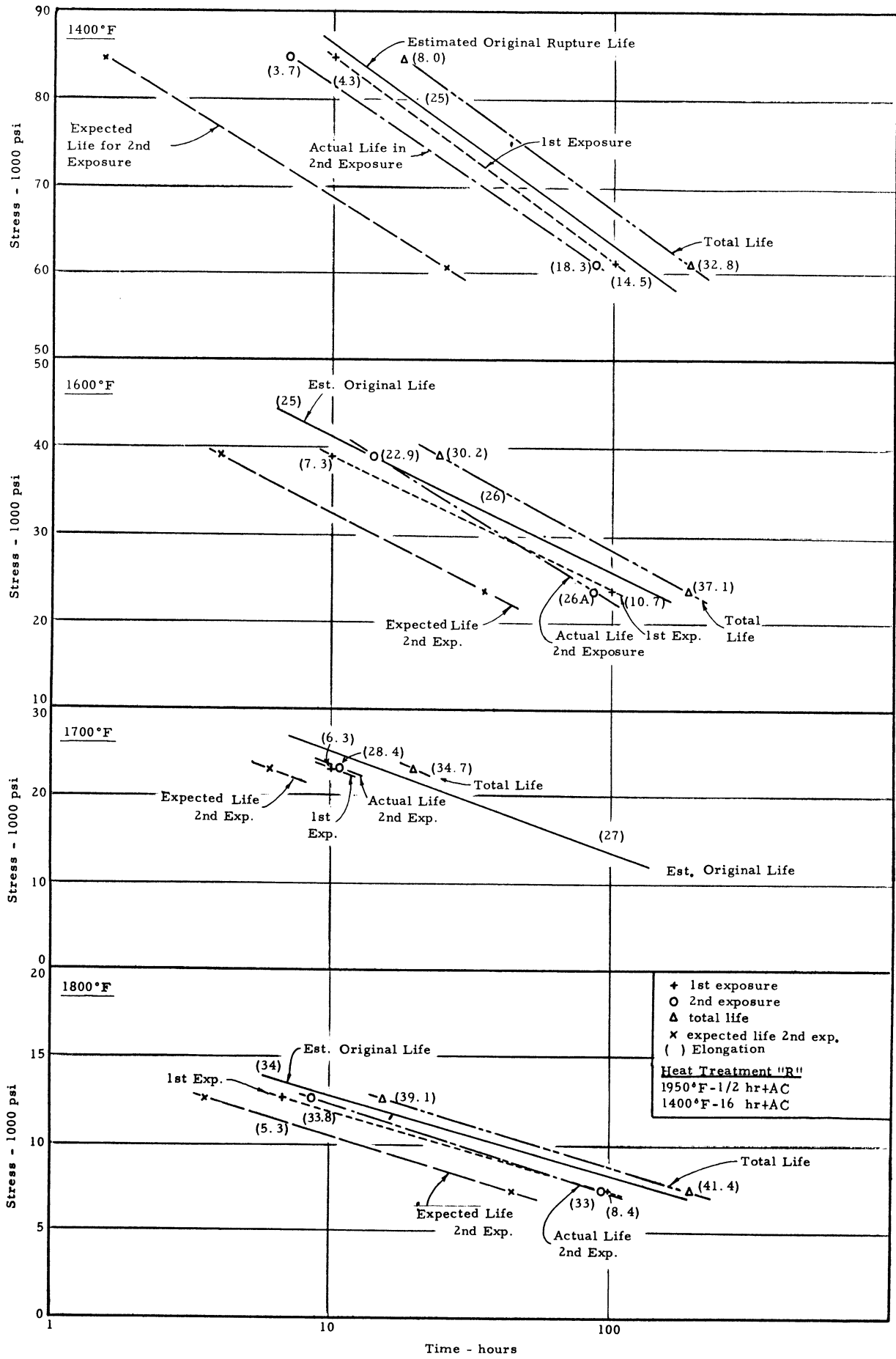


Figure 13 Effect of Re-Heat Treatment "R" on Rupture Life After Initial Creep-Exposure

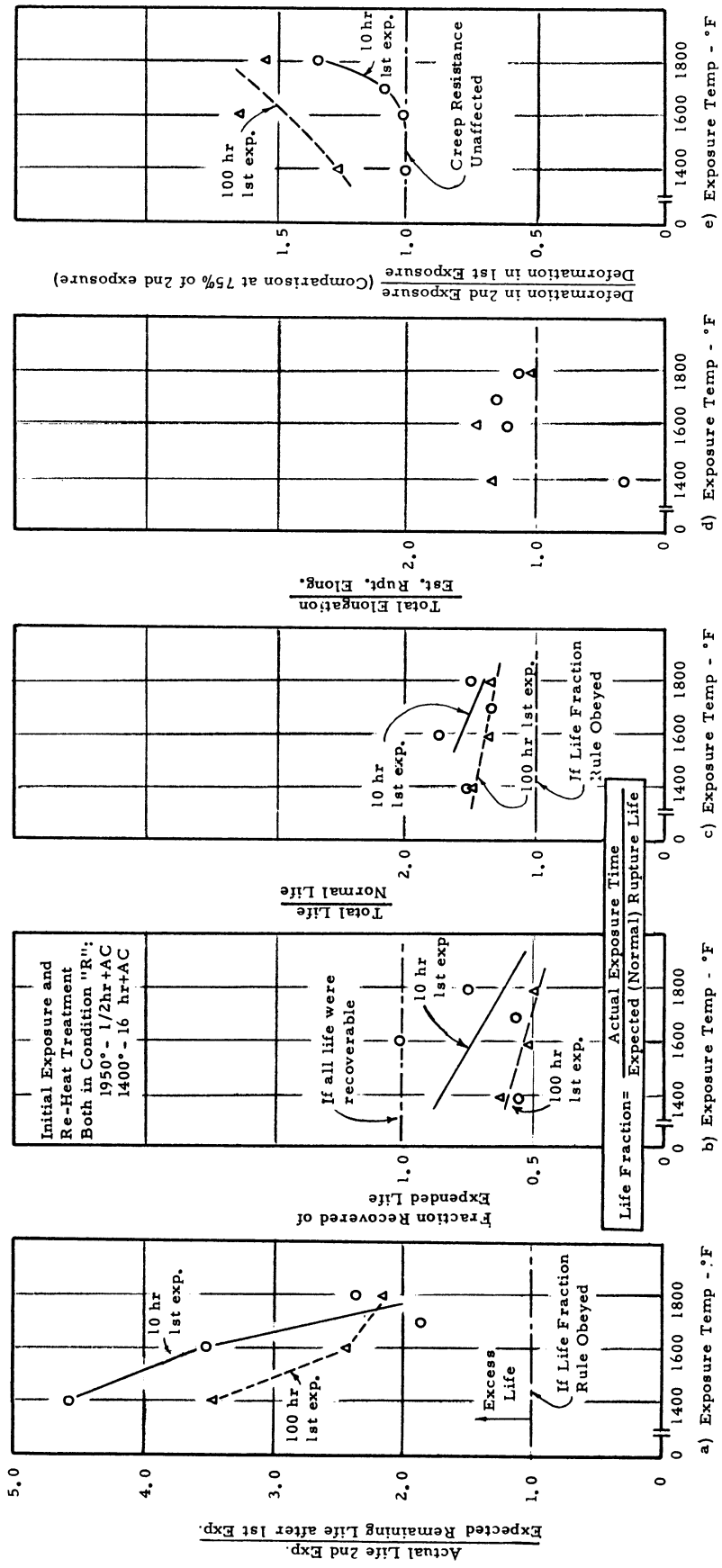


Figure 14 Effect of Re-Heat Treatment to the "R" Condition and Re-Machining on Ratios of Actual Behavior to Theoretical Behavior of Rene' 41 After a First Creep-Exposure of 10 or 100 Hours at 1400°, 1600°, or 1800°F.

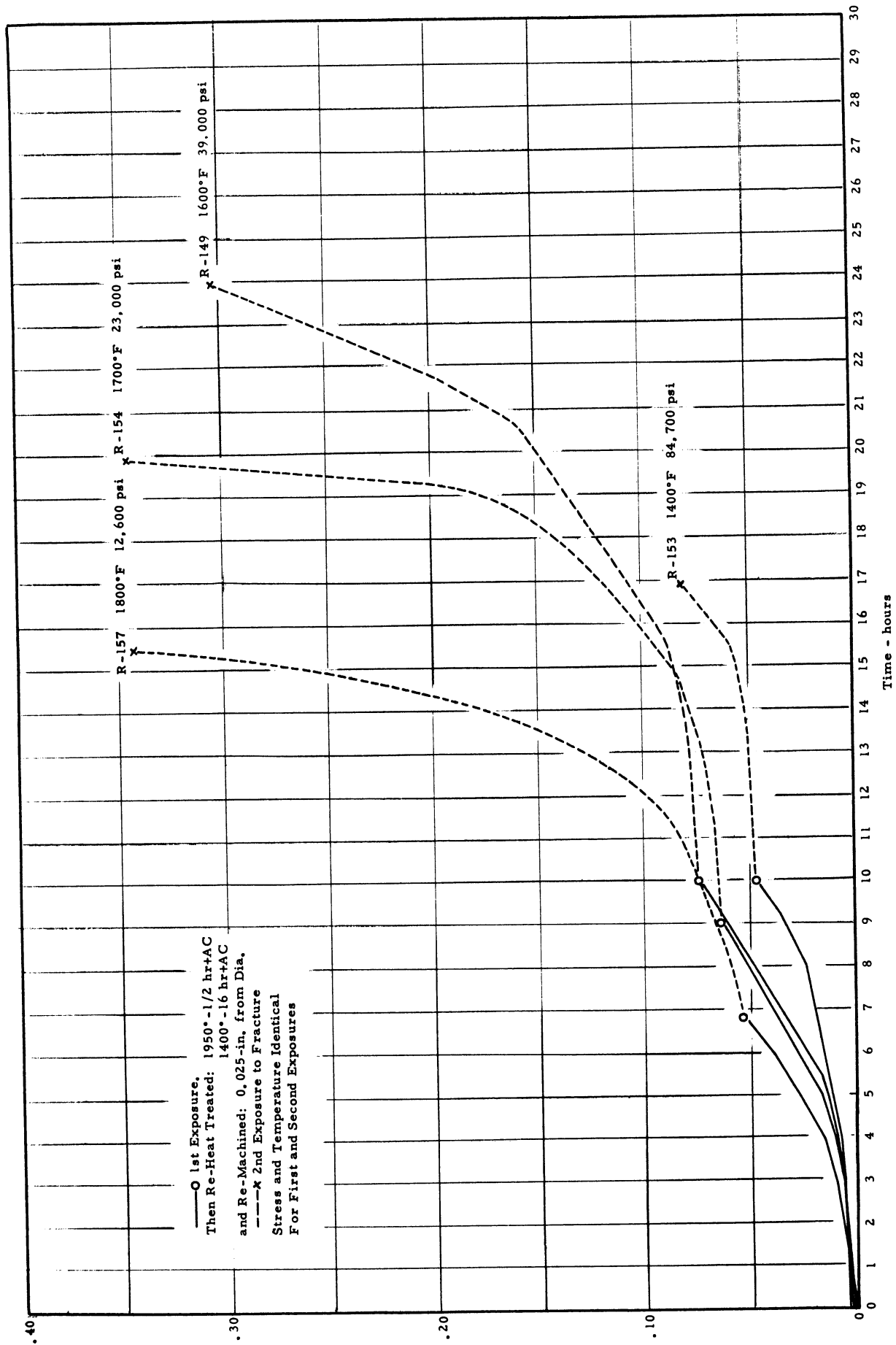


Figure 15 Effect of Re-Heat Treatment and Re-Machining On Creep of Rene 41 After Initial Creep-Exposure For 6, 9-10 Hours

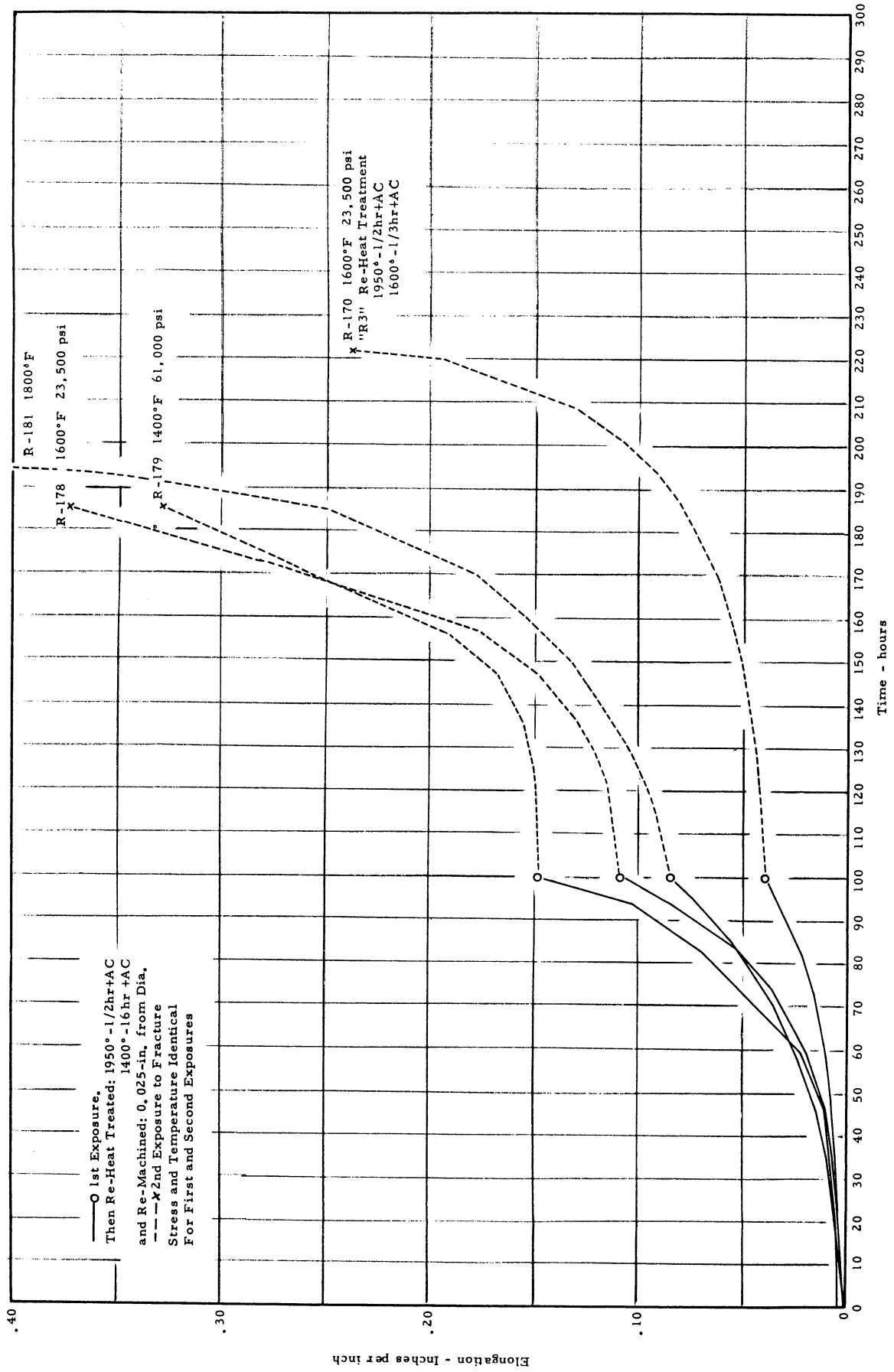
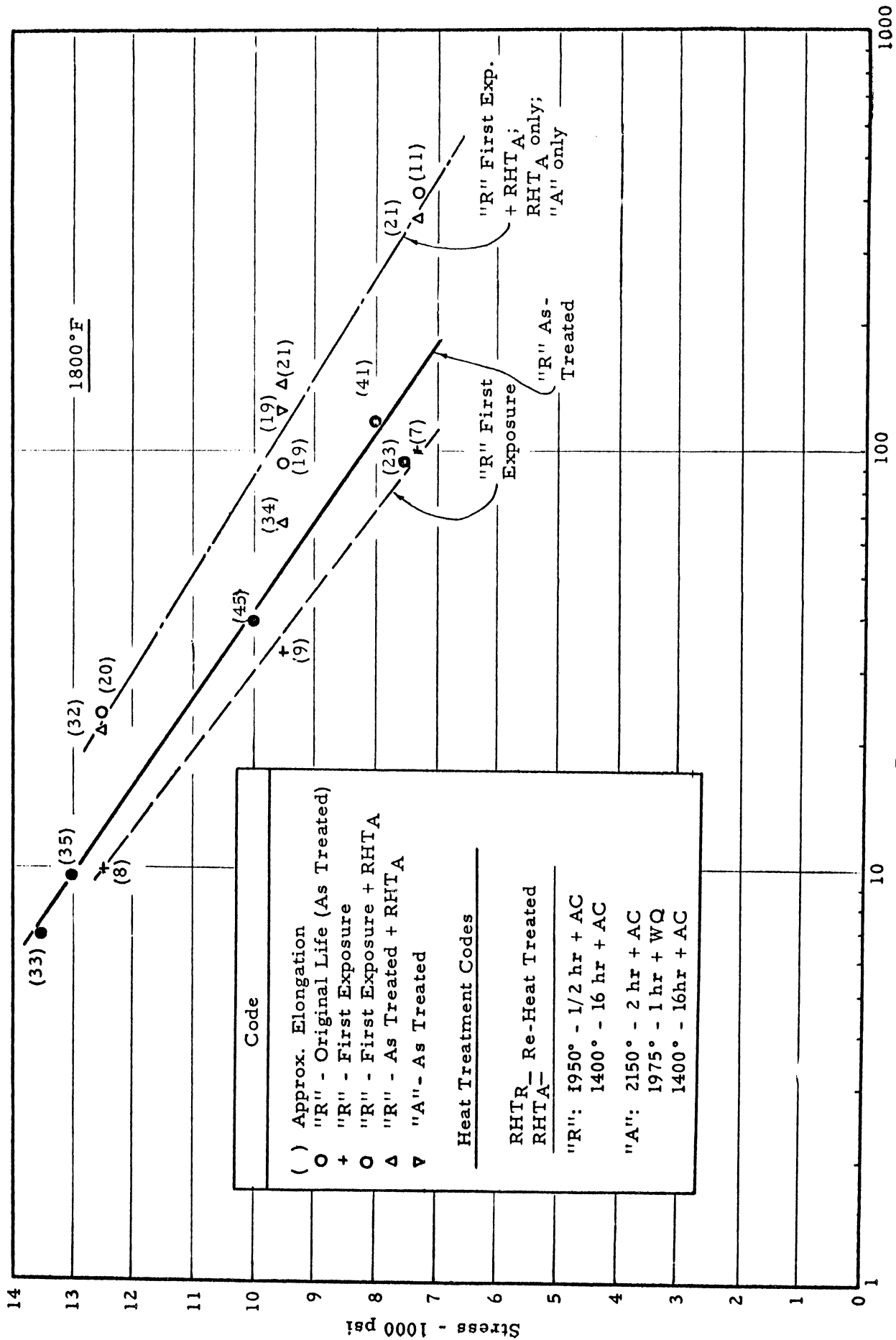


Figure 16 Effect of Re-Heat Treatment and Re-Machining on Creep of Rene' 41 After Initial Creep-Exposure for 100 Hours



Code	
()	Approx. Elongation
○	"R" - Original Life (As Treated)
+	"R" - First Exposure
○	"R" - First Exposure + RHTA
Δ	"R" - As Treated + RHTA
▽	"A" - As Treated

Heat Treatment Codes
RHTR- Re-Heat Treated
RHTA-
"R": 1950° - 1/2 hr + AC
1400° - 16 hr + AC
"A": 2150° - 2 hr + AC
1975° - 1 hr + WQ
1400° - 16hr + AC

Figure 17 Effect of Various Re-Heat Treatments on Rupture Life of Rene' 41 at 1800°F

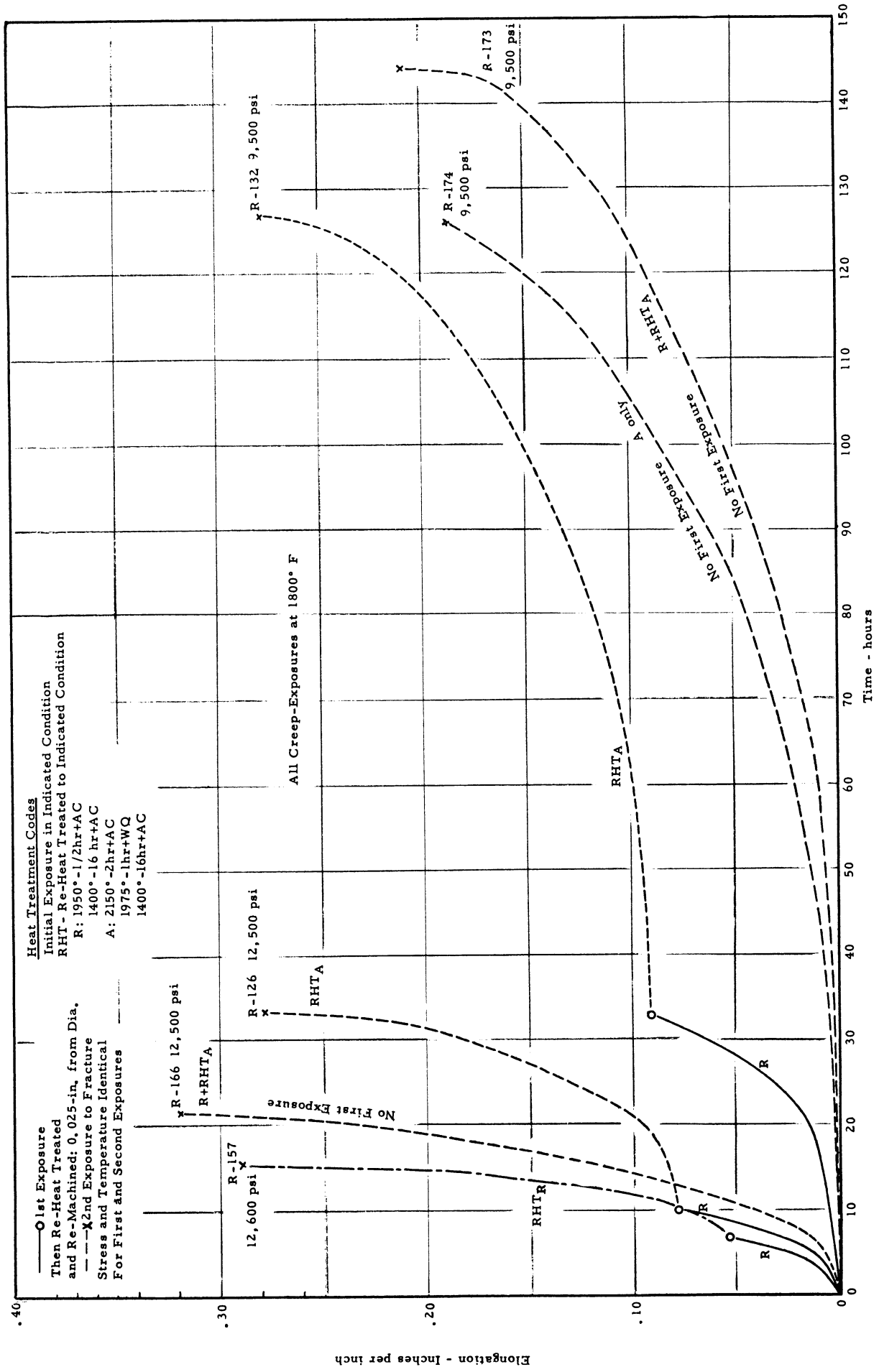


Figure 18 Effect of Type of Re-Heat Treatment (Followed By Re-Machining) On Creep of Rene 41 After Initial Creep-Exposure at 1800° F For 6, 8-33 Hours

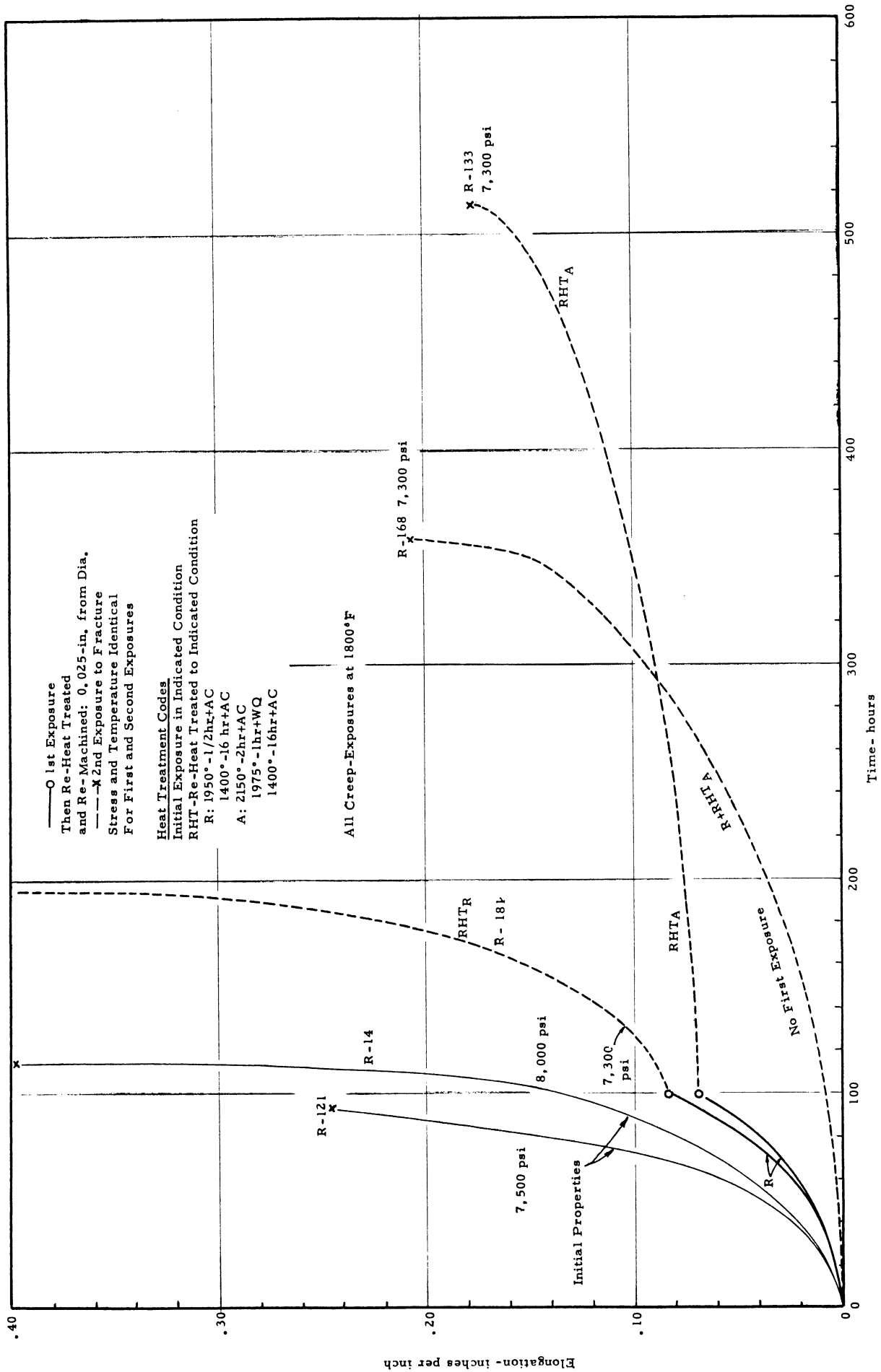


Figure 19 Effect of Type of Re-Heat Treatment (Followed By Re-Machining) On Creep of Rene 41 After Initial Creep-Exposure at 1800°F For 100 Hours

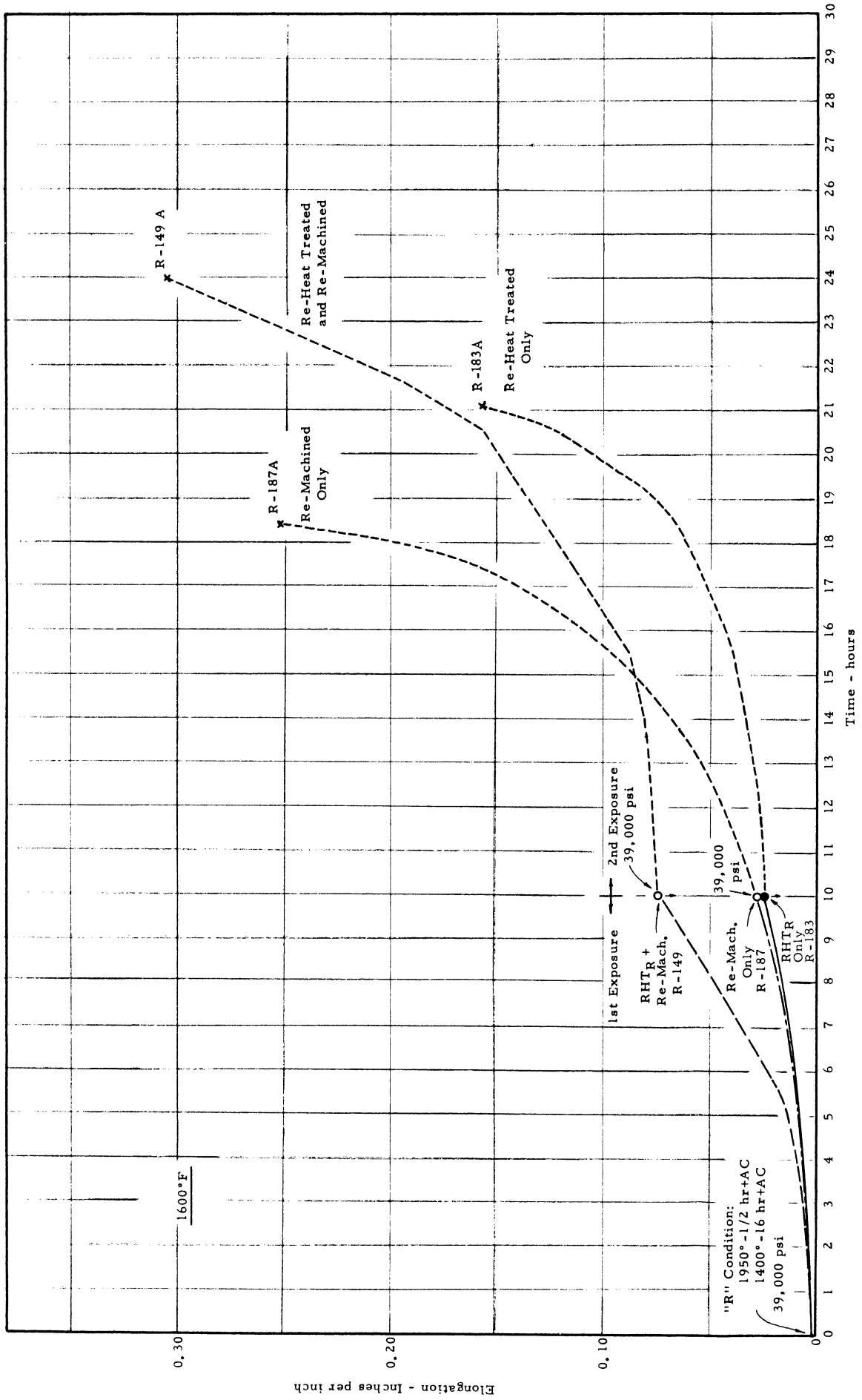


Figure 20 Effect of Re-Heat Treatment and Re-Machining on Creep of Rene 41 After Initial Creep-Exposure at 1600°F

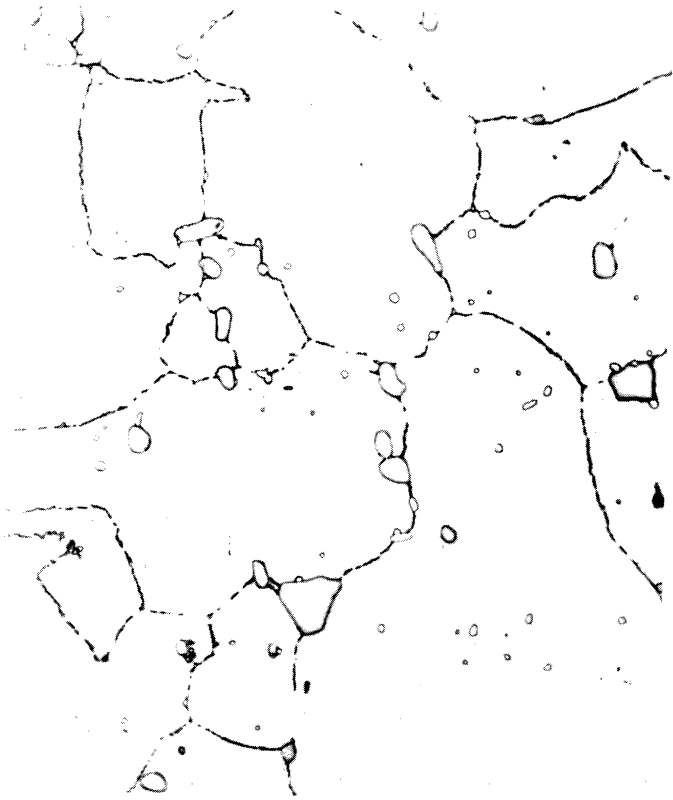


Figure 21

1000x

As Heat Treated "R" Condition



Figure 22

1000x

Specimen R-104 Exposed Without Stress
100 Hours at 1800°F

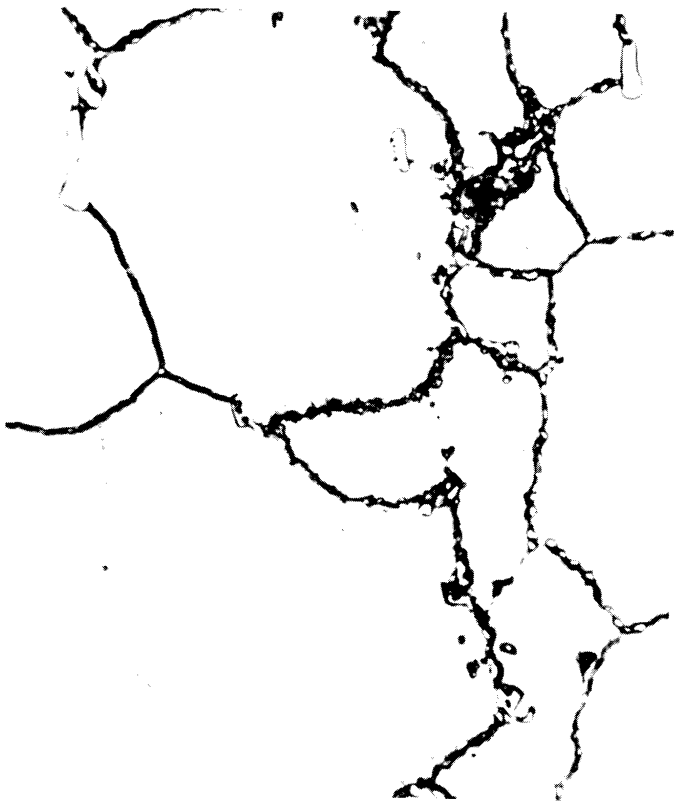


Figure 23

1000x

Specimen R-105 Re-Heat Treated After
100 Hours at 1800°F (Includes One Hour
Re-Solution at 2150°F)



Figure 24

1000x

Specimen R-111 Re-Heat Treated After
100 Hours at 1800°F (Includes Two Hour
Re-Solution at 2150°F)



Figure 25 1000x
Optical Micrograph of Spec. R-150



Figure 26 2200x
Electron Micrograph of Spec. R-150

Specimen R-150 Creep-Exposure 10 Hours at 1400°F to 3.52 Percent Deformation, Then Re-Heat Treated to Condition "R"

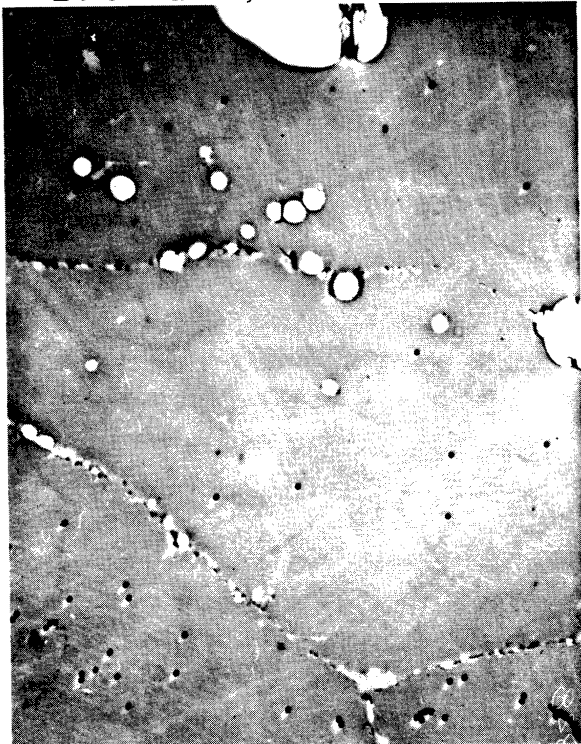


Figure 27 2200x

Electron Micrograph of Spec. R-172
Creep-Exposure 100 Hours at
1400°F to 19.0 Percent Deformation,
Then Re-Heat Treated to Cond. "R"

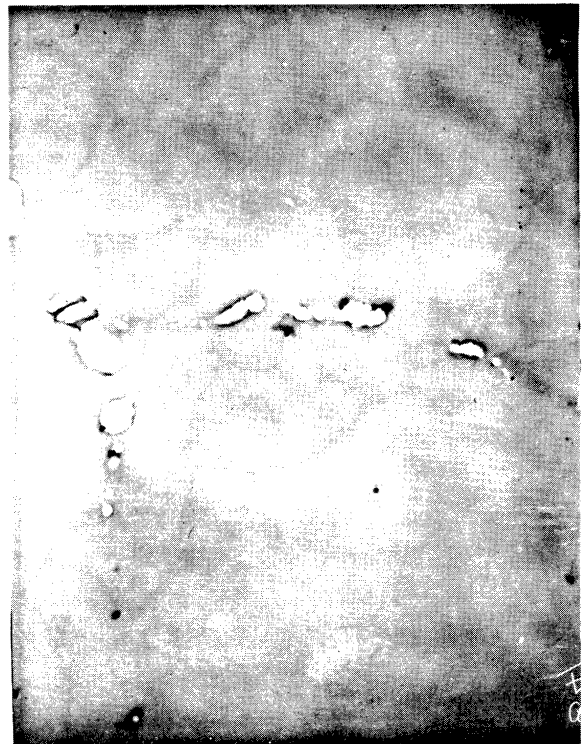


Figure 28 2200x

Electron Micrograph of Spec. R-148
Creep-Exposure 10 Hours at 1600°F
to 6.20 Percent Deformation, Then
Re-Heat Treated to Cond. "R"

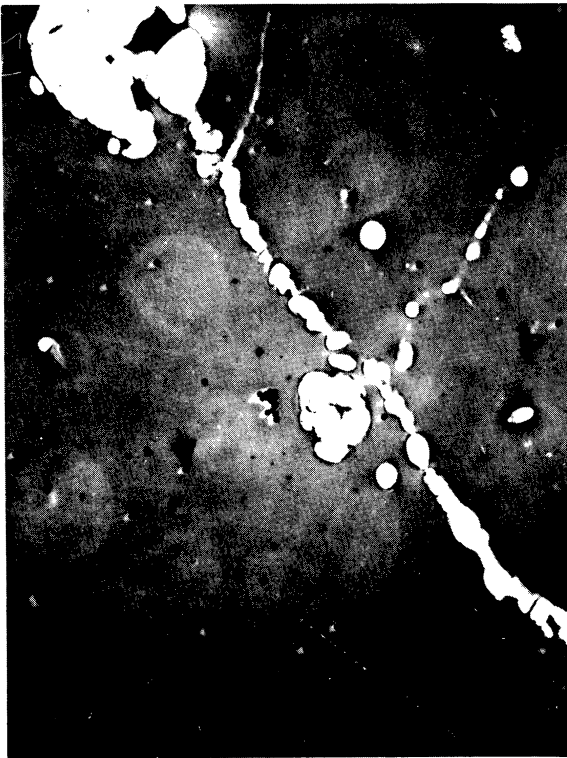


Figure 29 2200x

Electron Micrograph of Spec. R-185
Creep-Exposure 100 Hours at 1600°F
to 7.38 Percent Deformation, Then
Re-Heat Treated to Cond. "R"

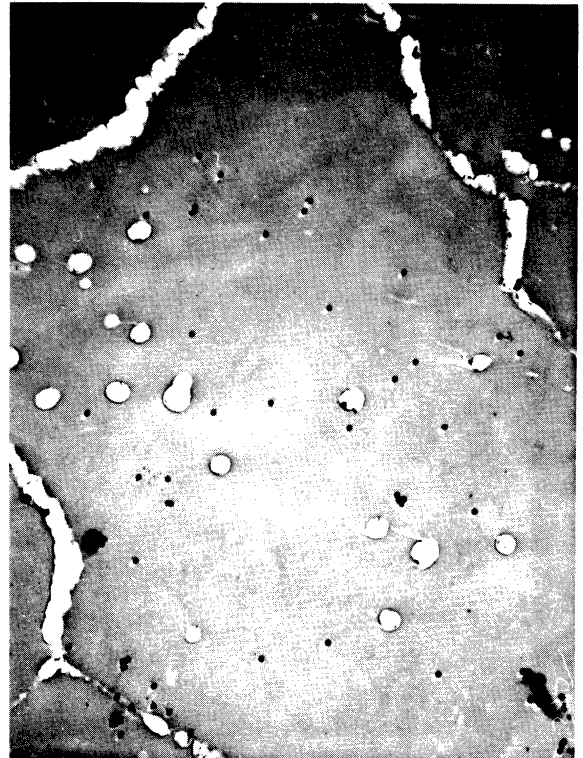


Figure 30 2200x

Electron Micrograph of Spec. R-151
Creep-Exposure 10 Hours at 1700°F
to 3.57 Percent Deformation, Then
Re-Heat Treated to Cond. "R"

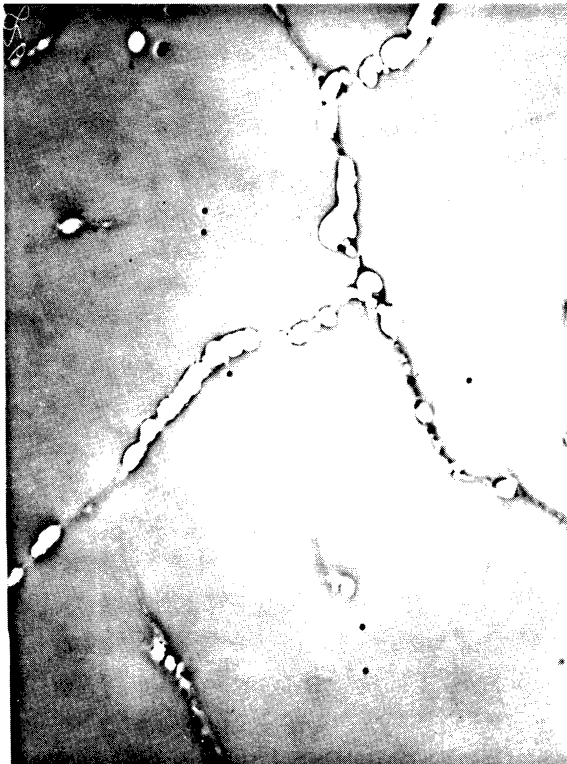


Figure 31 2200x

Electron Micrograph of Spec. R-155
Creep-Exposure 10 Hours at 1800°F
to 5.34 Percent Deformation, Then
Re-Heat Treated to Cond. "R"

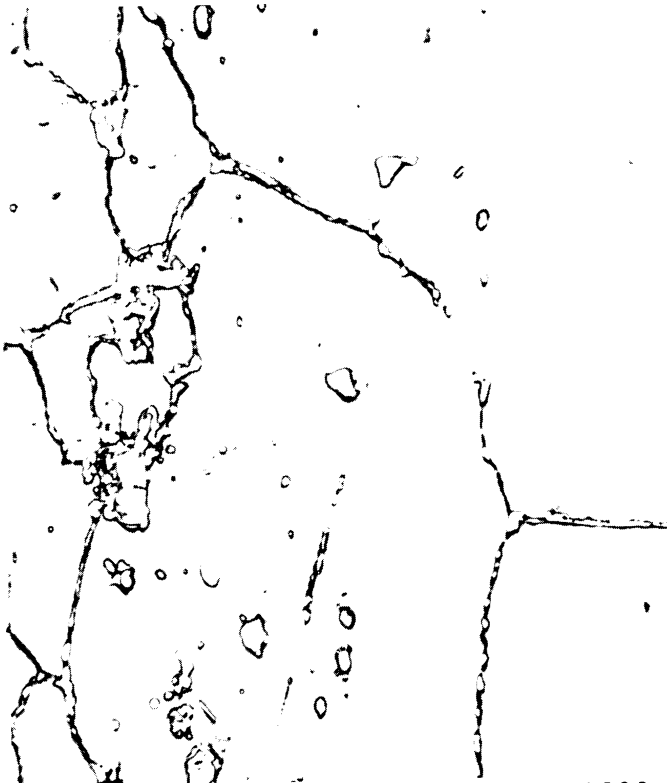


Figure 32

1000x

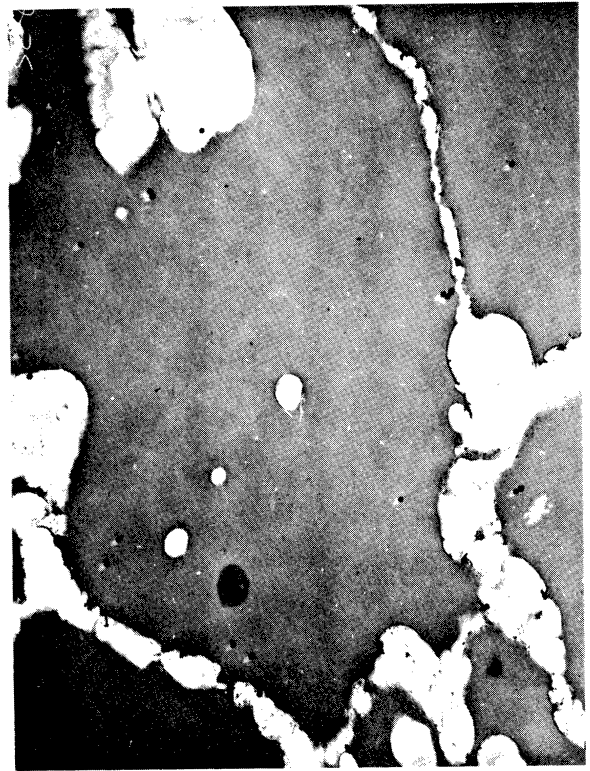


Figure 33

2200x

Optical Micrograph of Spec. R-197

Electron Micrograph of Spec. R-197

Specimen R-197 Creep-Exposure 100 Hours at 1800°F to 8.06 Percent Deformation, Then Re-Heat Treated to Condition "R"

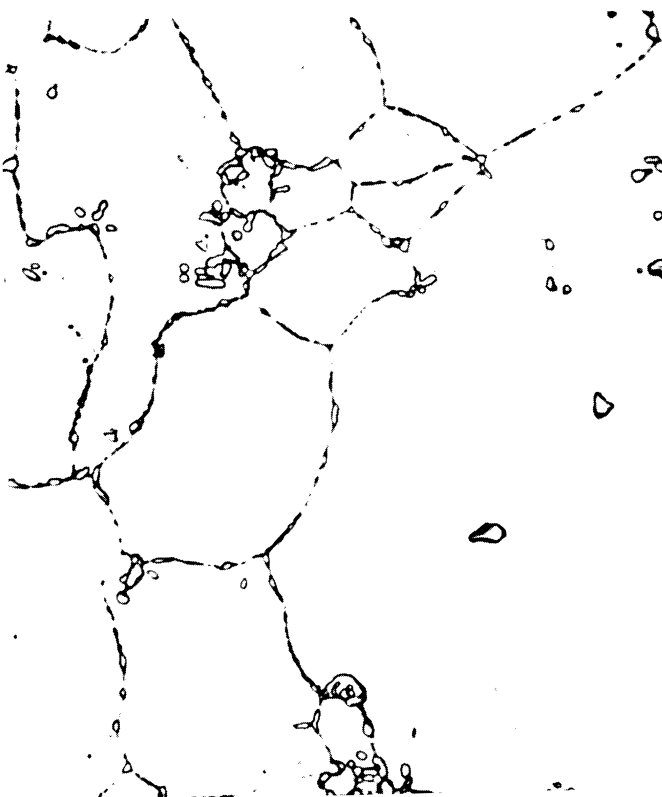


Figure 34

1000x



Figure 35

2200x

Optical Micrograph of Spec. R-124

Electron Micrograph of Spec. R-124

Specimen R-124 Creep-Exposure 100 Hours at 1800°F to 3.46 Percent Deformation, Then Re-Heat Treated to Condition "A"

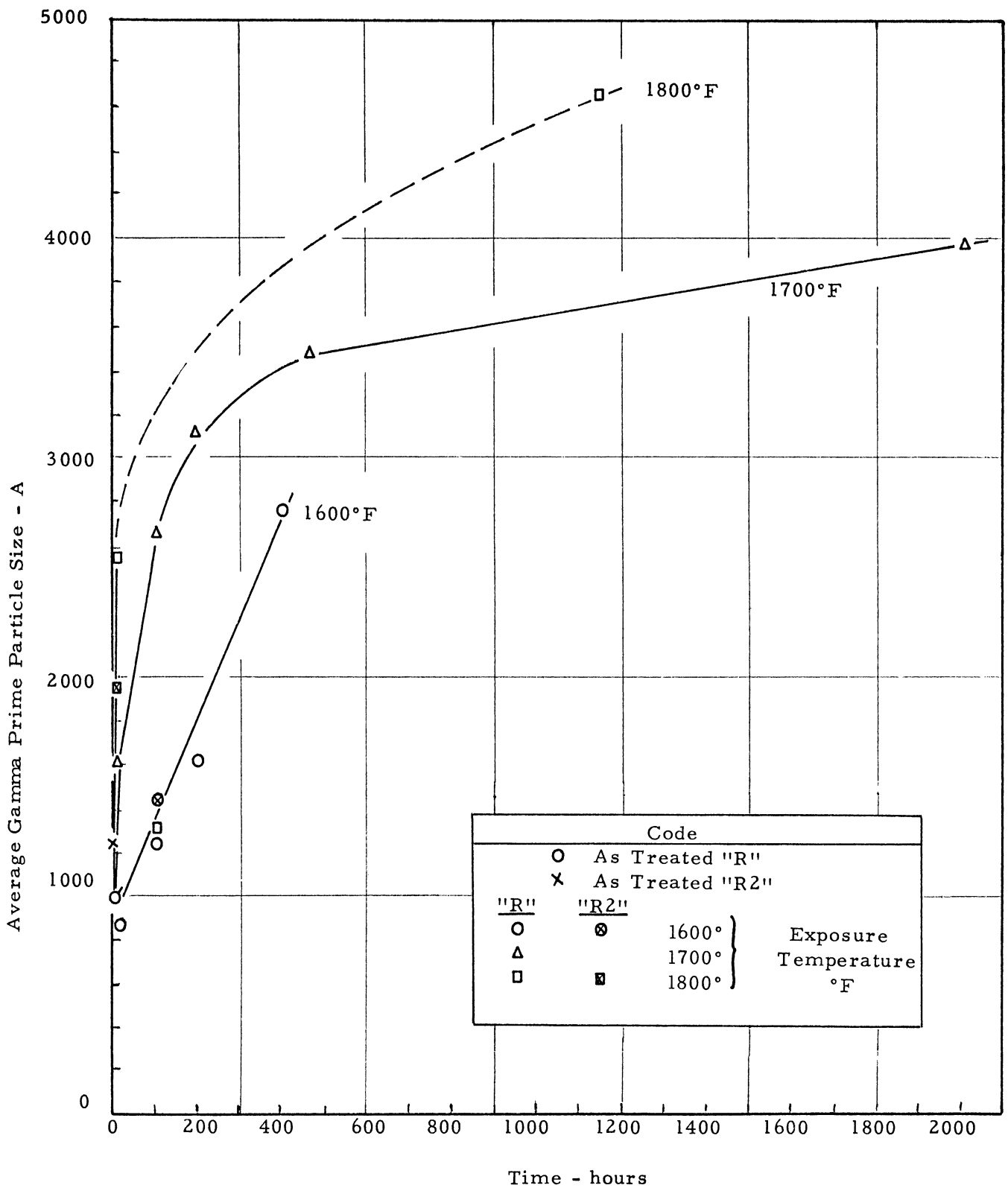


Figure 36 Effect of Aging Time and Temperature on Average Gamma Prime Particle Size in Rene' 41

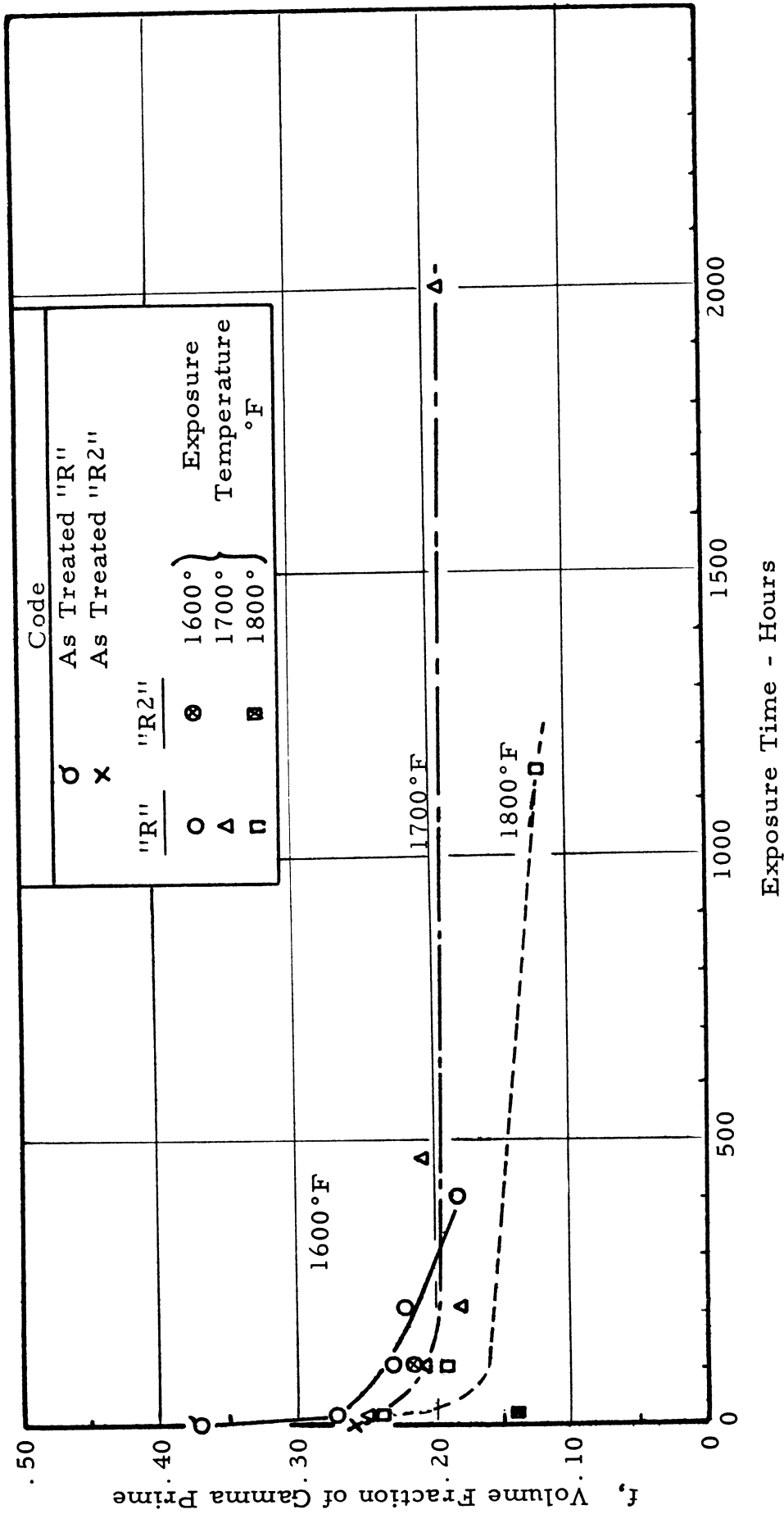


Figure 37 Effect of Exposure Time on Volume Fraction of Gamma Prime in Matrix of Rene' 41

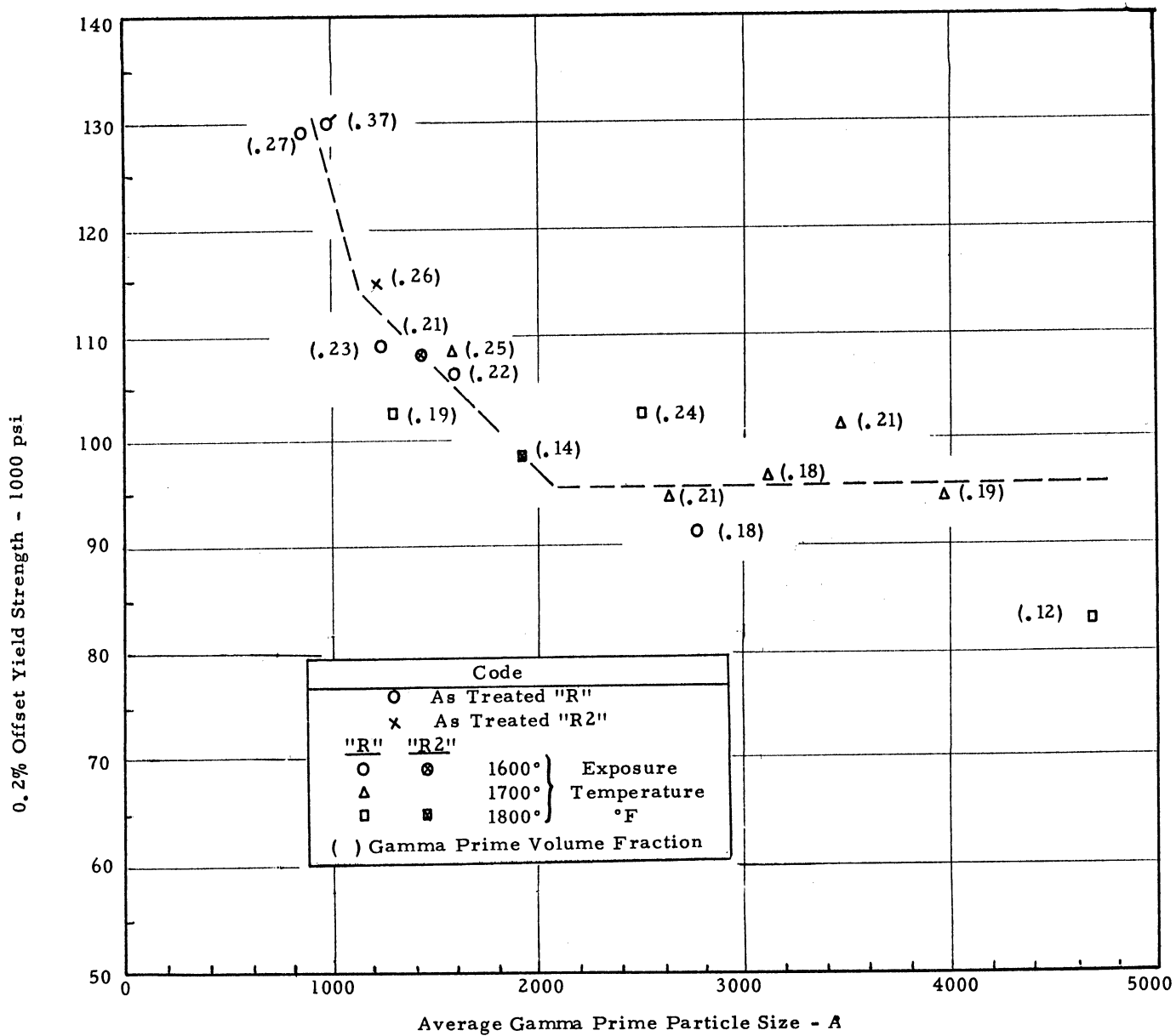


Figure 38. Effect of Gamma Prime Particle Size on Yield Strength of Rene' 41

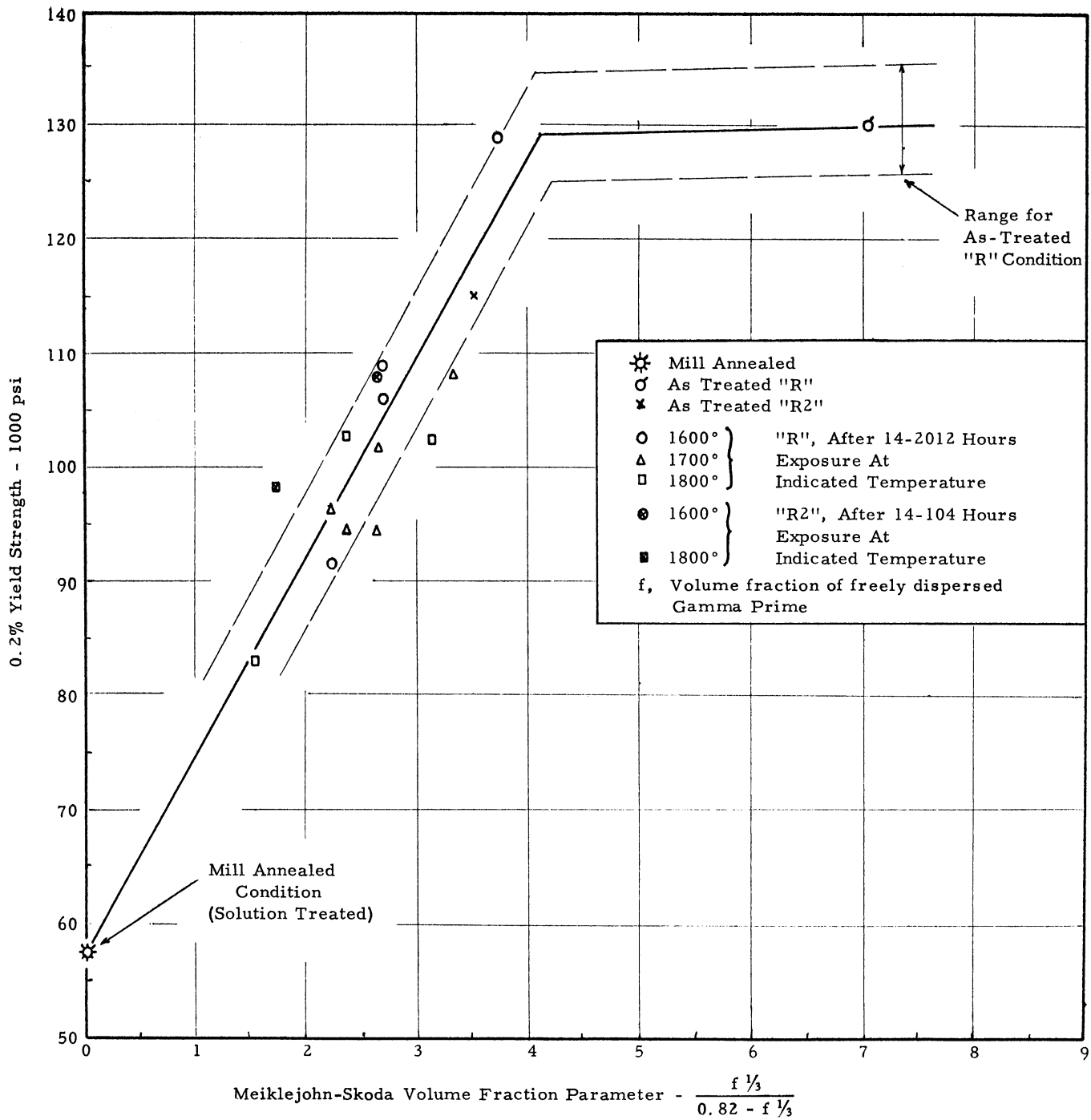


Figure 39 Correlation of Meiklejohn-Skoda Volume Fraction Parameter With Room Temperature Yield Strength of Rene' 41 After Unstressed Exposure

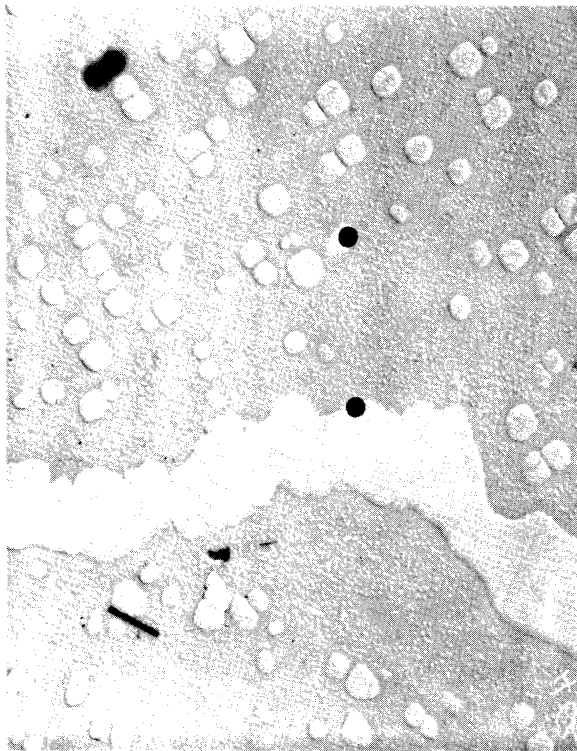


Figure 40 8200x
Collodion Replica of Spec. R-32

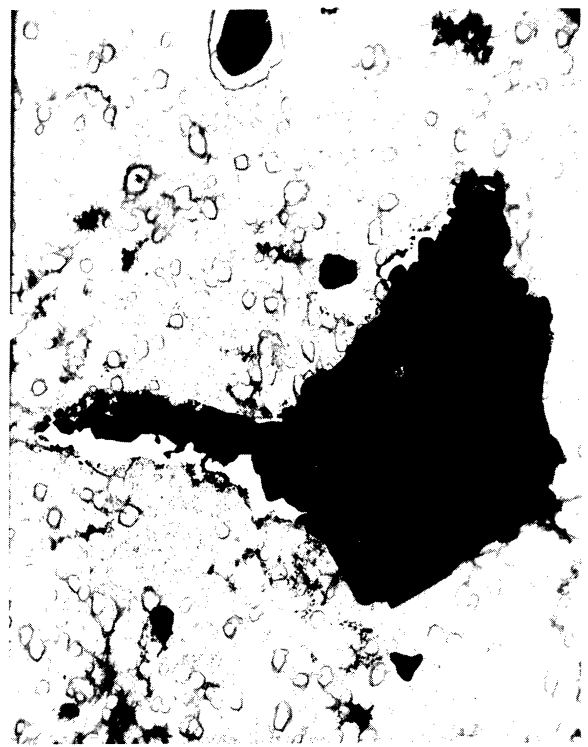


Figure 41 4800x
Carbon Extraction Replica of Spec. R-32

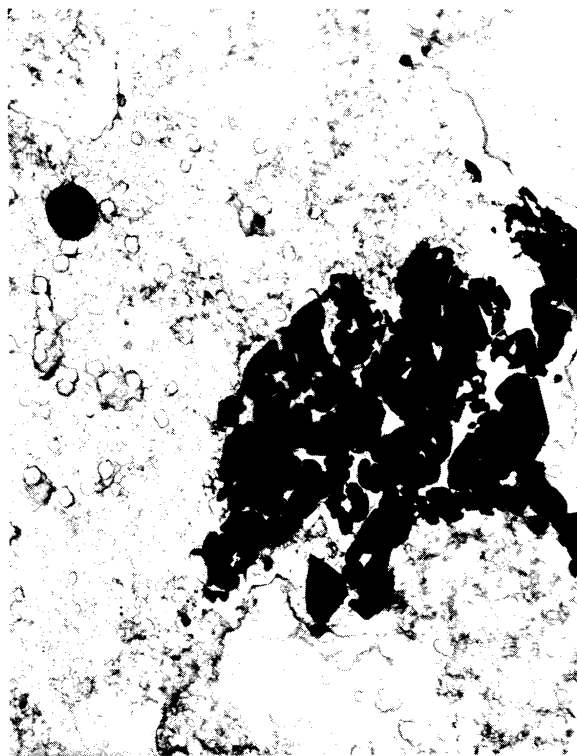


Figure 42 4800x
Carbon Extraction Replica of Spec. R-32



Figure 43 3500x
Collodion Replica of Spec. R-104

Spec. R-32 and Spec. R-104 Exposed Without Stress 100 Hours at 1800°F



Figure 44 8200x
Collodion Replica of Spec. R-104

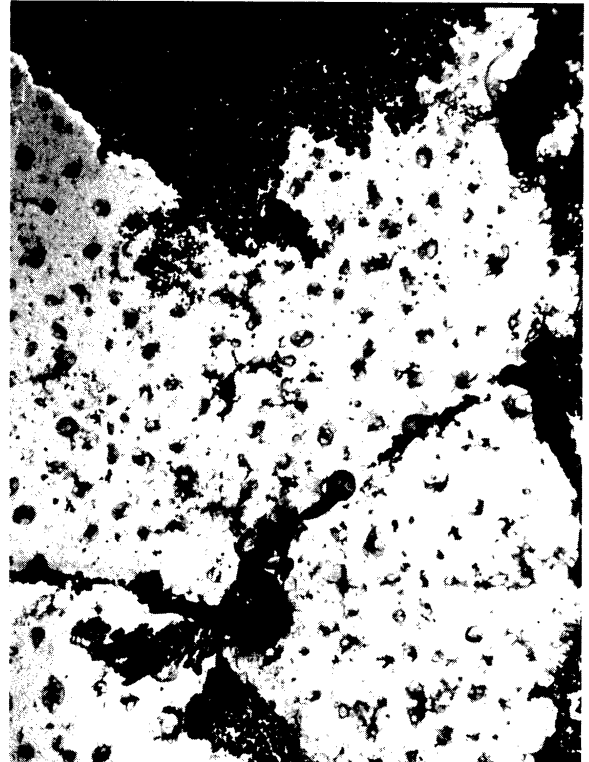


Figure 45 2200x
Carbon Extraction Replica of Spec. R-104

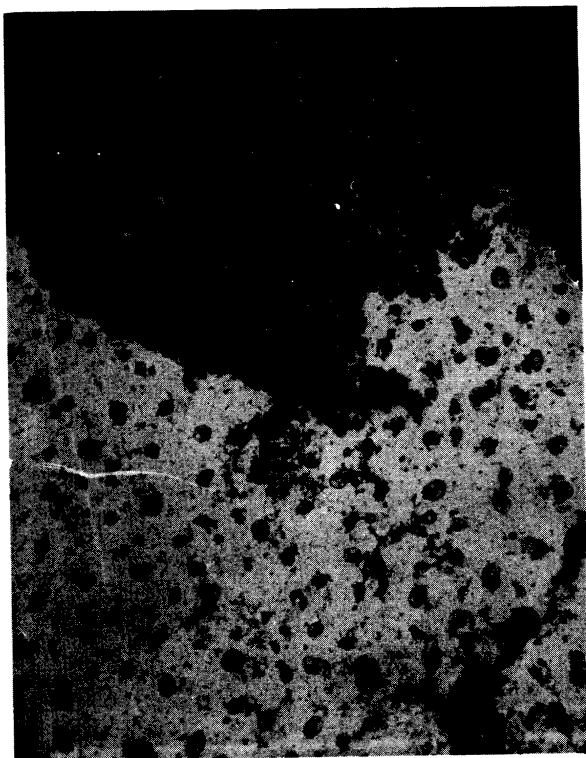


Figure 46 2200x
Carbon Extraction Replica of Spec. R-104



Figure 47 2200x
Carbon Extraction Replica of Spec. R-104
(Diffraction obtained from outlined area)

Spec. R-104 Exposed Without Stress 100 Hours at 1800°F



Figure 48 4800x

Carbon Extraction Replica of Spec. R-104
(Diffraction obtained from
outlined area)

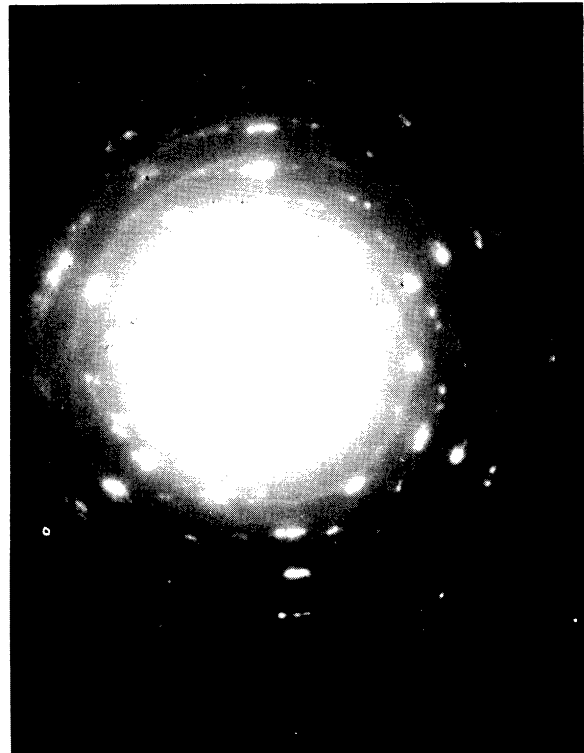


Figure 49

Electron Diffraction Photo of Selected
Area of Figure 47

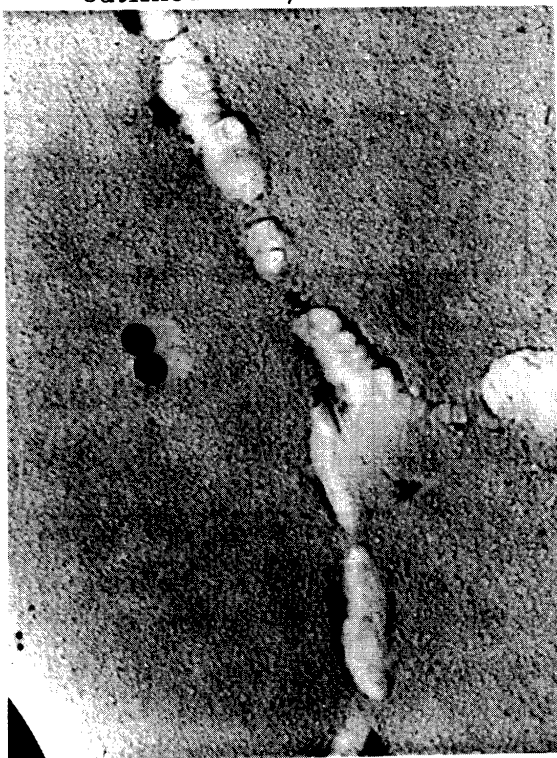


Figure 50 16,000x

Electron Micrograph of As-Treated
Condition "R" (1950° F Solution)

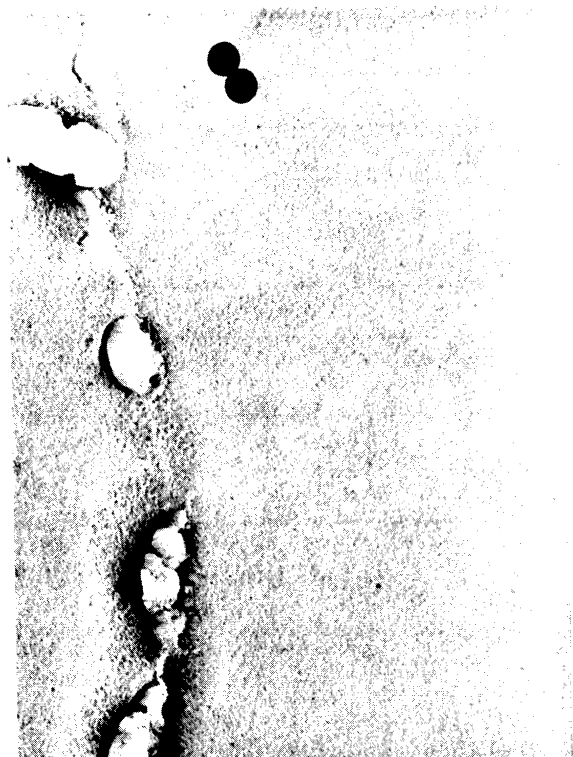


Figure 51 16,000x

Electron Micrograph of Spec. R-124
Re-Heat Treated to Condition "A"
(2150° F Solution) After 100 Hours
Creep-Exposure at 1800° F

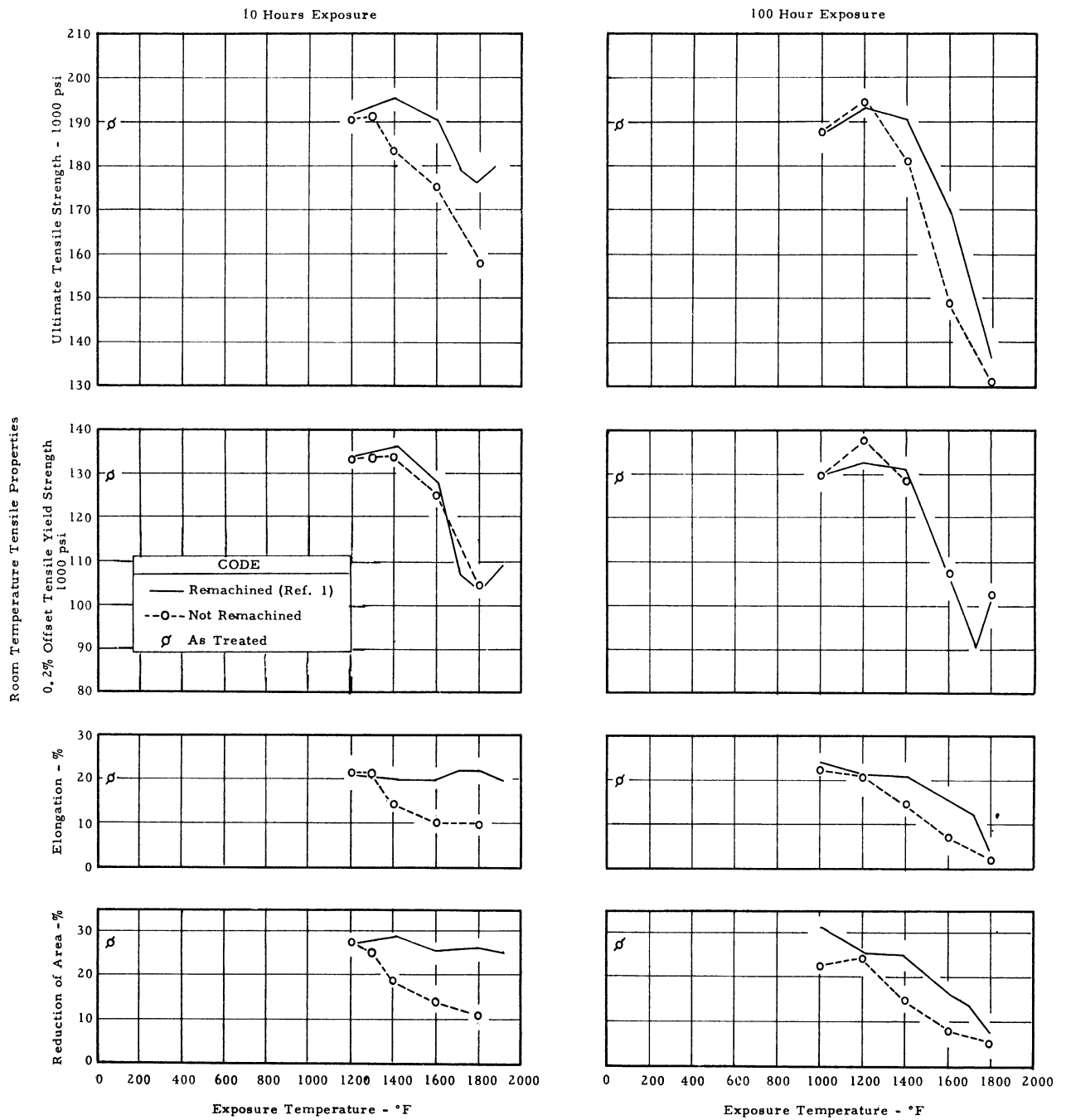


Figure 52 Effect of Remachining on Curves of Room Temperature Tensile Properties Versus Exposure Temperature of Rene' 41 Exposed Without Stress for 10 or 100 Hours,

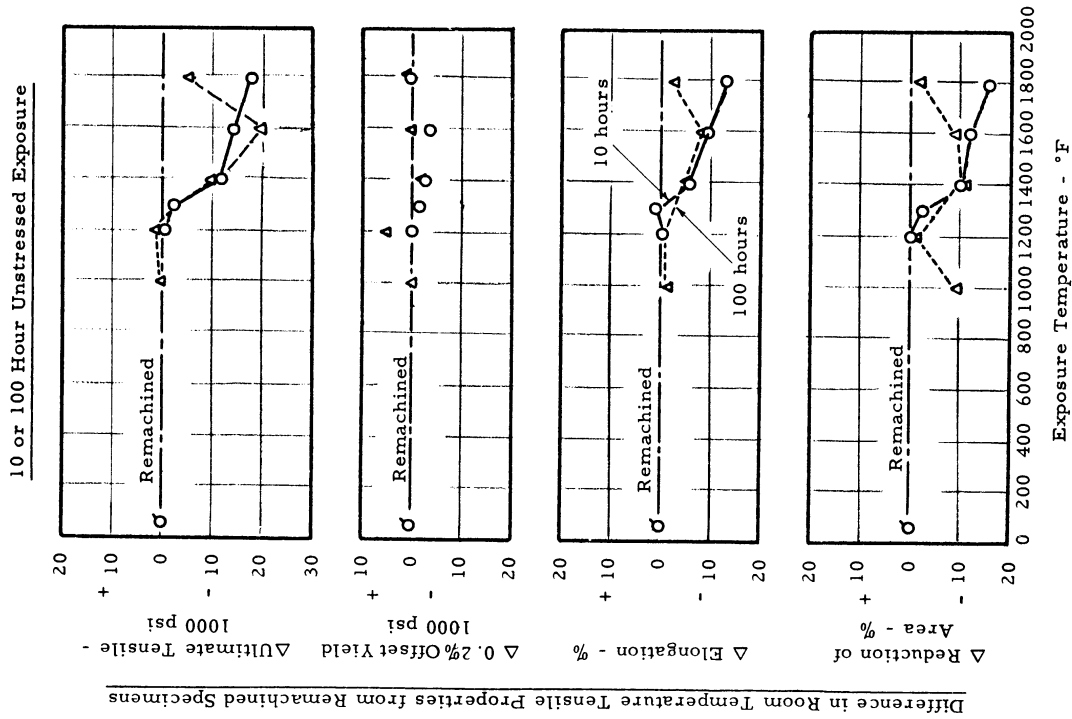


Figure 53a Effect of Exposure Temperature and Time On Difference in Room Temperature Tensile Properties Between As-Exposed and Re-Machined Specimens of Rene' 41 After Unstressed Exposure

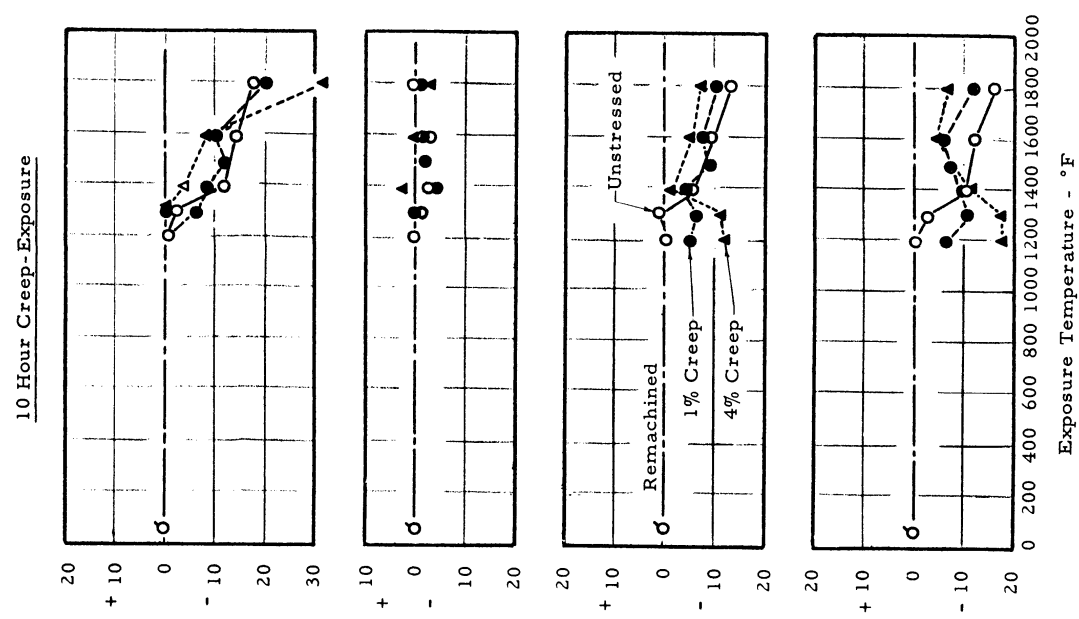


Figure 53b Effect of Exposure Temperature and Amount of Prior Creep On Difference in Room Temperature Tensile Properties Between As-Exposed and Re-Machined Specimens of Rene' 41 After 10 Hours Exposure

Code	
σ	As-Treated
---	Remachined
Not Re-Machined:	
—○—	Unstressed
---●---	1% Creep
---▲---	4% Creep
---△---	Unstressed, 100 hr Exposure
	10 hour Exposure

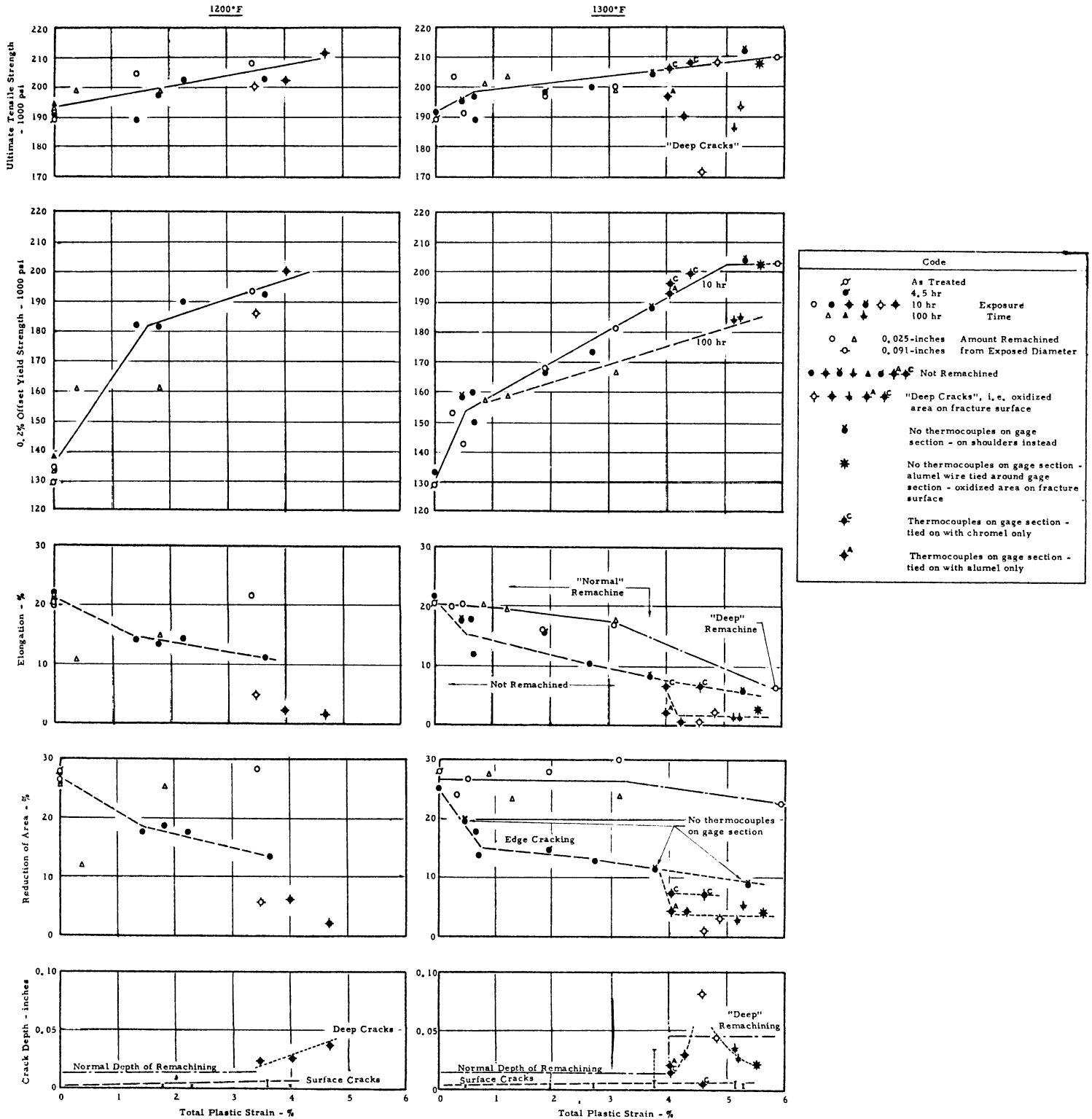


Figure 54 Effect of Prior Creep, Re-Machining, and Thermocouple Practice On Room Temperature Tensile Properties And Cracking Tendencies of Rene' 41 Exposed at 1200° and 1300° F

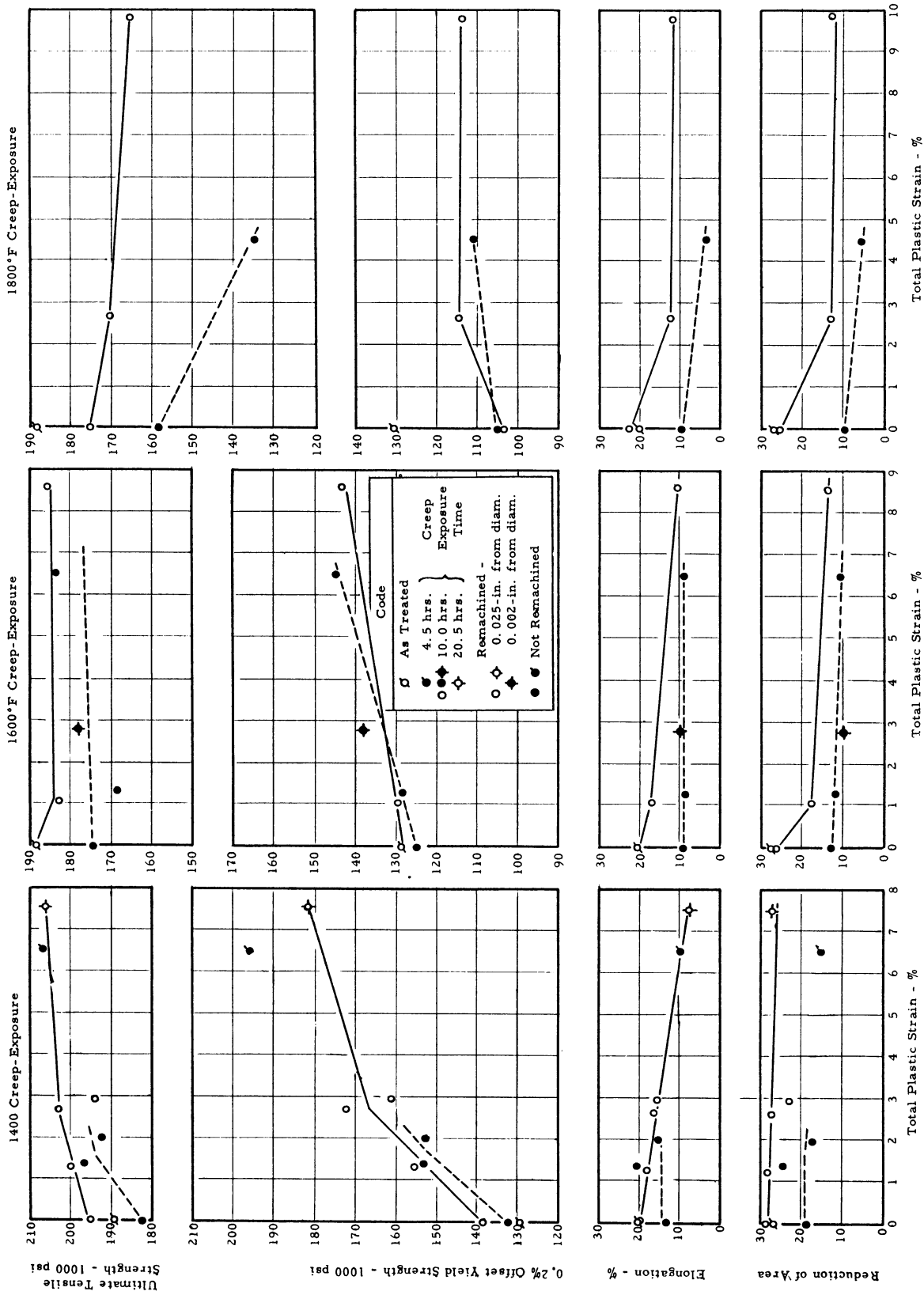
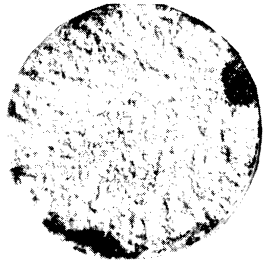
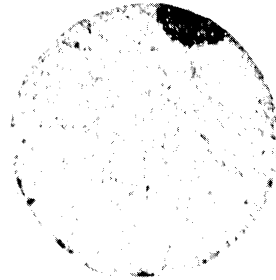


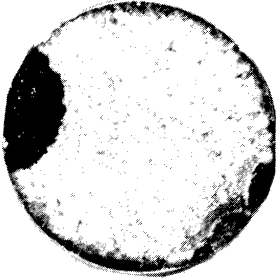
Figure 55 Effect of Prior Creep And Re-Machining On Room Temperature Tensile Properties of Rene 41 Exposed at 1400°, 1600°, and 1800°F



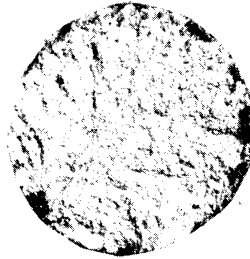
Spec. R-146
Exposed 10 hours at
1200°F to 4.70 percent
deformation
(Not Re-Machined
Before Tensile Test)



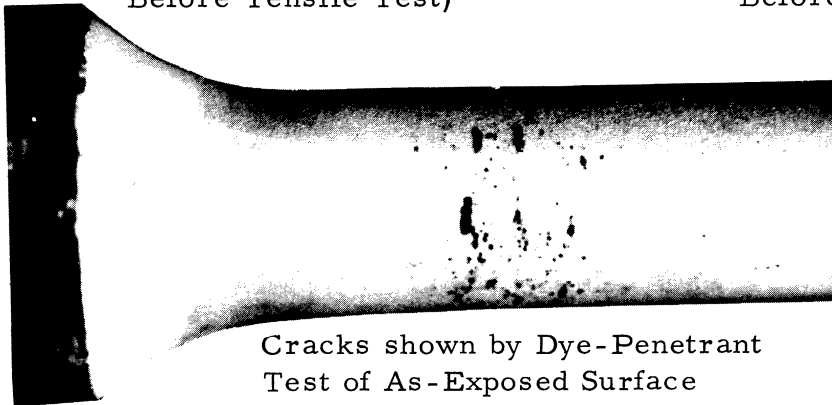
Spec. R-127
Exposed 10 hours at
1300°F to 4.30 percent
deformation
(Not Re-Machined
Before Tensile Test)



Spec. R-63
Exposed 10 hours at
1300°F to 4.60 percent
deformation
(Re-Machined
Before Tensile Test)

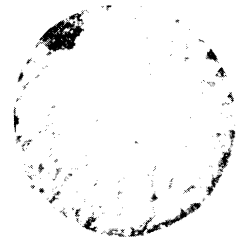


Spec. R-147
Exposed 97.3 hours at
1300°F to 5.21 percent
deformation
(Not Re-Machined
Before Tensile Test)



Cracks shown by Dye-Penetrant
Test of As-Exposed Surface

Spec. R-140
Exposed 10 hours at 1300°F
to 4.85 percent deformation



Fracture Surface
(Re-Machined Before
Tensile Test)

Approx. 4x magnification

Figure 56 Examples of Deep Cracks In Rene' 41 Exposed to Creep at 1200° or 1300°F (Low Ductility and Oxidation on Fracture Surface for Subsequent Tensile Test at Room Temperature)

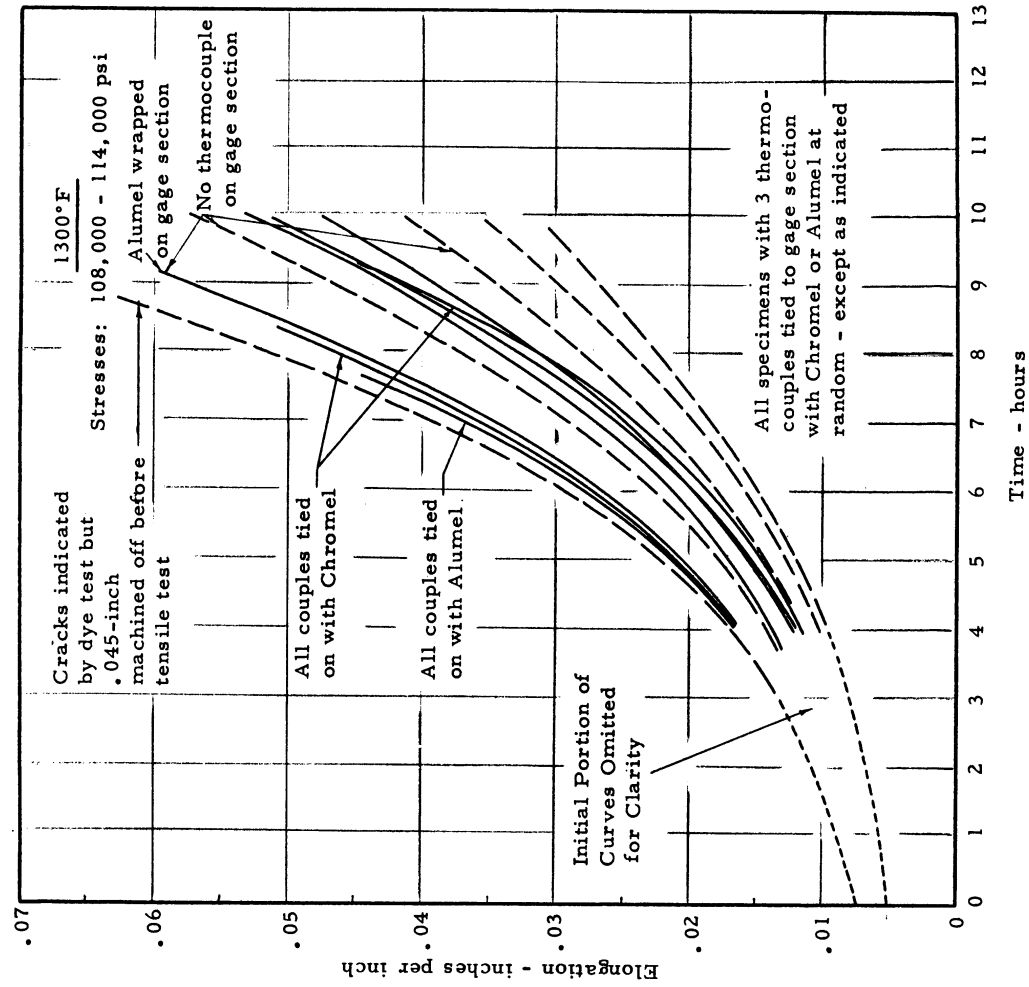
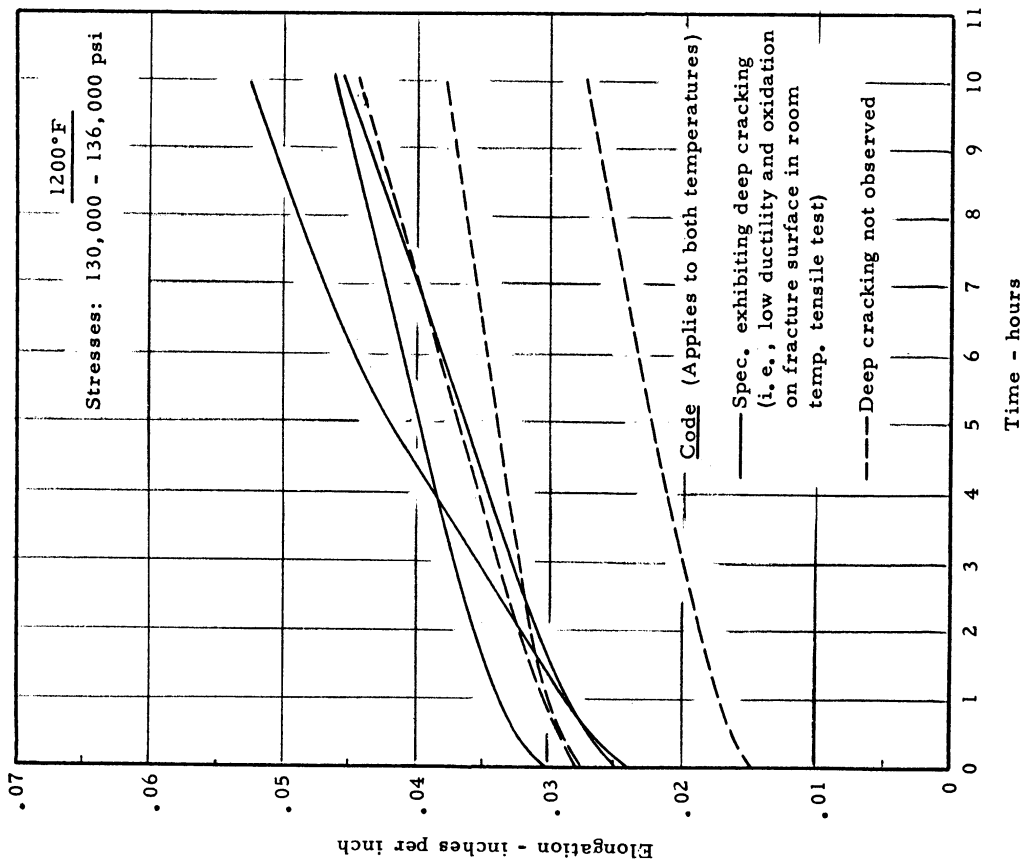


Figure 57 Examples of Creep Curves of Rene' 41 Specimens Exhibiting Deep Cracking After 10 Hours Creep-Exposure at 1200° or 1300°F.

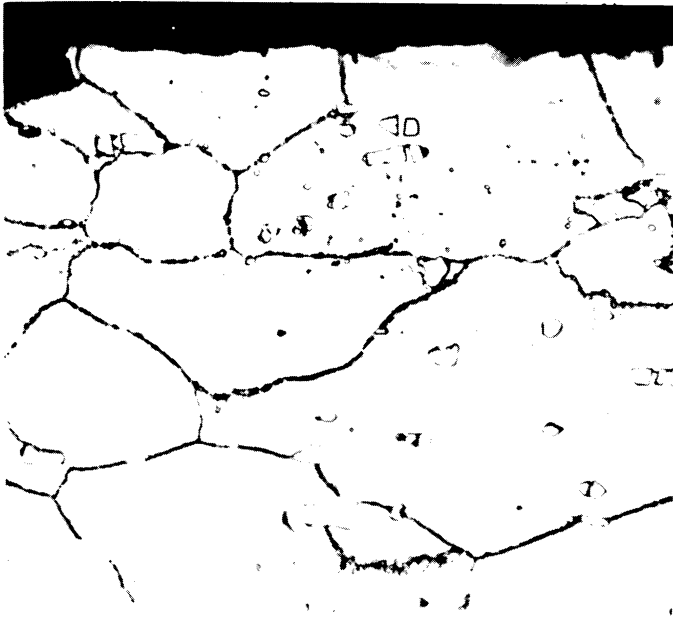


Figure 58 Spec. No. R-90 (Section Showing Surface) Exposed Without Stress 100 Hours at 1000°F

Subsequent Tensile Properties

Elongation: 22.9%

Reduction of Area: 23.2%

Corresponding Re-Machined Spec.

Elongation: 24.4%

Reduction of Area: 32.4%

500x



Figure 59 Spec. No. R-99 (Section Showing Surface Attack) Creep-Exposure at 1300°F for 100 Hours to 0.63 Percent Deformation

Subsequent Tensile Properties

Elongation: 17.6%

Reduction of Area: 17.2%

Approx. Properties of Re-Machined Spec.

Elongation: 20%

Reduction of Area: 24%

500x

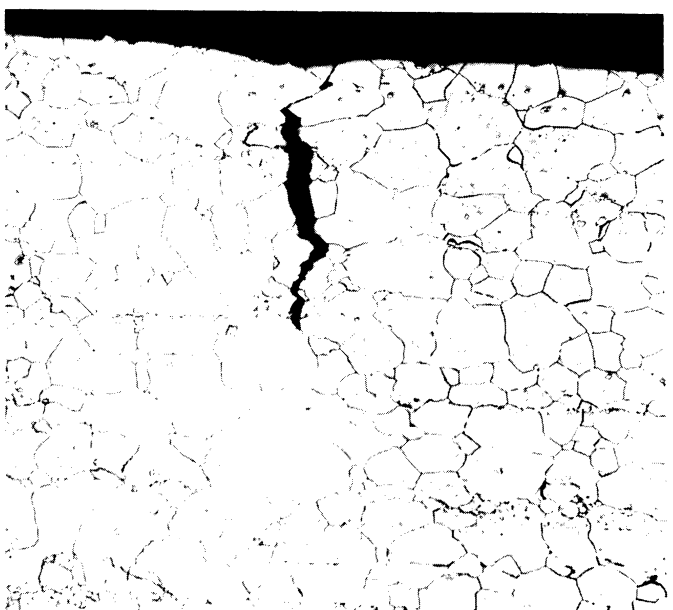


Figure 60 Spec. No. R-95 (Section Showing Surface Attack and Isolated Crack) Creep-Exposure at 1300°F for 10 Hours to 2.71 Percent Deformation

Subsequent Tensile Properties

Elongation: 10.2%

Reduction of Area: 12.9%

100x



Figure 61 Spec. No. R-93 (Section Showing Surface Attack) Exposed Without Stress 100 Hours at 1400°F

Subsequent Tensile Properties

Elongation: 14.9%

Reduction of Area: 14.9%

Corresponding Re-Machined Spec.

Elongation: 22.0%

Reduction of Area: 24.9%

500x



Figure 62 Spec. No. R-92 (Section Showing Surface Attack) Exposed Without Stress 100 Hours at 1600°F

Subsequent Tensile Properties

Elongation: 6.8%

Reduction of Area: 8.3%

Corresponding Re-Machined Spec.

Elongation: 15.1%

Reduction of Area: 16.6%

500x

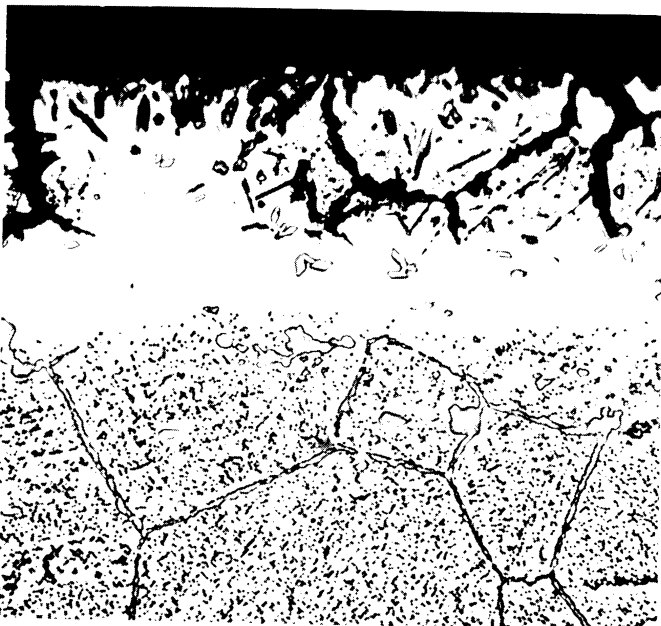


Figure 63 Spec. No. R-91 (Section Showing Surface Attack) Exposed Without Stress 100 Hours at 1800°F

Subsequent Tensile Properties

Elongation: 2.8%

Reduction of Area: 5.0%

Corresponding Re-Machined Spec.

Elongation: 4.2%

Reduction of Area: 5.9%

500x

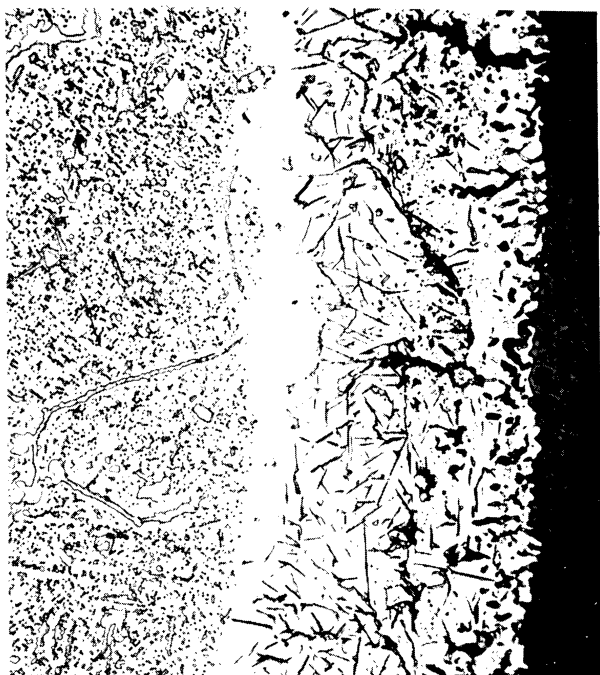


Figure 64 500x
Longitudinal Section of Spec. D-2

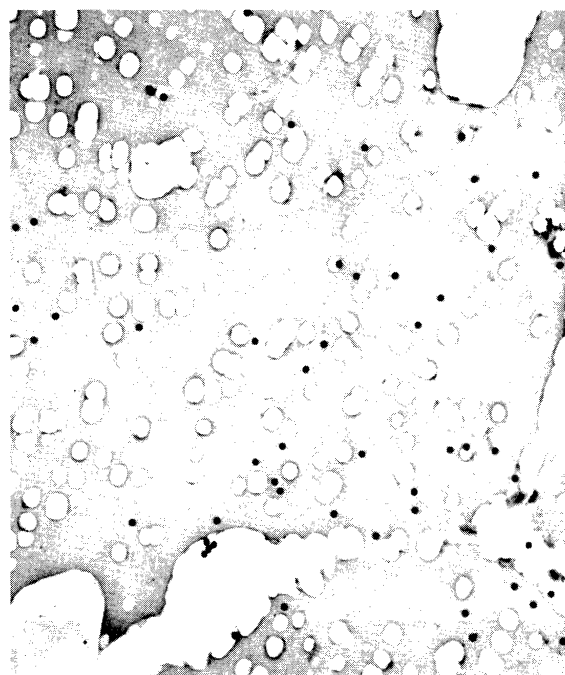


Figure 65 3500x
Electron Micrograph of Spec. D-2

Specimen D-2: Exposed Without Stress 474 Hours at 1700°F

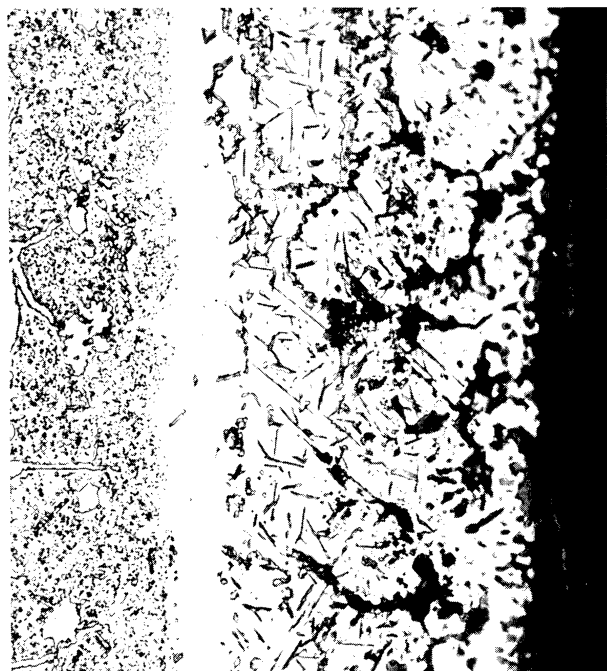


Figure 66 500x
Longitudinal Section of Spec. D-5

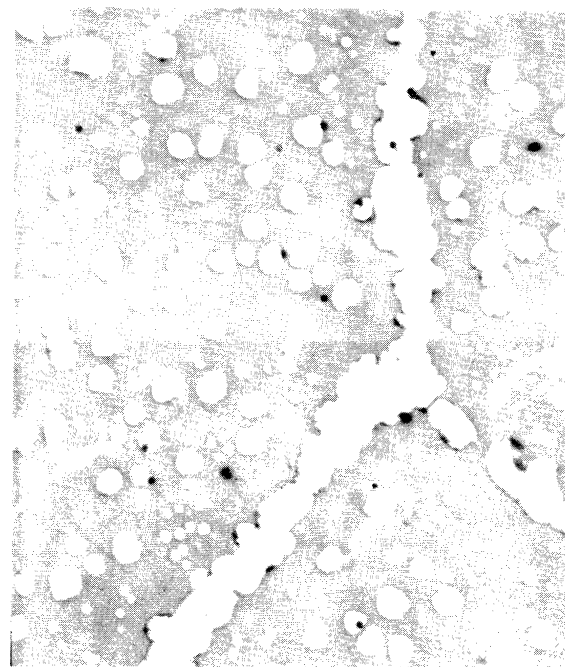


Figure 67 3500x
Electron Micrograph of Spec. D-5

Specimen D-5: Exposed Without Stress 2012 Hours at 1700°F

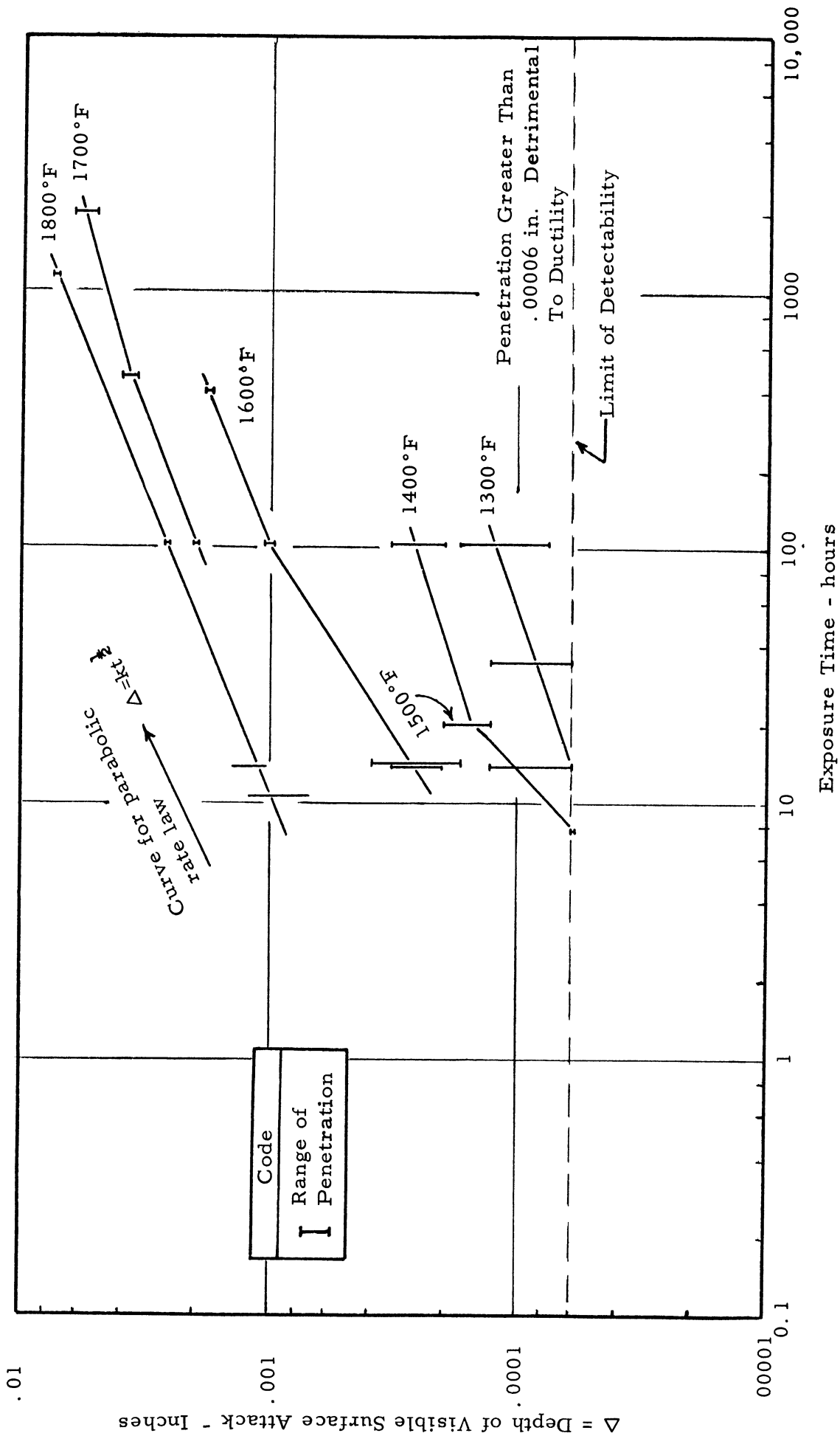


Figure 68 Effect of Exposure Temperature and Time on Depth of Visible Surface Attack in Rene' 41

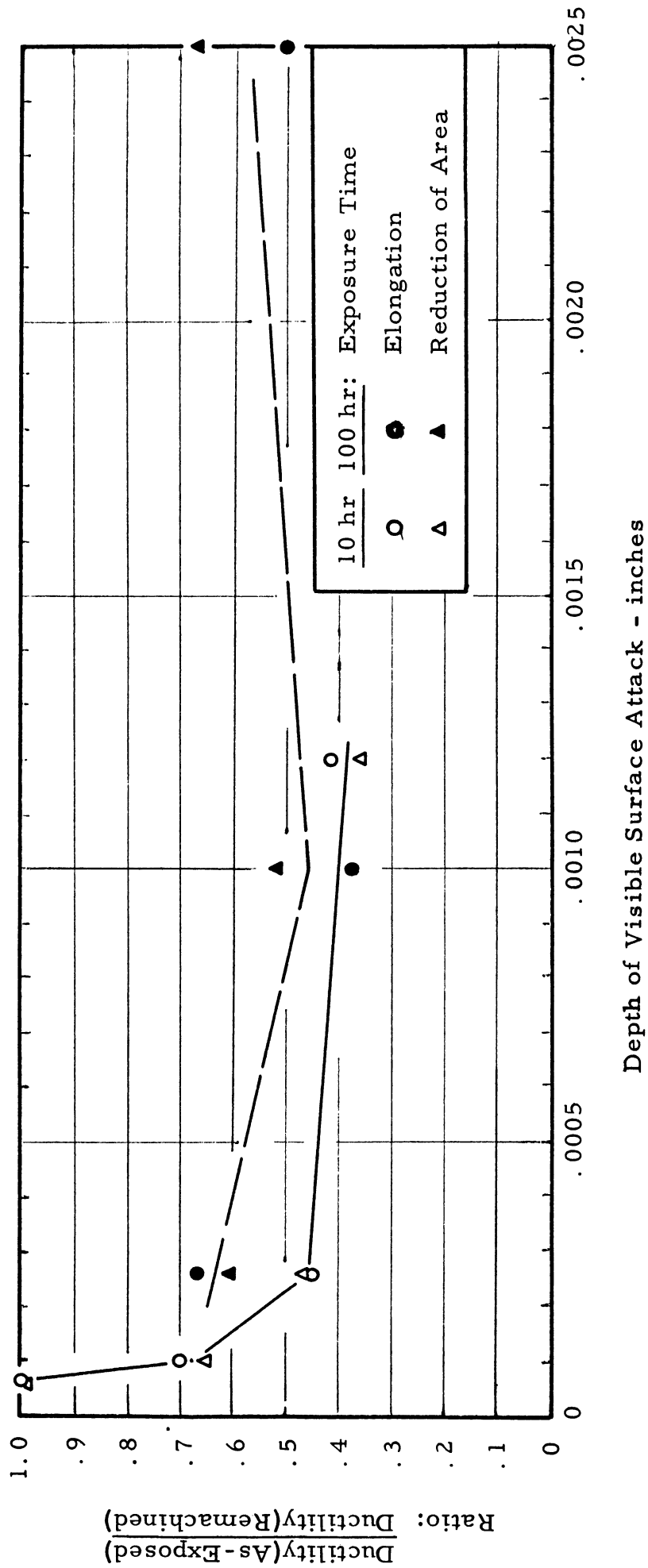


Figure 69 Effect of Visible Surface Attack on Room Temperature Tensile Ductility of Rene' 41 Exposed Without Stress at 1300° - 1800° F

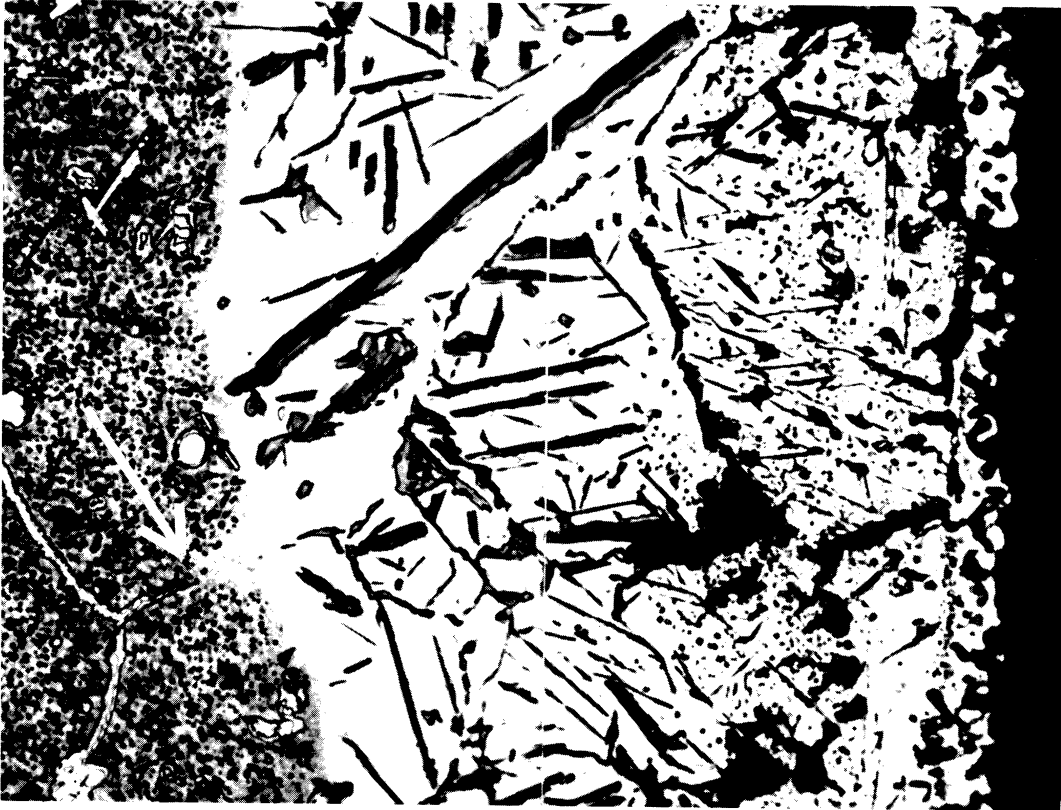


Figure 70

1000x

Section of Spec. D-2 Showing Attacked Surface Layers
(Arrow shows solution of grain boundary phase in
advance of general attack)

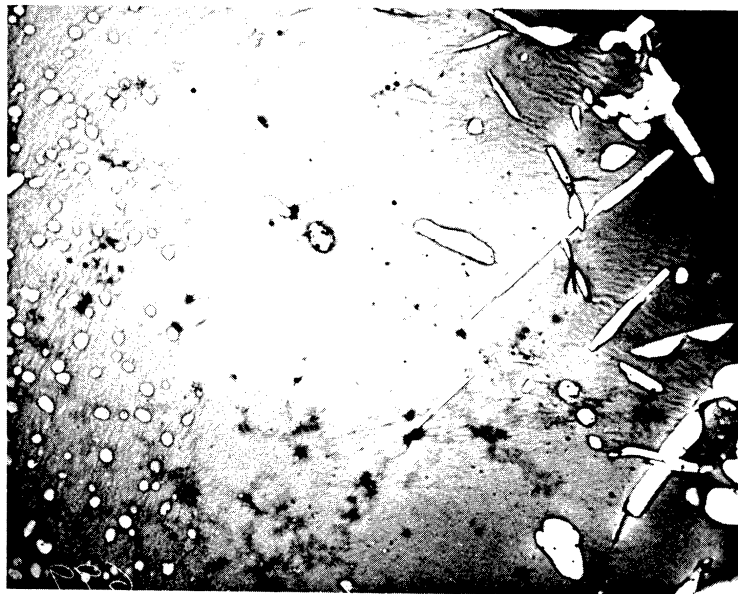


Figure 71

2200x

Electron Micrograph of "Depleted" Layer of Spec. D-2
Spec. D-2 Exposed 474 Hours at 1700°F In Dilatometer Furnace



1000x

Section of Spec. D-5 Showing Attacked Surface Layer
(Exposed 150 Hours at 1800°F In Dilatometer)

Figure 72

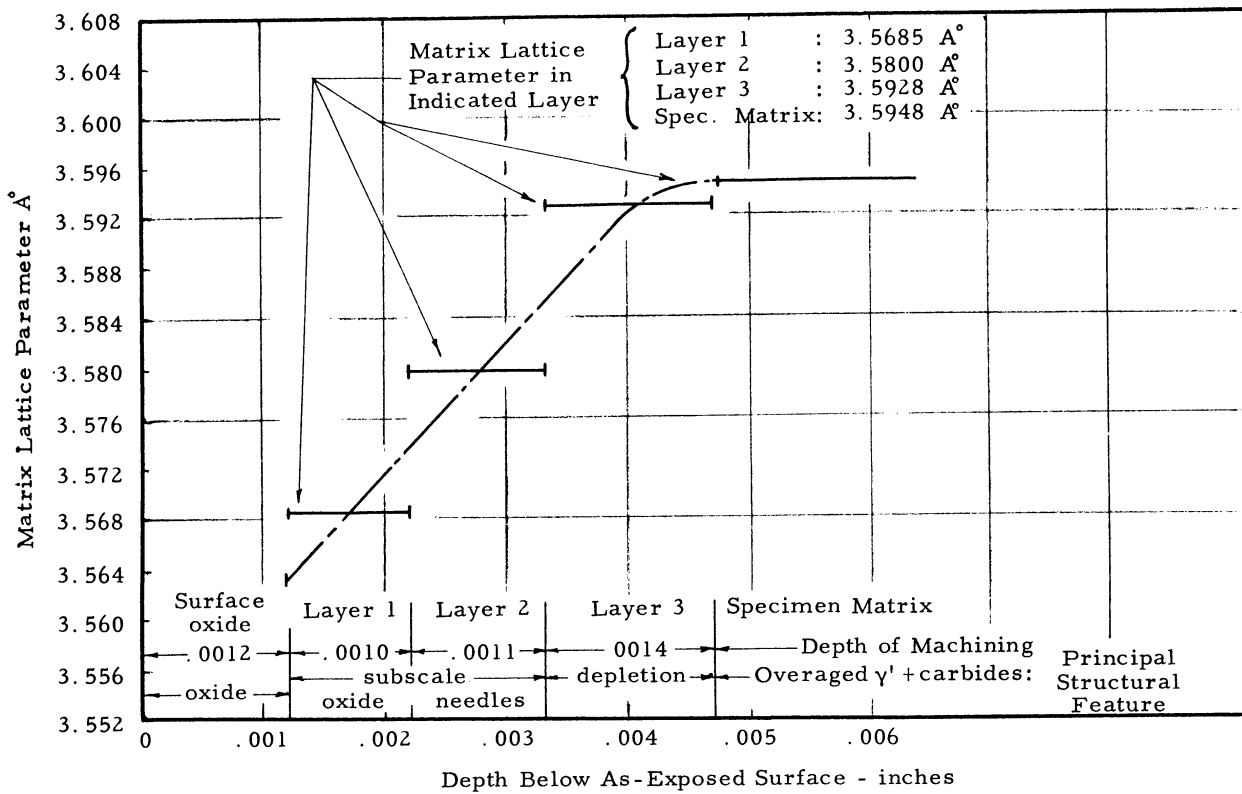


Figure 73 Effect of Surface Attack on Matrix Lattice Parameter of Spec. D-2

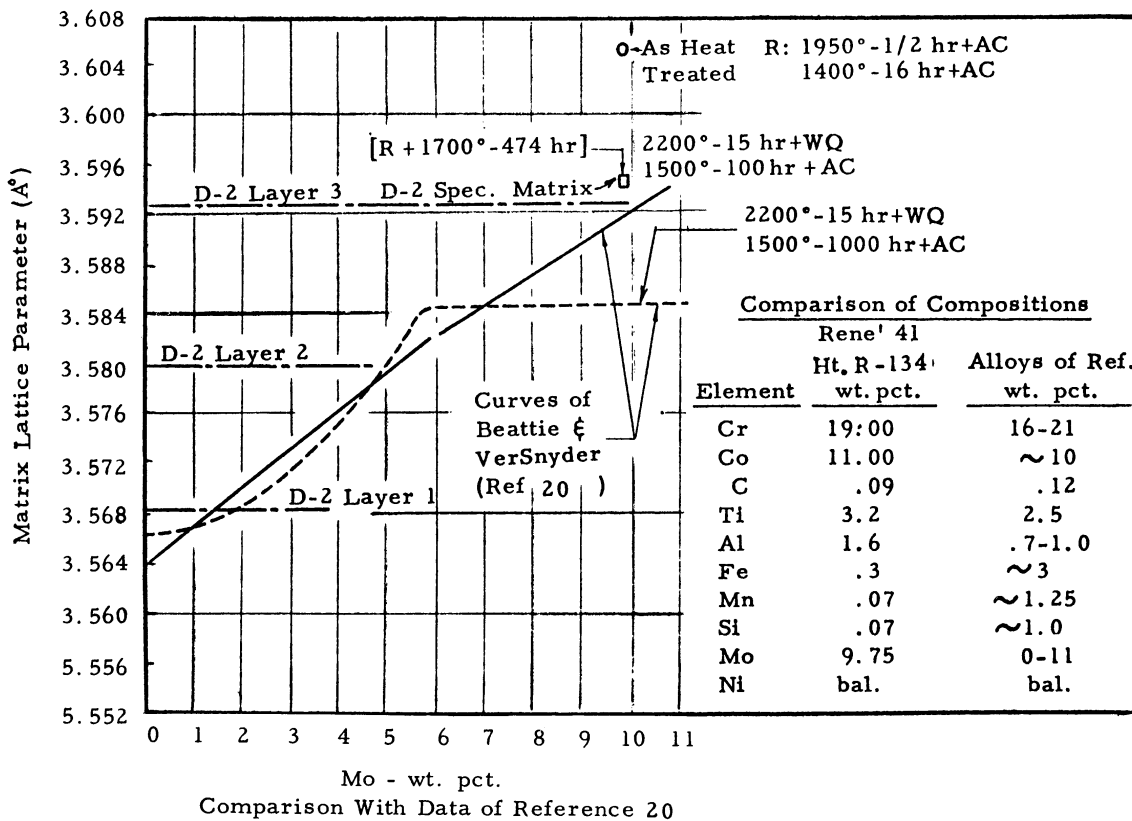


Figure 74 Lattice Parameter Data for Specimen D-2 Compared to Data of Beattie and VerSnyder For Effect of Molybdenum Content on Lattice Parameter of Nickel-Base Alloys

THE UNIVERSITY OF MICHIGAN, Ann Arbor, Mich.
EFFECT OF CREEP-EXPOSURE ON MECHANICAL PROPERTIES OF RENE' 41: Part II, Structural Studies, Surface Effects, and Re-Heat Treatment, by Jeremy V. Gluck and James W. Freeman, **November** 1961. 103p. incl. figs. tables and refs. (Project 7381; Task 73810) (ASD TR 61-73, Pt. II) (Contract AF 33(616)-6462)

Unclassified report
The effect of creep-exposure on room temperature mechanical properties of Rene' 41 was studied for temperatures of 1200-1800°F and times up to 200 hours. Unstressed exposures were for as long as 2012 hours at 1700°F. Thermally-induced structural changes reduced strength and ductility after exposures at 1400-1800°F. Reduced yield

(over)

strength was due to decreased volume fraction of gamma prime and secondarily to an increase in the particle size. Ductility was reduced by formation of massive grain boundary carbides. Up to 1500°F, creep caused strain hardening and Bauschinger effects. Except for surface effects, damage was restorable by re-heat treatment. Yield strength was restored by re-solution and re-aging to produce fine gamma prime. Complete re-solution of carbides was required to restore ultimate strength and ductility. Microcracking was not observed. Creep induced intergranular surface cracking at 1200-1300°F which reduced ductility. Surface effects for exposures above 1400°F were thermally induced. General principles were formulated for damage to properties of nickel-base alloys.

UNCLASSIFIED

THE UNIVERSITY OF MICHIGAN, Ann Arbor, Mich.
EFFECT OF CREEP-EXPOSURE ON MECHANICAL PROPERTIES OF RENE' 41: Part II, Structural Studies, Surface Effects, and Re-Heat Treatment, by Jeremy V. Gluck and James W. Freeman, **November** 1961. 103p. incl. figs. tables and refs. (Project 7381; Task 73810) (ASD TR 61-73, Pt. II) (Contract AF 33(616)-6462)

Unclassified report
The effect of creep-exposure on room temperature mechanical properties of Rene' 41 was studied for temperatures of 1200-1800°F and times up to 200 hours. Unstressed exposures were for as long as 2012 hours at 1700°F. Thermally-induced structural changes reduced strength and ductility after exposures at 1400-1800°F. Reduced yield

UNCLASSIFIED

(over)

UNCLASSIFIED

strength was due to decreased volume fraction of gamma prime and secondarily to an increase in the particle size. Ductility was reduced by formation of massive grain boundary carbides. Up to 1500°F, creep caused strain hardening and Bauschinger effects. Except for surface effects, damage was restorable by re-heat treatment. Yield strength was restored by re-solution and re-aging to produce fine gamma prime. Complete re-solution of carbides was required to restore ultimate strength and ductility. Microcracking was not observed. Creep induced intergranular surface cracking at 1200-1300°F which reduced ductility. Surface effects for exposures above 1400°F were thermally induced. General principles were formulated for damage to properties of nickel-base alloys.

UNCLASSIFIED

UNCLASSIFIED

UNCLASSIFIED

UNCLASSIFIED

UNCLASSIFIED

UNCLASSIFIED

<p>THE UNIVERSITY OF MICHIGAN, Ann Arbor, Mich. EFFECT OF CREEP-EXPOSURE ON MECHANICAL PROPERTIES OF RENE' 41: Part II, Structural Studies, Surface Effects, and Re-Heat Treatment, by Jeremy V. Gluck and James W. Freeman, November 1961. 103p. incl. figs. tables and refs. (Project 7381; Task 73810) (ASD TR 61-73, Pt. II) (Contract AF 33(616)-6462)</p> <p style="text-align: center;">Unclassified report</p> <p>The effect of creep-exposure on room temperature mechanical properties of Rene' 41 was studied for temperatures of 1200-1800°F and times up to 200 hours. Unstressed exposures were for as long as 2012 hours at 1700°F. Thermally-induced structural changes reduced strength and ductility after exposures at 1400-1800°F. Reduced yield</p> <p style="text-align: right;">(over)</p>	<p>THE UNIVERSITY OF MICHIGAN, Ann Arbor, Mich. EFFECT OF CREEP-EXPOSURE ON MECHANICAL PROPERTIES OF RENE' 41: Part II, Structural Studies, Surface Effects, and Re-Heat Treatment, by Jeremy V. Gluck and James W. Freeman, November 1961. 103p. incl. figs. tables and refs. (Project 7381; Task 73810) (ASD TR 61-73, Pt. II) (Contract AF 33(616)-6462)</p> <p style="text-align: center;">Unclassified report</p> <p>The effect of creep-exposure on room temperature mechanical properties of Rene' 41 was studied for temperatures of 1200-1800°F and times up to 200 hours. Unstressed exposures were for as long as 2012 hours at 1700°F. Thermally-induced structural changes reduced strength and ductility after exposures at 1400-1800°F. Reduced yield</p> <p style="text-align: right;">(over)</p>	<p>UNC L A S S I F I E D</p>	<p>UNC L A S S I F I E D</p>
<p>strength was due to decreased volume fraction of gamma prime and secondarily to an increase in the particle size. Ductility was reduced by formation of massive grain boundary carbides. Up to 1500°F, creep caused strain hardening and Bauschinger effects. Except for surface effects, damage was restorable by re-heat treatment. Yield strength was restored by re-solution and re-aging to produce fine gamma prime. Complete re-solution of carbides was required to restore ultimate strength and ductility. Microcracking was not observed. Creep induced intergranular surface cracking at 1200-1300°F which reduced ductility. Surface effects for exposures above 1400°F were thermally induced. General principles were formulated for damage to properties of nickel-base alloys.</p>	<p>strength was due to decreased volume fraction of gamma prime and secondarily to an increase in the particle size. Ductility was reduced by formation of massive grain boundary carbides. Up to 1500°F, creep caused strain hardening and Bauschinger effects. Except for surface effects, damage was restorable by re-heat treatment. Yield strength was restored by re-solution and re-aging to produce fine gamma prime. Complete re-solution of carbides was required to restore ultimate strength and ductility. Microcracking was not observed. Creep induced intergranular surface cracking at 1200-1300°F which reduced ductility. Surface effects for exposures above 1400°F were thermally induced. General principles were formulated for damage to properties of nickel-base alloys.</p>	<p>UNC L A S S I F I E D</p>	<p>UNC L A S S I F I E D</p>
<p>UNC L A S S I F I E D</p>	<p>UNC L A S S I F I E D</p>	<p>UNC L A S S I F I E D</p>	<p>UNC L A S S I F I E D</p>